Temporal changes of the benthic environmental conditions in a subarctic fjord with aquaculture activity

A geochemical and micropaleontological study

Hege Kristine Vågen

Master Thesis
Environmental geology – environmental stratigraphy
60 credits

Institute of Geosciences
The Faculty of Mathematical and Natural Sciences
UNIVERSITY OF OSLO

06/2018

TEMPORAL CHANGES OF THE BENTHIC ENVRIONMENTAL CONDITIONS IN A SUBARCTIC FJORD WITH AQUACULTURE ACTIVITY

A geochemical and micropaleontological study

Hege Kristine Vågen

Master Thesis
Environmental geology – environmental stratigraphy
60 credits

Institute of Geosciences
The Faculty of Mathematical and Natural Sciences
UNIVERSITY OF OSLO

06/2018

2018

Temporal changes of the benthic environmental conditions in a subarctic fjord with aquaculture activity

Hege Kristine Vågen

http://www.duo.uio.no/

Trykk: Reprosentralen, Universitetet i Oslo

Abstract

The Norwegian fjords host a large and increasing number of fish farms. Aquaculture activities produce high quantities of organic matter. The organic matter is released into the surrounding water and eventually end up on the seafloor. Increased organic matter supply to the sea floor sediment can potentially have negative effects on the benthic environment. It is therefore important to monitor how fish farming affect the benthic environmental status.

By analysing two sediment cores collected in the northern Norwegian fjord Kaldfjorden, this thesis has investigated the temporal changes in several geochemical parameters since the time before 1900 and towards the present time. Kaldfjorden has had an active aquaculture industry since the early 1970s. Both cores were radiometrically dated to 1900. The parameters investigated on each sediment core were total organic carbon (TOC), total nitrogen (TN), heavy metals, grain size distribution and calcium carbonate content. Benthic foraminifera were used to study the ecological status through time. The aim of the study is to establish the fjords reference condition (i.e before human impact), and investigate whether there can be observed any changes in the analysed parameters in recent times. This study shows that the sediments in both the inner and outer part of Kaldfjorden has received a high and increasing supply of sediment and organic matter from around 1960-1970 and towards the present. There is a different depositional environment in the outer and inner Kaldfjorden, which is reflected in the differences in benthic foraminiferal accumulation rate (BFAR) and the foraminiferal species assemblages. The diversity of foraminifera and the BFAR is naturally high in Kaldfjorden. The increase of organic matter to the sea floor sediments since the 1970s has not had a major influence on the diversity of the foraminiferal assemblages. However, the assemblage species composition of the inner fjord has changed in recent times, with an increasing presence of the opportunistic foraminifera *S. fusiformis*. Increased relative abundance of the *S. fusiformis* occurs in upper core samples at both stations. This could be views as an early warning sign that the assemblages are showing some degree of stress related to the increased organic matter supply.

Acknowledgements

Firstly, I would like to tribute my gratitude to my supervisors Elisabeth Alve and Silvia Hess. They are two cool ladies who know their field of study! Throughout this process they have enthusiastically shared their knowledge on the environmental sciences, foraminifera and the importance of critical thinking. I thank Elisabeth Alve for introducing me to environmental stratigraphy during my first semester at UiO. Her course was inspiring, and I am so happy that I could continue my masters within this field. An equal thanks to Sivia Hess for her kindness and her willingness to always find time to help. Sivia's expertise in foraminifera has been crucial in helping me defining foraminifera species, and her tips and tricks greatly aided the foraminiferal picking process. A special thanks to my Tromsø-based supervisor Paul E. Renaud. I thank him for his very kind hospitality in Tromsø, his enthusiasm in my work and for being my inside source in Akvaplan Niva. An equal thanks to all my supervisors for good assistance and feedback on my paper.

Great gratitude is also directed to the entire "Jellyfarm team" for making the two weeks of field work in Tromsø a really fun, interesting and memorable experience. I would like to thank the Jellyfarm project and the University of Oslo for financing laboratory- and fieldwork. Also, a special thanks to Miljøringen who granted me with a student scholarship, which greatly aided travel expenses and other analytical expenses.

I would like to thank Mufak Said Naroz for technical support in the laboratory and Anouk Tosca Klootwijk for very helpful input. Furthermore, I would like to thank the people at Havforskningsinstituttet for being very enthusiastic in helping to supply me with CTD data.

Big appreciations must also be awarded to my family and friends for unconditional love and support. A special thanks to my coolest and sweetest grandma 'Slaugen' who was always so interested in my schoolwork, but passed away before seeing me graduate. A great thanks to my friend Kat and my sweet mum for a helpful proof reading. And lastly, thanks to Even, firstly just for being you, but also for making me laugh every day and being there for me through my ups and downs the last six months.

Table of Content

1 Introduction 1

2 Study area 6

2.1 Kaldfjorden 6

2.2 Geology 8

2.3 Hydrography 9

2.4 Wind and current system 16

2.5 Pollution history of Kaldfjorden 17

3 Material and methods 22

3.1 Sample collections and preparations 22

3.2 Sediment dating 25

3.3 Particle size distribution 25

3.4 Total Organic Carbon(TOC) and Total Nitrogen (TN) content 26

3.5 Heavy metal concentrations 27

3.6 Micropaleontological analysis 27

4 Results 29

4.1 Core description and water content 29

4.1.1 Station IN 29

4.1.2 Station OUT 30

4.2 Core dating and Sediment Accumulation Rate (SAR) 31

4.2.1 Station IN 31

4.2.2 Station OUT 33

4.3 Particle size distribution 34

4.3.1 Station IN 34

4.3.2 Station OUT 36

4.4 Total organic carbon (TOC) and nitrogen (TN) content 37

4.4.1 Station IN 37

4.4.2 Station OUT 38

4.5 C/N ratio 40

4.6 Heavy metal concentrations 40

4.6.1 Station IN 40

4.6.2 Station OUT 42

4.7 $CaCO_3$ content 43
4.8 Foraminifera 44
4.8.1 Station IN 44
4.8.2 Station OUT 49
5 Discussion 52
5.1 Sediment chronology 52
5.2 Depositional environment 53
5.2.1 Sediment characteristics and accumulation rate 53
5.2.2 Temporal TOC accumulation rates 55
5.2.3 Calcium Carbonate ($CaCO_3$) content 60
5.2.4 Sediment dispersal and bottom currents 61
5.3 Heavy metal concentrations 63
5.4 Foraminifera assemblages 63
5.4.1 Validation of foraminifera concentration and BFAR 63
5.4.2 Difference in species assemblage 65
5.5 The impact of anthropogenic organic carbon discharges in Kaldfjorden 69
6 Conclusions 73
References 75
Appendices: 81
Appendix A: Lab report from sediment dating 82
Appendix B: Results from geochemical analysis 88
Appendix C: Foraminifera data, total counts and diversity indices 90
Appendix D: Foraminifera data, relative species abundance (%) 91
Appendix E: Taxonomic list of benthic foraminifera 92

List of figures:

Figure 2.1: Overview map; location of Kaldfjorden in Norway. Core locations are indicated. …….6

Figure 2.2. A: The bathymetry of Kaldfjorden with core locations. Placement of S_1 and S_2 indicated. **B:** Depth cure map of Kaldfjorden. …….8

Figure 2.3: Map showing the geology surrounding Kaldfjorden. ……...9

Figure 2.4: Overview of the circulation patter of Coastal Water and Atlantic Water outside Troms county. Map of the seafloor topography on the coastal shelf and placements of Malangsdjupet, Malangen fjord and Tromsø Airport. ……...10

Figure 2.5: A: Monthly average precipitation for the period 1961-1990. **B:** Total annual precipitation for each year in the period 2008-2017. ……12

Figure 2.6: CTD data collected from inner, mid and outer Kaldfjorden in September ……14

Figure 2.7: Wind rose from Tromsø airport……...16

Figure 2.8: Map of Kaldfjorden including the placement of the active fish farms, inactive fish farms, factory location, sewage outlet, harbours and the placement of coring stations. ……...19

Figure 3.1 The vessel used to collect sediment cores in September 2017. …….……..23

Figure 3.2. A: Picture of the Gemini Corer used. B: Example of subsampling from the box corer. C: Illustration of the slicing of a sediment core retrieved from the box corer. 24

Figure 4.1: Water content (%) of both replicate cores from station IN and OUT **A:** IN-B and IN-C core. **B:** OUT-11 and OUT-15 core. ……30

Figure 4.2: Pictures of the OUT-15 core sediments under slicing. ……...31

Figure 4.3. Age model of dated core samples. Results from station IN (IN-C core) is marked with blue, and at station OUT (OUT-15 core) is marked with red. ……...32

Figure 4.4: A: The ^{137}Cs activity vs. core depth. **B:** The unsupported ^{210}Pb activity vs. core depth. ….....33

Figure 4.5: SAR vs. the dated core sample from each station. …….33

Figure 4.6: Percentage of particles within fraction of clay, silt and sand. **A:** Results from station IN. **B:** Results from station OUT. **C:** % of sand fraction from both cores vs. dated year of the core samples. ……35

Figure 4.7: Differential volume of the complete grain size range of core IN-C from station IN. ……....36

Figure 4.8: Differential volume of the complete grain size range of core OUT-15 from station OUT. ……...37

Figure 4.9: A: IN-B-core measured TOC_{63} and TN concentrations in percent. **B:** The IN-B-core calculated TOC_{63} and TN accumulation rate in g/m^2/year. …….38

Figure 4.10: A: OUT-15-core TOC_{63} and TN concentration in percent (%). **B:** The OUT-15-core calculated TOC_{63} and TN accumulation rate in g/m^2/year. …….39

Figure 4.11: The C/N ratio at Station IN (blue) and Station OUT (red). The deviation between the two sets of analysis is illustrated with error bars. …….40

Figure 4.12: Down core concentrations of heavy metals from IN-B-core with corresponding environmental classification, EcoQs. …….41

Figure 4.13: Down core concentrations of heavy metals from OUT-15-core with corresponding environmental classification, EcoQs (sed). ……. ……..42

Figure 4.14: Pictures of the typical sediment composition of the 63-500µm sample fraction from each station. A: Picture from station IN (IN-B core). B: Picture from station OUT (OUT-15 core). …….43

Figure 4.15. % weight (g) of the 63-500µm fraction of sediment that consisted of $CaCO_3$. ……44

Figure 4.16: Results from foraminiferal analysis at station IN. **A:** Foraminiferal concentration and BFAR **B:** Diversity index ES(100). **C:** Diversity index H'$_{(log2)}$ **D:** % agglutinated species. …….……45

Figure 4. 17: Two-dimensional MDS-plots showing the relative occurrence of selected species analysed in the samples from station IN and station OUT **A+B**: *S. fusiformis*, **C+D**: *H. balthica*, **E+F**: *B. marginata*, **G+H**: *M. barleeanus*, **I+J**: *E. vitrea*, **K+L**: *C. renifrome*, **M+N:** *C. laevigata /C. neoteretis* **O+P**: *P. osloensis*, **Q+R**: *C. lobatulus.* ……..……..47

Figure 4.18: Dendrogram showing the similarities between assemblages of all samples analysed. ……...49

Figure 4.19: Results from foraminiferal analysis at station OUT. A: Foraminiferal concentration and BFAR. **B:** Diversity index ES(100). **C:** Diversity index $H'_{(log2)}$. ……50

Figure 5.1: Combined results of TOC accumulation rate at station IN (blue) and station OUT (red). ……56

Figure 5.2: Results from analysis of 13 surface samples located from the inner fjord (SE) to the outer shelf (NW) in Malangen. **A:** TOC content (%) **B:** $CaCO_3$ content (%) **C:** Clay + silt content (%). ……..59

Figure 5.3: Results from foraminiferal analysis along the transect of Malangen. **A:** Benthic foraminifera pr. g dry sediment (ind/g) **B**: % calcareous benthic foraminifera along the fjord transect. ……65

List of Tables:

Table 2-1: A summary of temperature and salinity measurements of bottom water collected over the years. …13

Table 2-2: Position of CTD measurements, depth of CTD and actual water depth at the CTD-station. ……..14

Table-3.1: Overview of sample sites, water depth, core length collected material with corresponding equipment and overview of analysis preformed. ……23

Table 4-1: EcoQs classification intervals for foraminifera and heavy metal concentrations (mg/kg) in marine sediments. ……..29

Table 5-1: Classification of TOC_{63} content in marine sediments that are can be used as a supplementary parameter in classifying the EcoQs. ……..…58

Table 5-2: Table show the 9 most abundant species in each core from Kaldfjorden. ……..66

Table 5-2: Average results of analysed parameters of sediments accumulated before 1900, between 1900 and 1976 and in sediments younger than 1976 (post-aquaculture) at station IN and station OUT. ……69

Acronyms and Abbreviations:

BFAR	Benthic Foraminifera Accumulation Rate
CTD	Conductivity Temperature Depth
EcoQs	Ecological Quality status
ind/g	individuals pr. gram dry sediment
MAB	Maximum Allowed Biomass
MOM	Modelling – On growing fish-farm Monitoring
NRF	Norsk Forskningsråd
OM	Organic Matter
POM	Particulate Organic Matter
psu	practical salinity units
TOC	Total Organic Carbon
TN	Total Nitrogen
TPM	Total Particulate Matter
SAR	Sediment Accumulation Rate

WFD Water Framework Directive

WTBC West Troms Basement Complex

1 Introduction

Norway hosts one of the world's longest coastlines, stretching over 13 degrees of latitude. The coastline is highly dissected by a multitude of fjords and sounds that extend far into the interior mainland. Around eighty percent of the Norwegian population lives within 10 km of its coastline (Sætre, 2007), and the biggest cities are all situated around fjords. Fjords are commonly defined as deep, steep-sided estuaries which have been excavated or modified by land-based ice (Syvitski et al., 1987). Fjords are distinctive systems and have different physical, hydrological and biological conditions (Sætre, 2007; Syvitski et al., 1987). The archetypical fjord usually contains one or more submarine sills, which can divide it into partially isolated basins (Syvitski et al., 1987). Water masses within a fjord comprise both oceanic water entering at the mouth and fresh water from rivers and runoff along the coast. The sills can influence the circulation processes and water exchange to various degrees (Sætre, 2007; Syvitski et al., 1987).

Norway benefits well from many goods and services that the fjords offer. The spectacular sceneries of fjords are tourist magnets, and they are of great cultural and recreational value for the Norwegian population. They are also immensely important in an economical perspective as the sheltered cold-temperate seas of Norwegian fjords provide the basis of what has become one of the world's largest aquaculture industries.

Industrial aquaculture in Norway started in the early 1970, and since then there has been a steep increase in the production. In Norway, production of farmed fish (mostly salmon and trout) has increased from 410 thousand tons in 1998 to 1.3 million tons in 2016 (Directorate of Fisheries, 2018a). Marine fish farming activity has increased globally and a continued expansion of aquaculture is expected and could be viewed as an important strategy to ensure the ever-growing food demand (FAO, 2016).

There are several interests that can come into conflict when exploiting the coastal zone. In relation to the aquaculture industry, one important issue is the environmental concern related to the considerable amounts of effluent generated by the operations. Because high densities of fish are contained in open net pens there is a significant amount of waste and by-products released into the surrounding water (Ackerfors and Enell, 1994; Carroll et al., 2003; Valdemarsen et al., 2015). Apart from parasites (e.g. fish lice), chemicals (from the net pen construction and pharmaceuticals) and escape of farmed fish, a great concern is the large

quantities of organic waste consisting of excess feed and faecal matter that is released into the surrounding water. The annual organic waste discharge from aquaculture can be estimated based on the amount of fish food pellets given to the farmed fish. Discharge of organic matter in the form of fish faeces is between 11-15%, and the amount of spilled food is between 5-11% of the total food consumed by the fish (Brooks and Mahnken, 2003; Svåsand et al., 2016). Using these estimates, the Norwegian Institute of Marine Research has estimated that the total load of organic waste from Norwegian aquaculture was between 560 - 660 thousand tonnes in 2017 (Svåsand et al., 2017).

The surrounding water that receives the high discharges of nutrients (i.e. phosphorus and nitrogen from fish faecal matter) can respond by supporting dense plankton blooms (Jørgensen and Richardson, 1996). When the plankton blooms halts the algal detritus will sink and increase the delivery rate of organic material to the bottom sediments (Pinet, 2013). In addition, the suspended particulate organic matter (POM) will eventually settle at various distances from the fish farms (Kutti, et al 2007a; Jørgensen and Richardson, 1996). The organic material on the sea bed decomposes and this process consumes oxygen. If the supply of organic material is high, and consumes more oxygen than what is provided by bottom currents, the bottom water and pore water within the sediment can become hypoxic (having low levels of dissolved oxygen). Over time hypoxia can become so severe that anoxia (no oxygen at all) may occur in bottom waters (Jørgensen and Righardson, 1996; Pinet, 2013). Biological systems are dependent on oxygen and nutrients, and small changes in these parameters can lead to changes in the bottom faunal community. Since the settling organic matter is food for the benthic fauna, a typical first response is an increase in fauna abundance and biomass, whereas the faunal diversity usually decreases (Kutti et al., 2008; Kutti et al,, 2007b). If the loading continues it is possible that so called ‘dead zones’ can occur, and these have been found below fish farms (Brown et al., 1987).

Several authors have carried out research on the carbon discharge and its environmental impacts from Norwegian fjord fish farming. In general, what is found is that;

1. Most of the organic waste matter settles in close vicinity of the farm cages (Kutti et al., 2007a).

2. Its effect on benthic productivity and diversity varies considerably from place to place. The degree of impact is highly dependent on site specific environmental variables, the most

notable of these being current velocities and water depth (Carroll et al., 2003; Kutti et al., 2008; Kutti et al., 2007b; Sweetman et al., 2014; Valdemarsen et al., 2015).

3. The management practices (i.e. production intensity, fallowing periods and feeding rates) are important factors controlling the degree of degradation of the benthic community (Keeley et al., 2015).

One important step towards a common goal for sustainable management of marine coastal waters was the implementation of the EU Water Frame Work Directive (WFD, 2000/60/EC). The EU's WFD defines a common European classification system for water quality. For coastal waters there have been developed several guidelines for classification of different chemical pollutants and biological indicators. A consensus about what is meant by "good" or "poor" ecological quality status (EcoQS) of water has been reached. This framework also gives an indication to a classification termed "high" status, which corresponds to the values expected in a functional, healthy and sustainable ecosystem presumably unimpacted by anthropogenic activity (Curtin and Prellezo, 2010; Lyons et al., 2010).

All fjords are sites of net sediment accumulation (Howe et al., 2000). Sediment delivery rate to fjords is a mixture of river- and wind-transported material from terrestrial sources, open ocean sources (e.g. input from the coastal shelf, transported by currents), and internal fjord sources (e.g. biogenic input) (Syvitski et al., 1987). It has been estimated that the average sediment accumulation rate (SAR) in Norwegian fjords is between 1-7mm/year (Syvitski et al., 1987), where fjords that are recipients for large river discharges have the highest accumulation rates (Syvitski et al., 1987). The sediment fill in deeper fjord basins can preserve a continuous, high resolution record of what has been deposited. The sediment record can therefore be used to interpret and understand previous depositional environments and environmental changes (Howe et al., 2000). In coherence with the varying SAR within fjords, the natural (not influenced by anthropogenic activity) input, accumulation and burial of organic matter differs between fjords. However, the average natural accumulation rate of organic material in fjords is much higher compared to that of the global open ocean (Smith et al., 2015).

Fish farming companies in Norway are obliged to conduct regular environmental surveys to monitor the environmental conditions below and in close vicinity to the farm sites. The analyses of these surveys are performed on the surface sediments of the seafloor, and the

results are classified based on a similar classification system as WFD. The main purpose of environmental monitoring is to investigate the EcoQS or “health” of an area, and determine whether it has changed over time due to human impact (Dolven et al., 2013). Since the environmental impact from increased organic loading to a fjord is controlled by site specific environmental variables, it can be difficult to understand and foresee all the interactions that define the fjord assimilative capacity. It can also lead to uncertainties when comparing different fjords. Two neighbouring fjords might, for example, naturally have very different organic carbon accumulation rates and bottom water oxygen conditions. Knowledge about the pre-impacted (also termed “reference conditions”) at a given site in the fjord is therefore important when investigating the degree of environmental impact caused by humans (Alve, 1991). A fjord’s reference conditions are usually unknown because of limited available biological time series and sediment data.

By studying two sediment cores, one collected in the inner fjord and one from the outer fjord, the main aim of this thesis is to determine if there has been an environmental change from pre-aquaculture to the present-day conditions. The sediments of the two cores were dated using radiometric methods. This allows us to set an age to the core depths and additionally calculate the temporal SAR at each station. The reconstruction of the depositional environment is done in Kaldfjorden and is based on sediment core observations and analyses of grain size, carbonate content, total organic carbon (TOC), total nitrogen (TN) and heavy metals. The ecological response through time is investigated by the use of benthic foraminifera.

Benthic foraminifera are small (generally < 1 mm) protists that live on or within seafloor sediments. According to the World Foraminifera Database the current number of total valid recent and fossil species is over 43 thousand. Foraminifera typically produce a shell (also termed test) that is commonly made of calcium carbonate or agglutinated sediment particles (Murray, 2001). Foraminifera are present in high abundances in almost all marine environments, and their short generation time implies that they have potential to respond fast to environmental changes (Murray, 2001). The foraminifera tests are preserved in the sediment after the species is dead. Thus, the studies of foraminifera can record the *in situ* environmental ecological changes through time (e.g., Alve, 1995; Dolven et al., 2013). Increased pollution, changes in organic carbon supply and variations in oxygen, temperature and salinity can be reflected in foraminifera abundances and the assemblage composition

(Murray, 2001). Foraminifera are therefore a well-established paleoenvironmental reconstruction tool when there is limited biological time series, and are proven to be a promising tool for assessing the ecological quality of marine waters and sediment (Bouchet et al., 2012; Dolven et al., 2013; Murray and Alve, 2016).

Considering the ever-growing aquaculture industry in Norway, and limited information on the reference conditions of fjords, this thesis seeks to contribute to the pool of fjord sediment data and investigate the reference conditions of a northern Norwegian fjord with aquaculture. This has been studied in Kaldfjorden, in Troms county, which has hosted aquaculture activities since the early 1970s.

The two stations that have been investigated are located relatively far away from the fish farms (~500 m and ~1 km) in Kaldfjorden. This gives us a broader picture of the environmental conditions of Kaldfjorden, and allows investigation of whether organic waste from the operation is dispersed over a larger fjord area. Studying both the inner and outer fjord further allows for comparison of two potentially different depositional environments along the inner fjord to coast gradient. Are the two locations comparable in their depositional environment and in the foraminiferal assemblage? Is there evidence of a temporal change over the past century in organic carbon accumulation rates between the two stations? Can any changes be linked to the aquaculture operations in the fjord? If impacted, how severely? Can there be observed a change in the foraminiferal assemblage through time, and do any changes happen at both station? By combining the information from the mentioned analysed environmental parameters this thesis seeks to answer these questions. The work will contribute to further understanding of spatial variability in environmental conditions within the same fjord, and the temporal environmental impact over the past century in one of the many different fjord types that have aquaculture.

2 Study area

2.1 Kaldfjorden

Kaldfjorden is situated on the northern coast of the island Kvaløya in the municipality of Tromsø (Troms county; Figure 2.1). The fjord lies at 69º latitude, which is about six degrees north of the Arctic Circle. Owing to the high latitude the yearly budget of solar irradiation show a strong seasonality, with a continuously light summer, and mostly dark winter.

The fjord has a characteristic L- shape, with a north-south orientation in the central and outer part, and a west-east orientation in the inner part. The mouth of the fjord is located between Klubbeneset in the north and Røsnes in the south and stretches to the village of Kaldfjord, located around the head of the fjord. In 2017 Kaldfjord had 847 inhabitants and the number has been stable over the past decades (SSB, 2018).

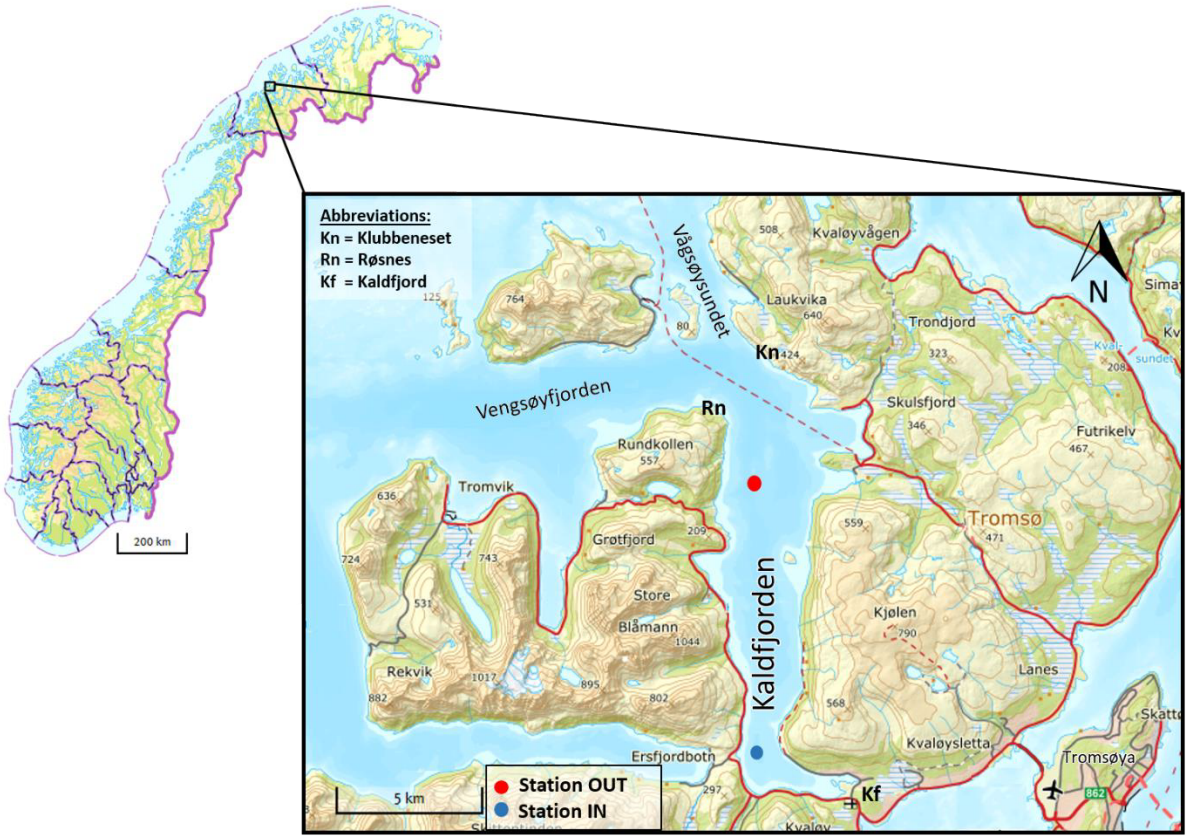

Figure 2.1: Overview map of location of Kaldfjorden in Norway. Core locations are marked with a red and blue circle. (Map modified from www.kartverket.no)

Kaldfjorden is approximately 15 km long, and has a maximum width of 4 km at the mouth; it narrows steadily towards the head of the fjord. Even though Kaldfjorden is situated close to the open ocean, the fjord has no direct contact with the Norwegian Sea, and all water

exchange happens between Vengsøyfjorden and Vågsøysundet (Figure 2.1). Kaldfjorden becomes progressively deeper seaward. The deepest part of the inner fjord area is 111m and reaches a max depth of 237m at the mouth of the fjord (Figure2.2B). Images from seismic profiling conducted 2013 by the University of Tromsø, depth curve maps and simple bathymetric pictures (MAREANO.no) show that the fjord has one partial sill at the mouth of the fjord (B_1 in figure 2.2A). The shallowest area of this sill is 75m but has a deeper channel of >150m on the western side and therefore it is not believed that it sufficiently restricts water movement between the deeper water masses of Vengsøyfjorden and Kaldfjorden (Eriksen, 2016). In the shallower area in the inner fjord there are two sills (S_1 and S_2 in Figure 2.2A). S_1 is 55 m and S_2 is 49 m at their deepest (Velvin et al., 2008). In this work inner Kaldfjorden/inner fjord is referred to the area up fjord of S_1 (Figure 2.2A).

The terrain surrounding mid and outer Kaldfjorden is steep sided with high mountains on both sides. Mountains on the west side reach up to 1000m above sea level. Below the waterline in the mid and outer fjord steep slopes, reflecting the surrounding terrain, continues down the side walls of the fjord. The vegetation consists generally of tundra plants that gradually disappear up the rocky hillsides. The Norwegian Water Resources and Energy Directorates (NVE) map-tool for registration of information related to landslides and avalanches have classified these outer coastal areas as hazardous areas, suggesting that there is a possibility that the fjord sometimes is supplied with debris. Several avalanches have been registered in the highest surrounding mountains (NVE, 2018). Topography surrounding the inner fjord is flatter, and this is also where the village Kaldfjord is situated.

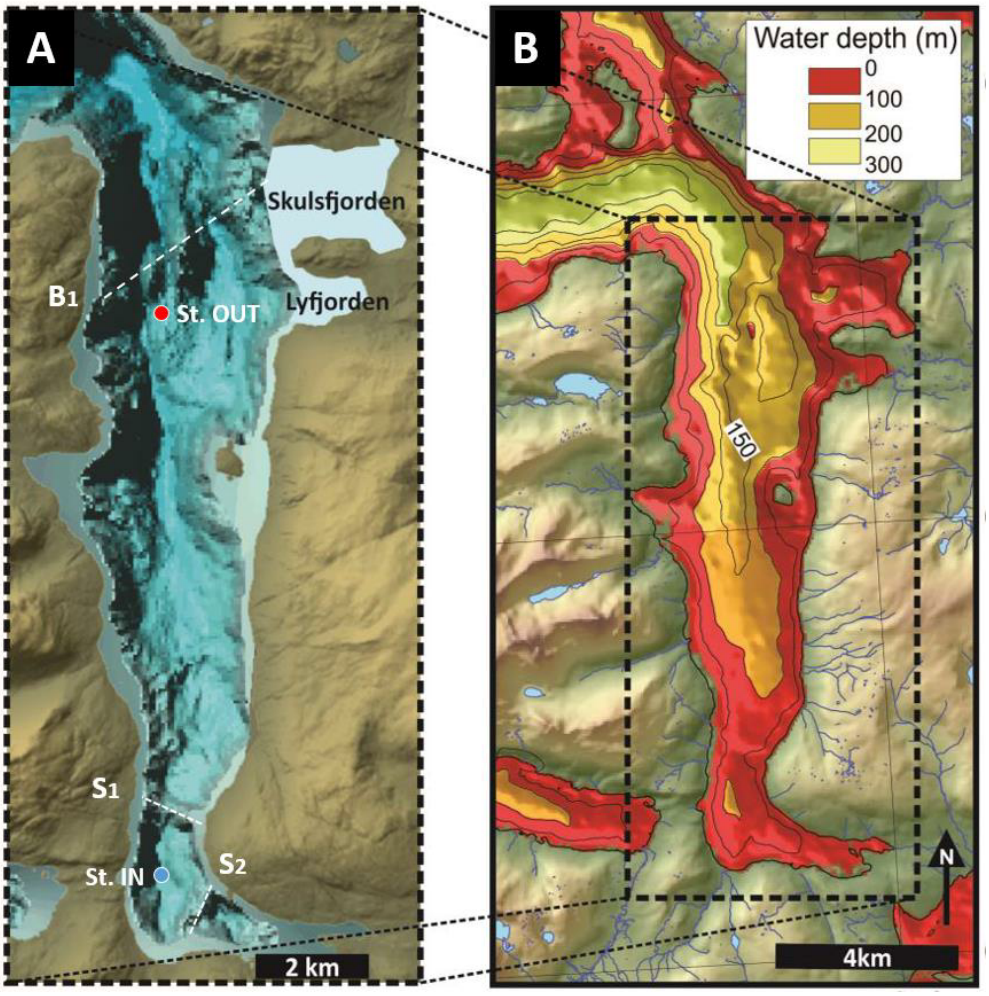

Figur 2.2: A: The bathymetry of Kaldfjorden mapped by MAREANO.no. It visualises the uneven seafloor topography. The shallowing barrier in the outer-fjord is indicated with B_1. S_1 and S_2 indicate the placement of the two sills in the inner part of Kaldfjorden. Placement of station OUT (red circle) and station IN (blue circle) are marked in figure A. B.: Depth curve map of Kaldfjorden (Figure modified from Hermansen, 2015).

2.2 Geology

The bedrock of Troms can be divided into two main components, Precambrian bedrock and the bedrock from the Caledonian orogeny. The Precambrian bedrock is prominent in the outer coastal areas, but lies hidden beneath Caledonian nappes further inland (Bergh et al., 2010; Zwaan, 1995). This coastal region with bedrock of Precambrian age is geologically known as The West Troms Basement Complex (WTBC) and is separated from Caledonian nappes by a series of Caledonian and post-Caledonian thrust faults (Figure 2.3). Although the WTBC lies just beside the Caledonian nappes, the area has experienced little influence from the Caledonian orogeny (Bergh et al., 2010). Kaldfjorden is located in the WTBC, and the bedrock of the surrounding fjord mainly consist of granite, also known as Erfjordsgranitten, which has been dated to be 1800-1770 million years old. In the very inner part of the fjord the

bedrock consist of quartz diorite and tonalitic and mafic gneiss of assumed Neoarchean to Paleoproterozoic age (Bergh et al., 2010). The sub-areal profile of a fjord can say something about how easily the local rock can be eroded (Syvitski et al., 1987). Considering the age of the bedrock and the height of the mountains surrounding Kaldfjorden, the bedrock is presumably resistant to weathering.

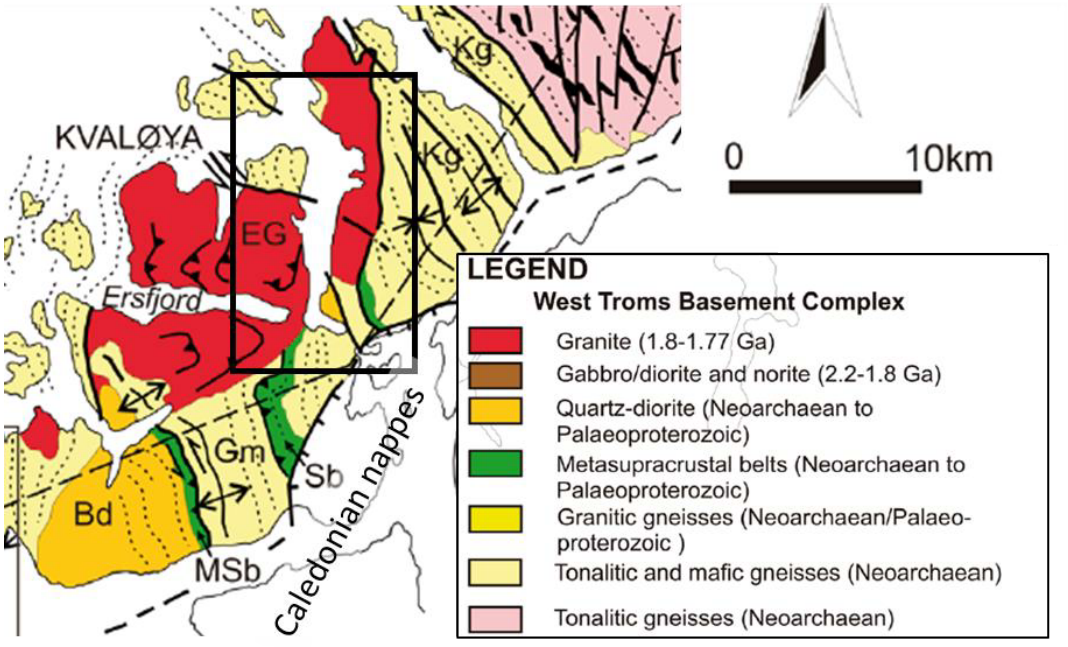

Figure 2.3. Map showing the distribution of bedrock surrounding Kaldfjorden. (Illustration modified from Bergh et al. (2010)).

2.3 Hydrography

A water body is described based on the physical parameters such as salinity, temperature and oxygen saturation (Sætre, 2007). The density of a water body is a function of temperature, salinity and pressure. Water masses with different densities will not as easily be mixed, and can lead to stratification of the within the water column. The northern Norwegian coastline is influenced by two northward-flowing current systems: the Norwegian Atlantic Current and the Norwegian Coastal Current. Atlantic Water and the Coastal Water are separated by their density differences and, according to a general accepted definition, water of salinity above 35 psu originates from Atlantic Water, and that of salinity below 35 psu is Coastal Water (Aure and Østensen, 1993). The Norwegian Atlantic Current is an elongation of the North Atlantic Current that enters the Norwegian Sea between the Shetland and the Faroe Islands (Sætre,

2007). The current transports relatively warm (9°C) and saline >35 psu Atlantic Water north along the Norwegian coast (Aure and Østensen, 1993).

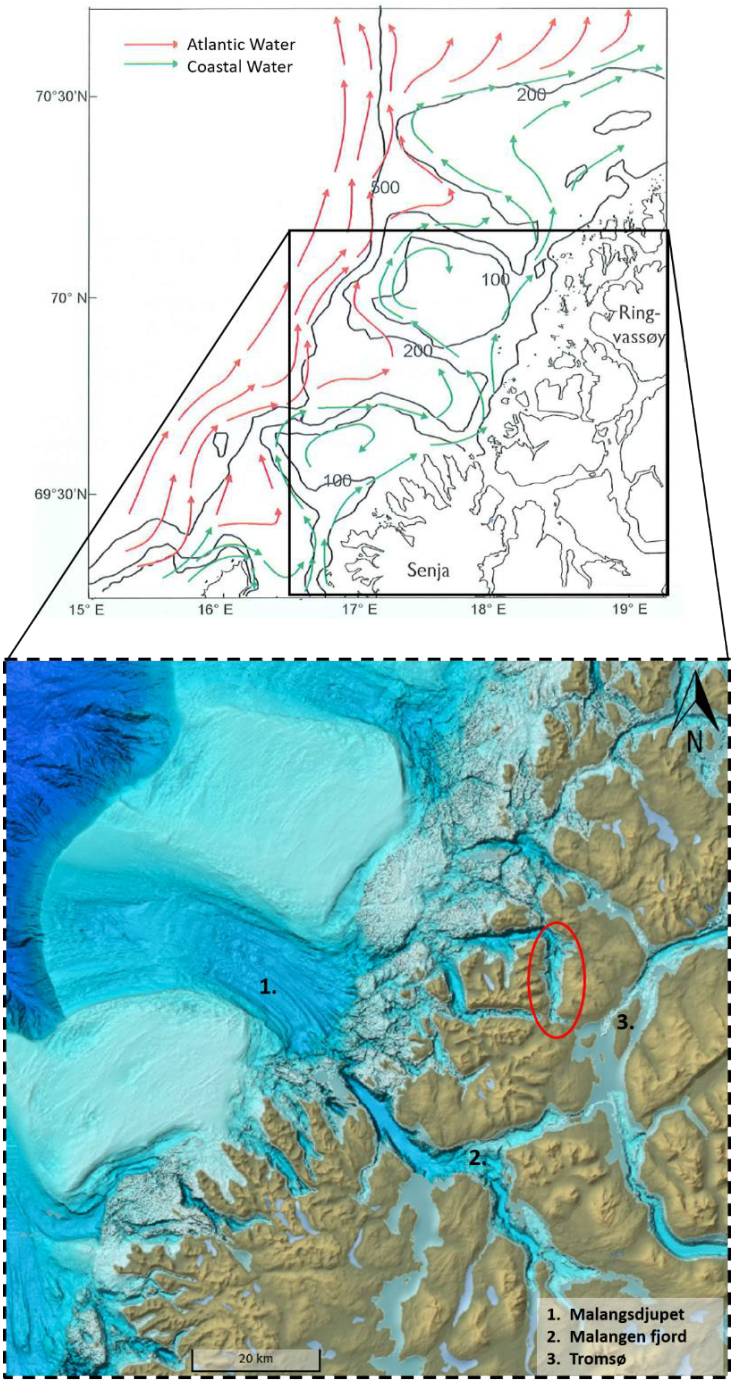

Figure 2.4: Above; Overview of the circulation patter of Coastal Water (green arrows) and Atlantic Water (red arrows) of surface water between 69º and 71º N (coastal shelf outside the Troms county) (illustration from Sætre, 2007). Below: A close up section of the seafloor topography surrounding Kaldfjorden. Kaldfjorden is encircled in with a red line. Location of Malangsdjupet (1.), Malangen fjord (2.) and Tromsø Airport (3.) are indicated (background map from kartverket.no).

The Norwegian Coastal Current originates from the surplus of fresh water the Skagerak area receives from the Baltic Sea, and fresh water discharge from rivers along the coast (Aure and Østensen, 1993; Sætre, 2007). This water flows northward along the coast of Norway as a low-salinity westward- thinning wedge upon the more saline Atlantic Water. Along its northern route the Coastal Water continuously mixes with the deeper and westward lying Atlantic Water. Therefore, the salinity of the Coastal Water gradually increases, and stratification between the two water masses decreases, the further north it flows (Sætre, 2007). The mixing of the water masses is counteracting the natural cooling of the Coastal Water and is of great significance for the temperature conditions of the coastal area in northern Norway.

Three banks are situated on the shelf area outside the coast of Troms and are separated from each other by deeper troughs. One of the troughs, Malangsdjupet, lies just outside Kaldfjorden (Figure 2.4). The water mass distribution is influenced by the bottom topography (Sætre, 2007; Sundby, 1984). The banks allow an oscillation inflow of Atlantic Water that intrudes into the troughs between the three bank areas (Sundby, 1984). It is believed that the intrusion of Atlantic water into the troughs is more common during the winter months, when stratification of the water masses are less pronounced (Sætre, 2007; Sundby, 1984). There is no observed sill outside Vengsøyfjorden, and it is therefore assumed that the water masses within the fjord mix well with those of the adjacent shelf and Malangsdjupet.

There are no rivers that discharge into Kaldfjorden, and the main freshwater supply comes from small streams located around the fjord, together with runoff from land. Data from the closest representative weather station at Tromsø Airport reveal that the mean annual precipitation in the defined Normal period (1961-1990) was approximately 1000 mm (Figure 2.5A). More recent measurements from the period 2008 – 2017 reveal that precipitation varies from year to year but is on average still stable at around 1000 mm (Figure 2.5B) (Eklima.no). Runoff from land is normally very low or absent during the late autumn to early spring, because freshwater is stored on land as snow and ice. Even though precipitation is usually low during the late spring to early summer (Figure 2.5A), this is the time in which the coastal water receives highest freshwater supply due to snow melt.

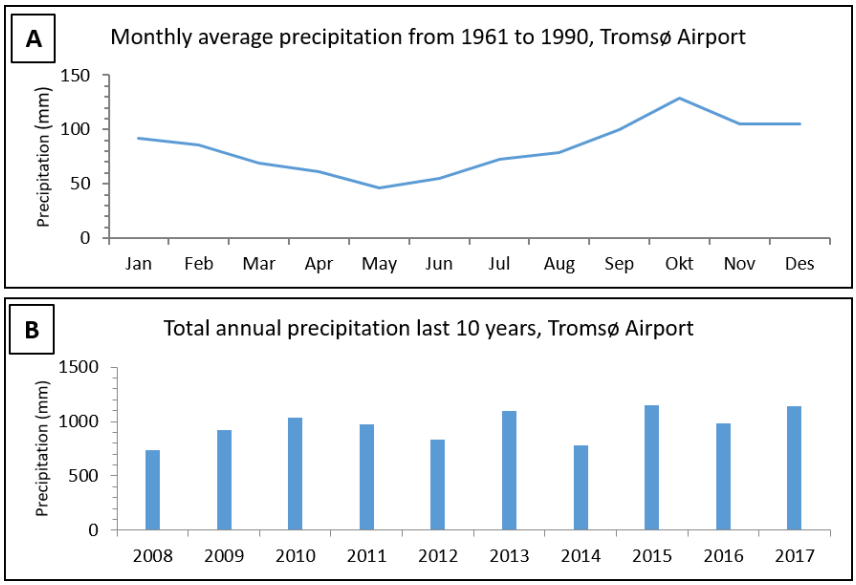

Figure 2.5: A: Monthly average precipitation for the period 1961-1990. Average annual precipitation in this period was 1000 mm. B: Total annual precipitation for each year in the period 2008-2017. The illustration shows the variation between each year. Total average precipitation from 2008-2017 is 966 mm. Both measurements of precipitation are collected from a weather station at Tromsø Airport (data from Meteorologisk Institutt, www.eklima.no).

Hydrographic measurements can be retrieved using a conductivity, temperature and depth (CTD) sensor. Several CTD measurements have been conducted in Kaldfjorden over the years and temperature and salinity of bottom waters collected from inner and mid/outer Kaldfjorden, including one measurement from Vengsøyfjorden, are presented in Table 2-1. Hydrographic measurements were also performed during sample collections for the present thesis, in September 2017, and the results are presented in Figure 2.6. Due to technical difficulties on board, the CTD data collected are unfortunately missing data from the bottom waters. The location, depth of CTD measurements and actual depth collected in September 2017 are showed in Table 2-2. A combination of all available CTD data are used in as a basis to interpret the general hydrographic characteristics of the water masses in the inner and outer Kaldfjorden through the year. However, there will always be yearly variations.

Table 2-1: A summary of temperature and salinity measurements of bottom water collected over the years.

Temperature and salinity measurements in bottom waters in inner and mid/outer Kaldfjorden					
Inner Kaldfjorden					
Date	Water depth(m)	Temp (°C)	Salinity (psu)	Oxygen saturation (%)	Source:
FEB (01.02.2001)	85	5	33.9	90	Mikkola et al., 2000
APR (06.04.1998)	94	2.9	33.8		Østrem, 2018
MAY (21.05.2012)	90	4.0	34.2		Velvin & Worum, 2012
JUN (06.06.2001)	65	3.5	34.5		Pedersen & Mikkola, 2001
JUN (19.06.2008)	100	4.0	33.9	65	Velvin et al., 2008
JUN (28.06.2001)	90	4.0	34.5		Pedersen & Mikkola, 2001
AUG (18.08.2008)	100	6.0	34.4	95	Velvin et al., 2008
SEP (04.09.2017)	80	7.1	34.1	90	This thesis
SEP (25.09.2008)	100	6.0	34.0	80	Velvin et al., 2008
SEP (20.09.2000)	100	7.7	34,8	90	Mikkola et al., 2000
NOV (06.11.2008)	100	6.0	34.0	70	Velvin et al., 2008
NOV (10.11.2013)	64	8.2	33.6		Østrem, 2018
Outer Kaldfjorden					
APR (06.04.1998)	150	3.0	34.0		Østrem, 2018
APR (26.04.2007)	44	3.6	33.8		Østrem, 2018
JUN (06.06.2001)	120	3.5	34.8		Pedersen & Mikkola, 2001
JUN (28.06.2001)	110	4.0	34.5		Pedersen & Mikkola, 2001
SEP (04.09.2017)	112	6.5	34.4	91	This thesis
OCT (26.10.2006)	79	7.7	34.1		Østrem, 2018
NOV (22.11.2016)	70	7.4	33.6		Eriksen, 2016
DEC (01.12.2017)	150	8.0	34.0		Walker, 2018
FEB (19.02.2018)	100	3.0	33.8		Walker, 2018
Vengsøyfjorden					
APR (06.04.1998)	134	3.5	34.0		Østrem, 2018

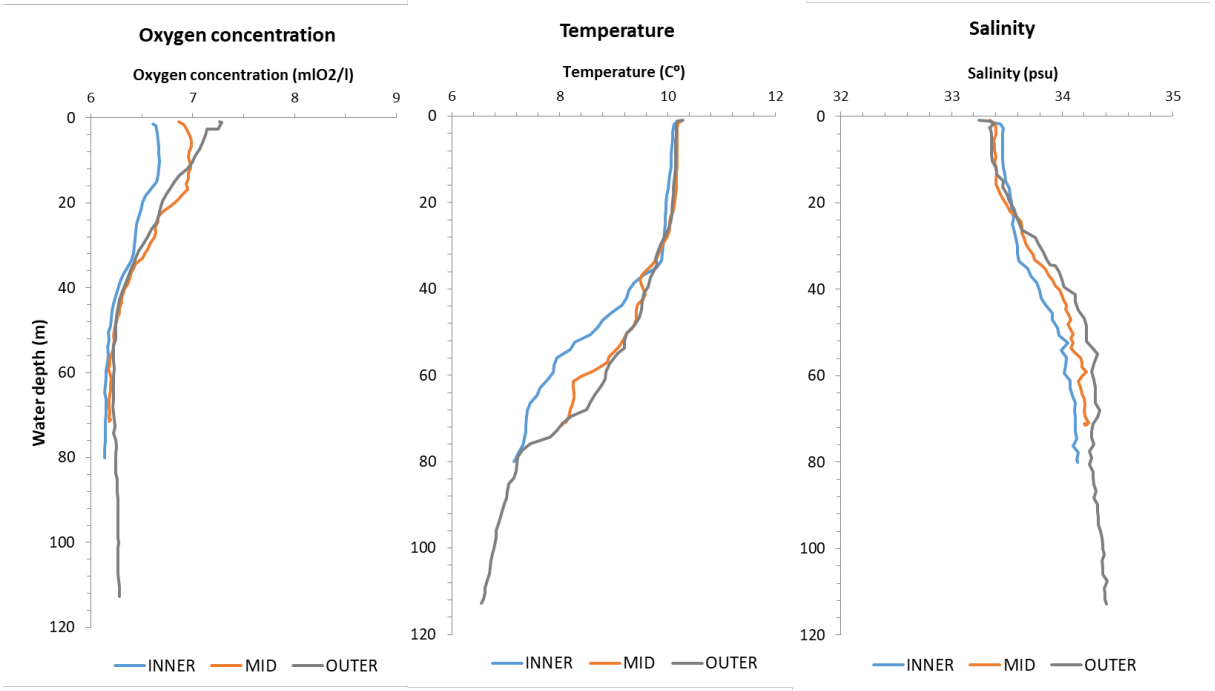

Figure 2.6: Oxygen (ml-O_2/L), temperature (°C) and salinity (psu) measured in the inner, mid and outer Kaldfjorden on a cruise in September 2017. OBS: data from the bottom waters at station INNER, MID and OUTER are missing.

Table 2-2: Position of CTD measurements, depth of CTD and actual water depth at the CTD-station.

CTD station name:	INNER	MID	OUTER
Position	69˚ 41'88 N, 18˚ 39'58 E	69˚ 46'57 N, 18˚ 40'09 E	69˚ 48'09 N, 18˚ 40'48 E
Depth CTD (m)	80	71	112
Actual depth at station (m)	111	140	236

The salinity in the surface water is lowest during the snow melt season in late spring. This, together with the higher surface temperature occurring in these months, causes a shallow strong pycnocline <20 m to be present in these months (Pedersen and Mikkola, 2001; Velvin et al., 2008). Many fjords have their major freshwater inputs at the head of the fjord that can drive a typical estuarine circulation. Estuarine circulation is driven by net transport of brackish surface water out of the fjord and with an underlying compensating current transporting water into the fjord (Syvitski et al., 1987). If fresh water runoff to Kaldfjorden is sufficient there could be a seasonal estuarine circulation during early spring. Increased bottom water salinities observed during early spring in northern Norwegian fjords indicate that there is usually a renewal of deep waters within fjord basins during this period (Wassmann et al., 1996). The pycnocline observed in early spring weakens and deepens during the summer. CTD measurements collected in September (Figure 2.6) indicate that the water masses are

generally homogeneous with little or no apparent stratification present in early autumn. A vertically unstratified water column during winter is common in northern Norwegian fjords and is partly due to limited fresh water runoff leaving the surface and salinity remaining high and stable (Mankettikkara, 2013; Wassmann et al, 1996; Wassmann et al., 2000). CTD profiles collected during winter months reveal that Kaldfjorden is weakly stratified during November and December and vertically unstratified during January and February, with full mixing in the water column (Mikkola et al., 2000; Walker, 2018). High winter surface water salinities of over 33.5 in Kaldfjorden (Walker, 2018) will prevent formation of ice cover in the fjord (Mankettikkara, 2013).

Available data reveal that there is no great variation in bottom water salinity in Kaldfjorden through the year, which varies between 33.6 psu and 34.8 psu (Table 2.1). There is a seasonal trend in bottom water temperatures. The lowest temperatures of ~3-4 ◦C occur in late winter to early spring, gradually increase and are highest at ~7-8 ◦C in late autumn- early winter (Table 2.1). Though high salinities occur in the deep water of Kaldfjorden they do not exceed 35 psu and therefore, strictly speaking, only Costal Water is present in the fjord. There is insufficient data to confirm the absence of Atlantic Water; however further research could confirm or refute this.

CTD profiles from Kaldfjorden show that oxygen saturation usually has a gradual decreasing trend with depth, and oxygen saturation in bottom waters varies between 70-95%. In one oxygen measurement performed in the inner Kaldfjorden in June by Velvin et al., 2008, a decline in oxygen saturation was observed in bottom waters where oxygen saturation levels dropped from 85% (at 80 m depth) to around 65% (100 m depth). This indicates that significant O_2 consumption can occur in the inner Kaldfjorden during summer. Because of limited oxygen data from areas further out in Kaldfjorden annual variations in oxygen saturation is unknown.

In those instances where measurements in the inner and outer fjord were performed on the same day (Table 2.1 and Figure 2.6), there is a slight indication that bottom water oxygen concentrations, salinity and temperature are higher in the outer Kaldfjorden compared to the inner fjord. The difference is small and the CTD measurements all point in the direction that the water masses within inner and outer Kaldfjorden are well mixed.

2.4 Wind and current system

The wind rose from Tromsø airport (Figure 2.7) show there are strong prevailing south and south-westerly winds in the area. The topography surrounding Kaldfjorden suggests that the valley at the head of Kaldfjorden could be funnelling the winds in a southerly to northerly direction along the fjord. The high mountains on the western and eastern side will assumedly shelter the fjord from westerly and easterly winds and amplify the funnelling effect on the southerly winds.

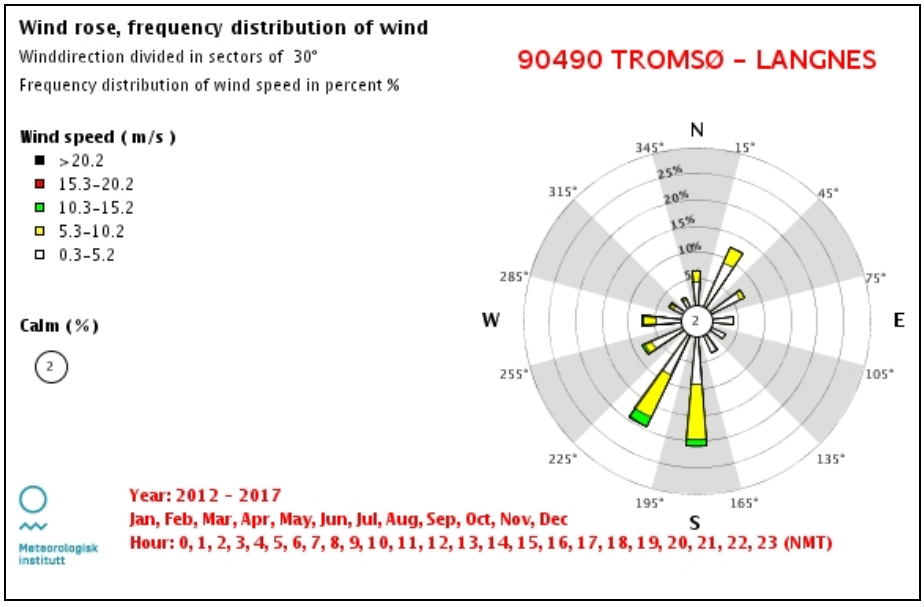

Figure 2.7: Wind rose showing the average wind direction and frequency of wind speed (%) in a 6 year period at the weather station at Tromsø airport (Metrological data gathered from eklima.no).

Measurements of the current conducted over a four-week period from February to March in the western outer Kaldfjorden show that the mean surface (0-5m) current speed was at 3.9 cm/s with a clear dominating northerly direction, transporting surface water towards the mouth of the fjord (Eriksen, 2016b). The mean current speed was similar in deeper water masses, but the main current direction showed a gradual change towards a southern direction (towards the head of the fjord) with increasing depth. Already at 15m depth the mean current direction was towards south. Although the mean current speed was 3.9 cm/s the maximum current observed at all depths was between 16 and 17 cm/s. This indicates that the current speed varies considerably. In waters below 5m depth a clear backflow towards the north was observed, which is likely caused by the tidal current (Eriksen, 2016). The tidal amplitude in Tromsø can be up to 4 meters (yr.no). Tidal currents can provide efficient flushing of the fjord basins and because of the high amplitude stagnant bottom waters in Northern Norway is

rarely recorded. Since any estuarine circulation is limited to seasonal fresh water input the strong southernly winds are likely to be the dominating contributor to transporting surface water north towards the mouth of the fjord.

2.5 Pollution history of Kaldfjorden

Aquaculture is the main industry operating in Kaldfjorden, and fish farms have been in the inner fjord since the early 1970s (Figure 2.8). Every fish farmer in Norway must have a license that provides permission both for the use of all production sites and for the Maximum Allowed Biomass (MAB). MAB states the maximum amount of fish (biomass), measured in tons, the fish farmer can have in the sea at once (Ministry of Fisheries, 2016). The MAB per license is 945 tons in Troms and Finnmark. Each production site, or fjord, can hold several MAB licenses. Kaldfjorden received the first MAB license in 1976 (Directorate of Fisheries, 2018b). Hansen, T. H., owner of Sjurelv Fiskeoppdrett (current company operating in Kaldfjorden), says that there was a small production active before 1976, but no permits were needed in the early 1970 and thus there is no available record of the production size before this year (personal communication, February 18, 2018). 1976 is therefore the date used as the beginning of fish farming in Kaldfjorden. In 2009 Sjurelv Fiskeoppdrett received its second MAB license. From 1976-2009 there was a maximum amount of 945tons, and from 2009 until today a maximum of 1890 tons of fish present in the open net pens at any time during the year. An estimate of 1,3 ton fish feed is needed for every ton fish produced (Svåsand et al., 2016). Following Brooks and Mahnken's (2003) estimates, it is reckoned when producing two MAB licences around 600 tons of fish feces and food spill is discharged into Kaldfjorden every year.

Sjurelv Fiskeoppdrett has owned the rights to farm in Kaldfjorden since 1984 and the company has relocated their farms several times. Figure 2.8 illustrates the location of the inactive and currently active fish farm localities. Sjurelv and Henrikvik, both located in the innermost part of Kaldfjorden, are the oldest localities. Sjurelv has been inactive since around 2001 and Henrikvik since around 2010. The three currently active fish farms are Kræmarvika (in operation since 1990), Rogndalen (since 1999) and Blåmansvik (since 2004). Rogndalen is the only farm located in the outer fjord and is the largest of the three farms with a total volume capacity of 24 000m^3 and can therefore hold ca. the total amount of the two MAB licenses. The two other active farms have a total volume capacity of 12 000 m^3.

The MAB can be distributed between the active farms, depending on the company's logistics on fallowing periods. Fallowing is the temporary retirement of a fish farm area. Its main purpose is to prevent negative environmental conditions beneath the fish farm which can again affect the farmed fishes health and also break any life cycles of parasites and diseases (Keeley et al., 2015). Data about in which year the single fish farms have had fish in them, and the total annual production for each year, are not available. We therefore don't know how concentrated or distributed the production has been in Kaldfjorden.

A factory and a sewage outlet located around the head of the fjord are two other potential pollution sources that have or currently are contributing to increased organic material supply to the fjord (Figure 2.8). The factory has hosted several companies but the only company that has had documented discharge of organic material was the shrimp factory, Tromsø Reker, that operated from ~1970 to ~2005. The factory had licence to discharge of processed water from the shrimp production into the innermost part of Kaldfjorden. The discharge from the factory was 50 000 p.e. (personal equivalent) (Mikkola et al., 2000). This unit is used to describe the pollution from organic rich waste-water. One p.e. expresses the amount of organic material that is decomposed by a biological oxygen demand measured over 5 days with 60g oxygen consumed per day (Sigvaldsen and Lindkjenn, 1992).

The sewage outlet was built in 1984 and discharges mechanically treated waste water into the fjord (Berg et al., 2009). The drain pipe discharges waste water about 170 m from land at 12 m water depth (discharge point indicated in Figure 2.8). The sewage outlet is connected to around 500 households, and waste water discharge is estimated to be around 500 p.e. (Berg et al., 2009). The sludge separator was operating in 2009, and is presumably still operating today.

Kaldfjorden is a popular fishing and whale watching spot, and because of this there is a lot of boat traffic in the fjord. The harbor situated in the inner fjord could potentially be a source of heavy metals related to anti-fouling impregnation usually used on boats.

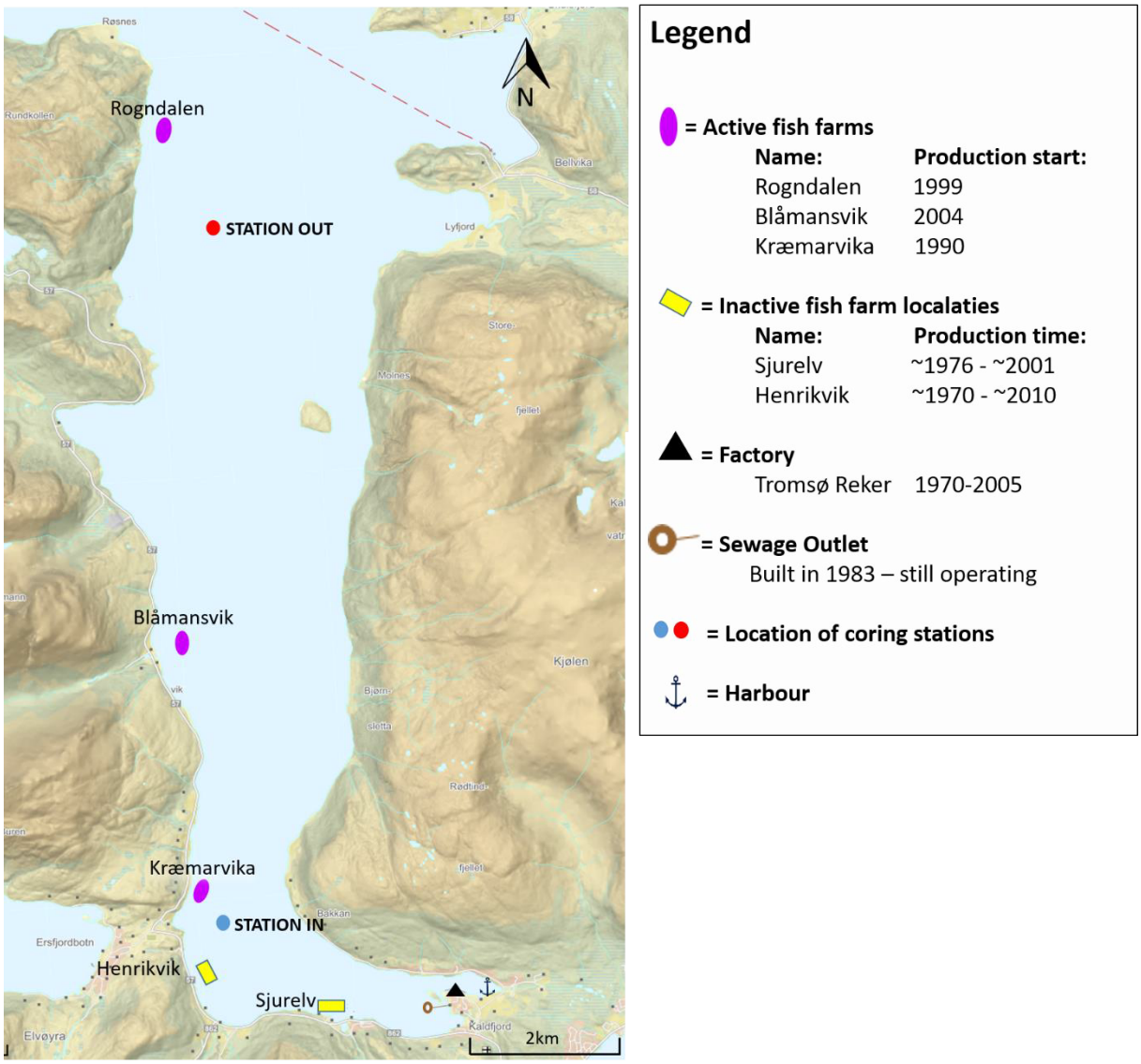

Figure 2.8: Map of Kaldfjorden including the placement of the active fish farms, inactive fish farms, factory location, sewage outlet, harbours and the placement of coring stations (background map from kartverket.no).

In addition to licenses, fish farmers in Norway are obliged to conduct regular environmental surveys (Modelling-Ongrowing fish-farm Monitoring, abbreviated MOM) in the recipient area of all active fish farms. The surveys are conducted in accordance with NS 9410:2016 (Norwegian standards for monitoring aquaculture operations), and the environmental conditions are classified according to standards set by The Norwegian Environmental Agency (Veileder M-608:2016). The classification system is based on numbering where 'high' EcoQs is given the classification 1, 'good' = 2, 'moderate'= 3, 'bad'= 4 and 'very bad' is classified with the number 5.

Previous environmental surveys conducted in Kaldfjorden in 2000 and 2008 reveals that sediment samples collected very close to our station IN (Figure 2.8) had high TOC content in

the surface sediments. In 2000 TOC content was highest and measured to be 38.3 mg/g and the diversity indices from same study revealed that the soft bottom fauna was classified within 1 (‘high’). In 2008 TOC content was reduced to 27,4 mg/g, but the diversity had reduced and was classified as 2 (‘good’) (Velvin et al., 2008). A MOM-survey conducted in spring 2012 revealed that sediments in the deeper part of the inner fjord (area close to station IN in Figure 2.8) still had high TOC content, but the diversity of soft bottom fauna was lower (Velvin and Worum, 2012). High abundance of a pollution tolerant polychaete worm was found, and the environmental conditions were classified as 3 (‘moderate’). However, the quantitative diversity indices from the same study showed values had classification 2 (‘good’) (Velvin and Worum, 2012). Heavy metal analysis preformed in the inner Kaldfjorden reveal that all metal concentrations were within class 1, except Hg concentrations that had concentrations classified as 2 (Velvin et al., 2008; Velvin and Worum, 2012)

The mentioned results found by previous environmental surveys only include results from close to our station IN. The area around the very innermost fjord, around the harbour, have previously been classified as 5. This innermost area of the fjord is documented to be heavily loaded with TOC with low diversity both in 2000, 2001 and 2008 (Mikkola et al., 2000; Pedersen and Mikkola, 2001; Velvin et al., 2008).

The reason that the two-inner fjord fish farm localities are now shut down could be due a combination of two reasons. Firstly, the already mentioned evidence that the inner Kaldfjorden area was enriched in organic material, and showed sign that it effected the ecological status. The second reason could be due to the massive herring school that appeared in Kaldfjorden in December 2012. The abundance of herring was so large that it depleted the oxygen saturation from 80–90% to 30% in short time, and killed 250 000 farmed salmon in inner Kaldfjorden (Tårnesvik, 2012). The herring school has appeared nearly every year since 2012 in Kaldfjorden (Walker, 2018). A multidisciplinary collaborative to understand the impact of these massive Winter Herring Abundance on the KaLdfjorden Environment (WHALE project) is currently being researched. Because of his event, and the convenient larger size, fish farm production in Kaldfjorden has been concentrated around Rogndalen since 2012.

Since pollution sources have been concentrated around the inner Kaldfjorden, there are fewer environmental surveys conducted in the outer fjord. MOM surveys conducted by Rogndalen

in 2011, 2013 and 2016 show that the environmental conditions beneath fish farm has been classified as 1 until 2016 when they were given a class 2 (Eriksen, 2016a).

3 Material and methods

3.1 Sample collections and preparations

The original plan was to collect one sediment core situated close to the fish farm Rogndalen and one from a control station with some distance from the fish farm. Station OUT, situated ca. 1 km south east of Rogndalen (location showed in Figure 2.1, 2.2 and 2.8), was therefore the original control station served as an example of a location presumably less affected from organic waste from the fish farm. Rogndalen fish farm is situated close to land, in a relatively shallow area of around 70m. The seabed surrounding the fish farm consisted of coarse shell-sand with several rocks which made coring difficult. After several unsuccessful deployments it was decided to change the coring location. Already having collected cores from a station in the outer fjord, collecting a core from the inner part of the fjord was decided to be an interesting contrast. The deepest part of inner Kaldfjorden was picked for the location of station IN.

No high-resolution bathymetry data of Kaldfjorden was available during the cruise and suitable soft bottom and flat seabed conditions were found by studying depth curve maps and by the use of an on-board echo sounder system. Overall, coring in Kaldfjorden was difficult and several deployments were unsuccessful.

The cruise was conducted as a part of the NFR founded ‘Jellyfarm’ project and all sediment samples used in this study were collected during a cruise from 4-8th of September 2017. The boat used was a local fishing vessel (Figure 3.1). Sediment cores from two sites were collected, one located in the outer part of the fjord (station OUT) and in the inner fjord (station IN) (Figure 2.1). At each site two replicate cores were collected and subsampled for further analyses (Table 3-1).

Figure 3.1 The vessel used to collect sediment cores in September 2017.

Table-3.1: Overview of sample sites, water depth, core length collected material with corresponding equipment and overview of analysis preformed. GC= Gemini Corer, BC= box corer

Station name	OUT	OUT	IN	IN
Replicate name	OUT-11	OUT-15	IN-B	IN-C
Position	69˚ 46'60N 18˚ 40'60E	69˚ 46'65N 18˚ 40'72E	69˚ 41'88N 18˚ 39'59E	
Water depth (m)	139	138	111	
Core length(cm)	23	16	17	17
Sampling equipment	GC	GC	BC	
Sediment dating		x		x
Particle size distribution		x		x
TOC/TN content		x	x	
Heavy metal concentrations		x	x	
Micropaleontological analysis		x		x

Sediment cores from station OUT were collected using a Gemini gravity corer. The Gemini corer has a set of twin cylinders each with an inner diameter of 8 cm (Figure 3.2A). When the two twin cylinders have descended into soft sediment, a lock is released and two flaps trap the sediment inside the cylinders. The core liners can therefore penetrate the sea floor with minimal disturbance of the sediments. The two replicate cores (OUT-11 and OUT-15) collected at station OUT were situated only a few meters apart and from similar water depths.

From station IN, sediment samples were collected with a box corer that collect a 1000 cm^2 section of undisturbed sediment from the sea floor. After retrieval, two small plastic core liners (4.7 cm inner diameter) were carefully pushed into the sediments confining an undisturbed sequence of the sediment within the cylinder. The procedure is illustrated in the

picture B in Figure 3.2. This method was used as a substitute for the Gemini corer, as this instrument was not available on the day of sampling. Only retrievals of Gemini and box cores with minimal disturbance of the surface sediments were accepted.

On board, all sediment cores were extruded with a piston and sub-sampled in 1 cm thick slices (Figure 3.2C). Slices were placed in plastic boxes and immediately stored in a freezer when back on land. After the cruise, the samples were transported frozen back to the University of Oslo (UiO).

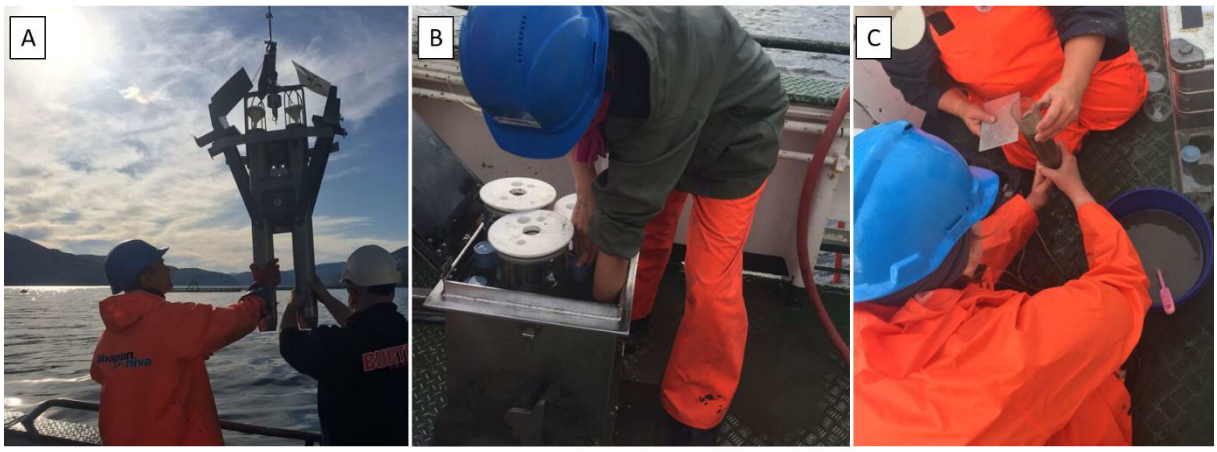

Figure 3.2. A: Picture of the Gemini Corer used. B: Example of subsampling from the box corer. Picture is not from sample collection at station IN. C: Illustration of the slicing of a sediment core retrieved from the box corer.

In the laboratory at UiO, the samples from all four cores were weighed in their wet (frozen) state before freeze-dried using a Christ Alpha 1-4LD plus and a Christ Alpha 1-4 freeze drier. The instrument removes the frozen water based on the physical phenomenon of sublimation, i.e. the direct conversion from solid to gaseous phase. Freeze-drying is a gentle process for drying products and removes water with minimal disturbance to the structure and porosity of the sediment. The water content was calculated by subtracting the dry weight from the frozen weight. Preserving the porosity of the dried sediment also simplified the later process of homogenizing the sediment samples.

Calculating the down-core water content was done as a first step to compare the similarities between the replicate cores. It also gives an indication about disturbances in the sediment record. The pseudo-replicates from station IN represented great consistency in their water content and further analyses were done on both cores. The surface of core OUT-11 was uneven and the surface sample therefore consisted of 0-2cm. In addition, one large and one smaller rock were present in the 2-5 cm section on OUT-11, which gave an aberration in the water content graph. For this study it is important to separate the top core sediments in

individual, undisturbed 1 cm slices, and it was therefore decided to do all further analysis on core OUT-15.

3.2 Sediment dating

Small samples (ca.7g) of dry sediment from each layer from the cores IN-C and OUT-15 were sent to the Environmental Radioactivity Laboratory at Liverpool University for geochronological dating. All samples were analysed for ^{210}Pb, ^{226}Ra and ^{137}Cs by direct gamma assay, using Ortec HPGe GWL series well-type coaxial low background intrinsic germanium detectors (Appleby et al. 1986). The laboratory report can be found in the Appendix A.

The relative short half life time (22.3 years) of ^{210}Pb, a natural radioactive isotope of lead, make it useful for dating recent sediments. ^{210}Pb is produced in the long ^{238}U decay series, and is the daughter nuclide of ^{226}Ra. Sediments are supplied with ^{210}Pb in two ways; supported ^{210}Pb (which is authigenic) and unsupported ^{10}Pb (which is derived from atmospheric fallout) (Appleby, 2001). It is assumed that the atmospheric influx of unsupported ^{210}Pb is constant over time at any given site, and that deposited ^{210}Pb is undisturbed (Appleby, 2001). By assuming supported ^{210}Pb activity is equal to the measured ^{226}Ra activity, the decay of unsupported lead isotopes activity is calculated by subtracting supported ^{210}Pb from the measured total ^{210}Pb activity (Appleby, 2018, appende A).

To validate the ^{210}Pb dating, an independent dating technique that looks at fallout peaks of the artificial radionuclide ^{137}Cs was used. ^{137}Cs is found in the sediment records due to the onset of atmospheric testing of high-yield thermonuclear weapons. ^{137}Cs reaches a peak in 1963, shortly after testing was banned (Appleby, 2001). The ^{137}Cs peaks of these known events can be used to calibrate the ^{210}Pb dating. When ^{210}Pb /^{226}Ra reach equilibrium, further dating of the sediments is no longer possible with this method and samples below this point can be extrapolated if necessary.

3.3 Particle size distribution

Particle size distribution analysis was carried out using a Beckman Coulter LS 320 laser diffraction analyser. The instrument can measure particles sizes between 0.04 and 2800µm.

Grains larger than 2000µm, which is the upper limit of sand, were sieved out. Dry sediments were well homogenized before a small fraction of the material (0.4-0.9 g) was extracted and mixed with a deflocculating agent Calgon ($NaPO_3$). The sample mixture was placed in a sonic bath where it was shaken for a minimum of 3 minutes. This procedure was applied to separate any aggregates in the sediment. After treatment the mixture with sediment was poured into the Beckman Coulter keeping the obscurity between 9-12% before starting the analysis.

The instrument measures the size distribution of all the particles suspended by using the principle of light scattering (LS 320 manual). The particles flow by a laser beam, each casting a shadow that corresponds to a size group. The cumulative percentage of each size group is calculated. The procedure and analysis was run twice for each sample and the average value was calculated.

In order to calculate the fraction within particles >63 µm that consisted of carbonate, an additional analysis was done to 8 sub-samples from each core. 0.5 g were first washed over a 63 µm sieve, dried and weighed again. The samples were then treated with 6M HCl which dissolves inorganic carbonate in the sediments. All samples were then rinsed, dried and weighted again to calculate the percentage of sand fraction that consisted of carbonate particles.

3.4 Total Organic Carbon(TOC) and Total Nitrogen (TN) content

For the analysis of total organic carbon (TOC) and total nitrogen (TN), sub-samples of approximately 0,5 g homogenized sediment were pulverized in an agate mortar and treated with 15 ml of 1M Hydrochloric Acid (HCl), which removes inorganic carbon. The mixture was placed in a shaker for 1 hour before being neutralized by three repetitions of centrifuging and rinsing with distilled water. Samples were dried at 50ºC overnight. Analyses were performed using a Flash EA 1112 NC Analyser at the Department of Biosciences, UiO. Two repetitions of the measurements were done for both cores to avoid inaccuracy in the results. The average of the measurements was calculated.

TOC content within each sediment sample was normalized to the sand content of the samples according to Veileder M-633:2016, using the equation 3.4.

$$TOC_{63} = TOC_{bulk} + 18.0*(1-F) \quad \textbf{(3.4)}$$

TOC_{bulk} = measured content organic carbon (mg/g)

F= fraction of particles smaller than 63µm

The C/N ratio was calculated by dividing the carbon content by the nitrogen content.

3.5 Heavy metal concentrations

Approximately 1g of dry sediment from each sample was pulverized and put in teflon containers and after weighed with high precision where the weight was noted. 20ml nitric acid (7M HNO_3) was added to each sample and the mixture was shaken for about an hour before being placed in an autoclave. Samples were heated under 200kPa (corresponding to 120°C) for 1 hour. The autoclave enables the acid to reach high temperatures and absorb any metals in the sediments without boiling or evaporating. 0.02 ml of the acid with dissolved metals was extracted, placed in separate containers and diluted 50 times with 1M HNO_3. The diluted samples were then analysed for chromium (Cr), copper (Cu), zinc (Zn), cadmium (Cd) and lead (Pb) using a Multicollector- ICPMS. Analysis for heavy metals was preformed according to Norwegian Standard (NS477/1994) and Veileder M-608:2016 was used to identify the EcoQs of the concentrations.

3.6 Micropaleontological analysis

Subsamples used for micropaleontological analyses were selected from every 3rd core sample in both cores. Additional subsamples from core intervals of interest were also selected and analysed.

A small sample (ca. 2 g) of homogenized dry sediment was accurately weighed before gently wet sieved through a 500 µm and 63 µm sieve. The 63 µm sieve size was used in as recommended for ecological studies in benthic foraminifera (Veileder M-633, 2016; Murray 2001). The 500 µm sieve was used to avoid the largest sediment particles. The 63-500 µm samples were dried at 50°C, and again weighed.

A small subsample from the fraction 63-500µm of the selected samples was evenly distributed on a faunal slide and foraminiferal tests were picked under a binocular microscope. Typically, >300 individuals were picked from each sample. The individuals were

identified to species level and counted. Weights of all picked and unpicked samples were noted. The counts are listed in Appendix C.

The absolute abundance was normalized to the dry weight of the sediment and expressed as individuals/g (ind/g). Benthic Foraminiferal Accumulation Rates (BFAR) (ind/cm^2 /year) were calculated following Herguera (1992). BRAR is based on calculated sediment accumulation rates (SAR) from core dating and concentration of benthic foraminifera (ind/g).

The diversity indices $H_{(log2)}$ (Shannon & Weaver, 1964) and ES_{100} (Hulbert, 1971) were calculated using the data program PRIMER (Plymouth Routines In Multivariate Ecological Research) version 6.1.13. These are the two most common measures of diversity and the results are used to classify the Ecological Quality Status (EcoQs) by comparing the numbers with classifications defined by Veileder M-633:2016. Both indices were calculated as their approach is different and they can give varying results.

PRIMER was also used to calculate the resemblance among all picked samples. The resemblance between samples were based on Bray-Curtis similarity coefficient (Roger Bray and Curtis, 1957). In PRIMER all samples were √-transformed before the resemblance analysis. Multi-Dimensional Scaling (MDS) plots were created in PRIMER to show the relative abundance of selected species in each core.

4 Results

Table 4-1 give an overview of classification intervals for marine sediment used to classify the ecological status of the sediment. Raw data for all results can be found in the Appendices (A-C).

Table 4-1: EcoQs classification intervals for foraminifera and heavy metal concentrations (mg/kg) in marine sediments. Heavy metal concentrations indicated by Veileder M-608:2016. Diversity indices based on H' and ES(100) for foraminifera in coastal marine environments indicated by Veileder M-633:2016.

EcoQS	Unit	Background	Good	Moderate	Poor	Bad
Heavy metals						
Cadmium (Cd)	(mg/kg)	<0.2	0.2-2.5	2.5-16	16-157	>157
Chromium (Cr)	(mg/kg)	<60	60-660	660-6000	6000-15500	>15500
Copper (Cu)	(mg/kg)	<20	20-84	-	84-147	>147
Lead (Pb)	(mg/kg)	<25	25-150	150-1480	1480-2000	>2000
Zink (Zn)	(mg/kg)	<90	90-139	139-750	750-6690	>6690
Diversity indices						
H'		5.0 – 3.4	3.4 -2.4	2.4 - 1,8	1.8 – 1.2	1.2 - 0
ES(100)		35 - 18	18 - 13	13 - 11	11 - 9	9 - 0

4.1 Core description and water content

4.1.1 Station IN

The two pseudo replicate samples from the box core both consisted of homogeneous dark grey sediment. There was no clear visible colour change up core. Surfaces were even and undisturbed and small shell fragments were abundant throughout the cores. The lower 5 cm of the cores consisted of compacted sediment with an average water content of 40% (Figure 4.1A). The sediment gradually became softer, less sticky and easier to slice up-core. The water content of both replicates had a steady continuous increase from 40% toward 63% calculated in the 1-2 cm section. The surface sample was loose and watery with a water content between 67% (in core IN-B) and 73% (core IN-C).

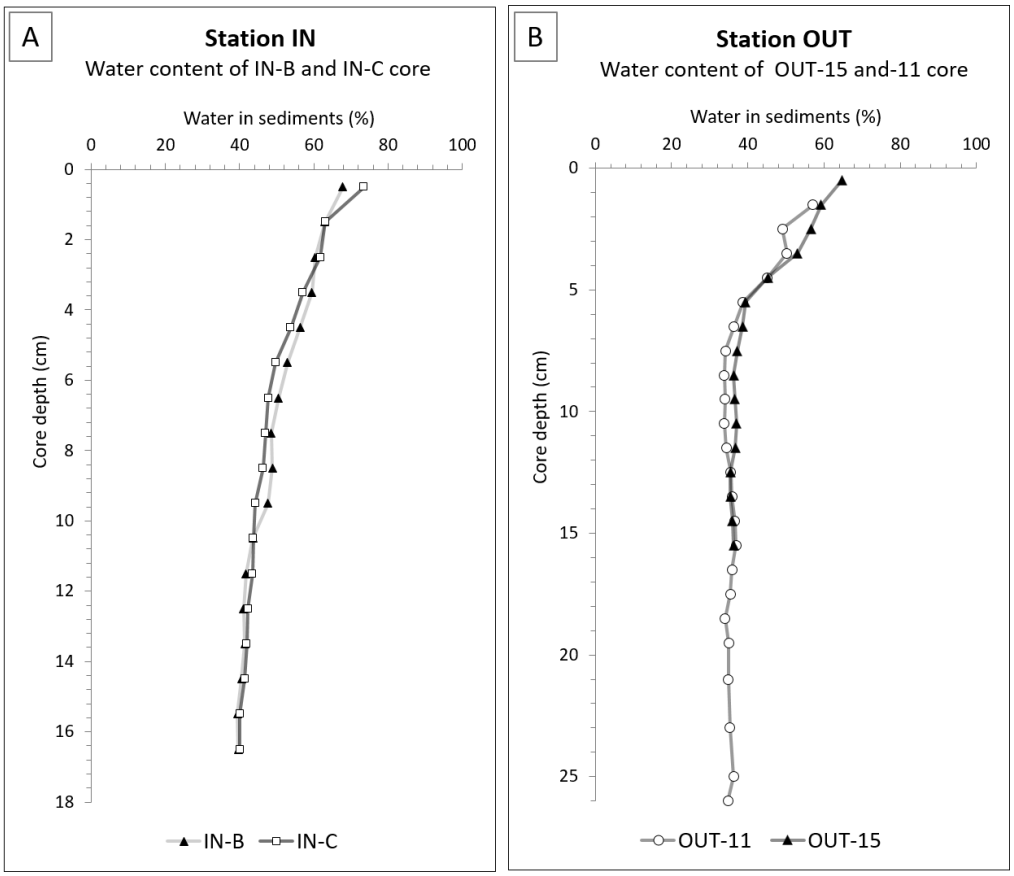

Figure 4.1: A: Water content (%) of both replicate cores collected from box core sediments at station IN (IN-B and IN-C core) **B:** Water content (%) of both replicate cores collected with the Gemini corer at station OUT (OUT-11 and OUT-15 core).

4.1.2 Station OUT

The two replicates collected from Station OUT had similar sediment characteristics to each other. Sediments in the lower part of the cores consisted of compacted light grey mud. At 15-14 cm core depth a few small pockets/streaks of browner sediment became visible, and the frequency of these pockets increased up core. From 6 cm to the surface, only the brown sediment, with higher abundance of shell fragments, was visible. The transition from the compacted light grey to the browner sediments was evident while sub-slicing the core as illustrated in Figure 4.2. What could be traces of small (~1-2 mm in diameter) burrowing holes were seen in both cores.

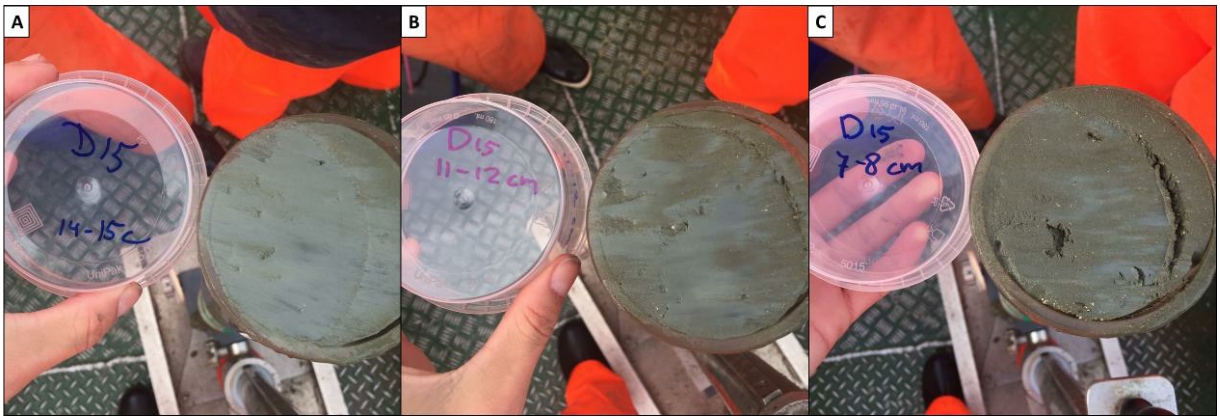

Figure 4.2: Pictures of the OUT-15 core sediments under slicing. **A:** Sediments at 14 cm core depth. **B:** Sediments at 11 cm core depth. **C:** Sediments at 7cm cored depth.

From the lowest part to 8 cm core depth, water content was relatively stable ranging between 34-36% for both cores (Figure 4.1B). The brown upper layers were less compacted and had a higher water content. Water content increased from 38% at 6 cm to 64% in the surface layer.

4.2 Core dating and Sediment Accumulation Rate (SAR)

4.2.1 Station IN

The Environmental Radioactivity Centre at the University of Liverpool could date the IN-C core down to 12 cm core depth. In the 11-12 cm sample the ^{210}Pb activity reached equilibrium with the supporting ^{226}Ra and this lowest sample was dated to 1900 (117 (± 9) years old) (Figure 4.3). Below this depth dating was not possible and the age differences between the two lowermost dated samples were used to extrapolate the dating for the rest of the core. All extrapolated dated core depths are marked with an asterisk (*) at the end of calculated date. The ^{137}Cs concentrations had a well-defined peak in the 6-7 cm sample (Figure 4.4A), which most probably can be linked to the peak levels of atmospheric fallout around 1963. ^{210}Pb dating place 1963 at a core depth of about 7cm, which is in good agreement with the ^{137}Cs record. The year 1976, which marks the start of fish farming in Kaldfjorden, is set to a core depth of 5.7 cm and marked with a red dotted line in figure 4.3 and 4.5.

The unsupported ^{210}Pb activity declined relatively uniformly with depth in sediments below 4 cm core depth (Figure 4.4B). Above 4 cm there was observed a reduced gradient which may indicate a recent increase in sediment accumulation rate (SAR) (Appleby and Piliposian, 2018). The trend of the up-core SAR at station IN is illustrated in figure 4.5. The mean

sedimentation rate of sediments below the 6-7 sample (~1967) section were calculated to be 0.059 (± 0.006) g/cm^2/year. Above 6 cm there is a small increase to 0.062 (±0.005) g/cm^2/year, which is stable up to 4.5 cm (~1989). In samples younger than 1989 a significant increase in SAR occurs in all samples towards the surface of the core. The average sedimentation rate in the upper 4 cm is calculated to be 0.0077 (±0.004) g/cm^2/year. The full laboratory report on sediment chronology and SAR is presented in Appendix A.

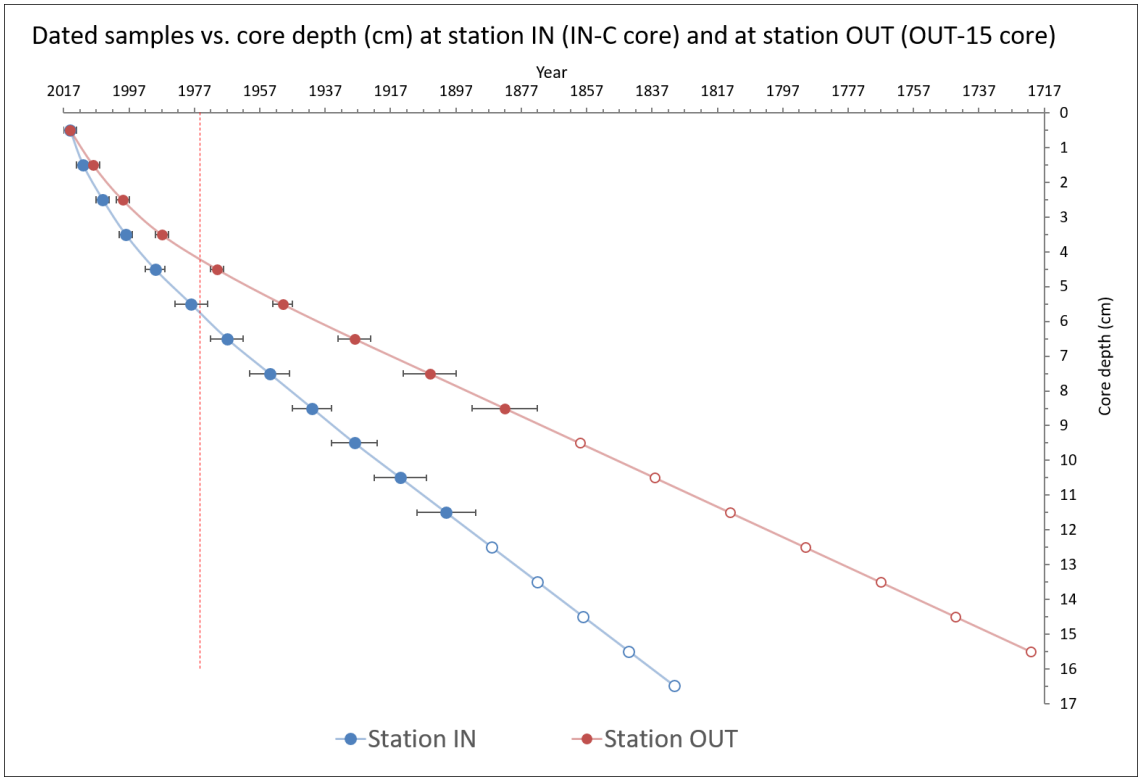

Figure 4.3. Age model of dated core samples. Extrapolated core depths are indicated with unshaded markers. Note that the error margins increase downcore. Results from station IN (IN-C core) is marked with blue, and at station OUT (OUT-15 core) is marked with red. Vertical red dotted line marks approximately the year 1976.

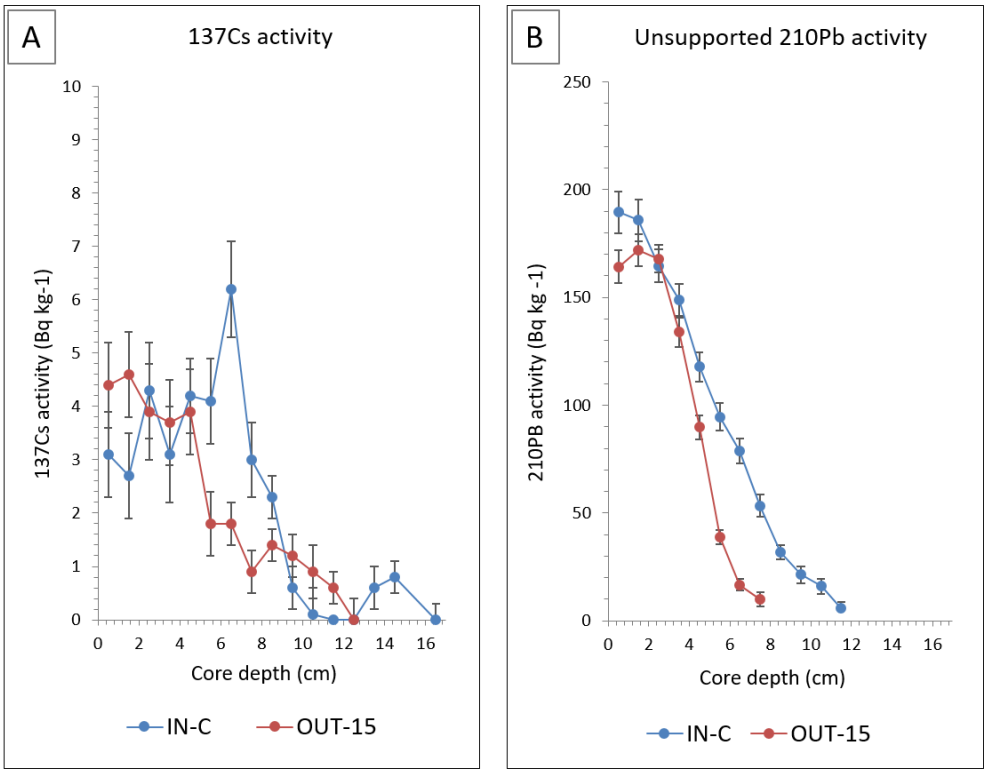

Figure 4.4: A: The ^{137}Cs activity vs. core depth of IN-C core (blue) and OUT-15 core (red). **B:** The unsupported ^{210}Pb activity vs. core depth of IN-C (blue) and OUT-15 core (red).

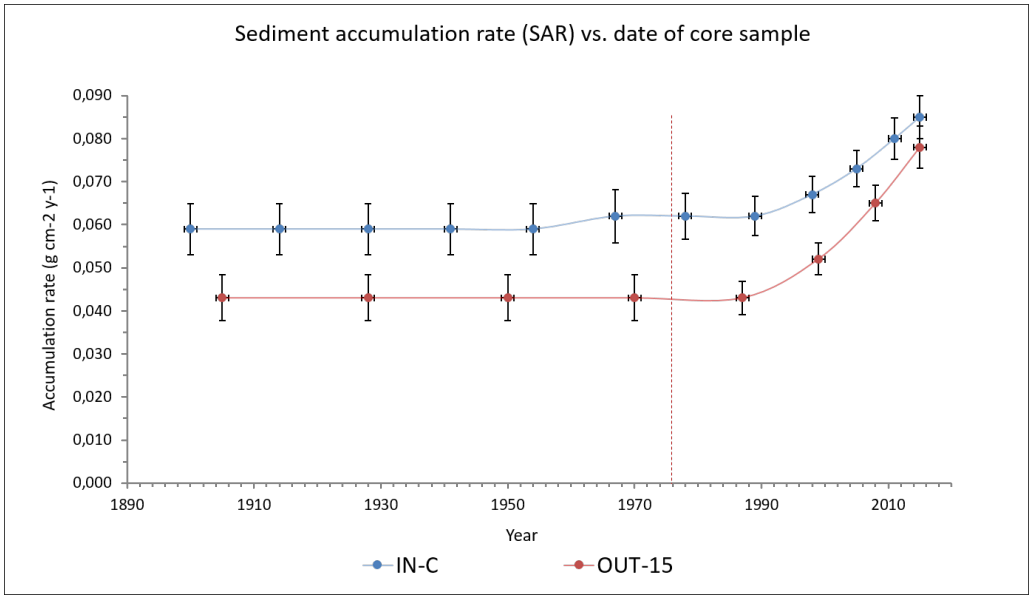

Figure 4.5: SAR vs. the dated core sample from each station. Station IN (IN-C core) is marked with blue line, and SAR at station OUT (OUT-15 core) is marked with red line. The red stippled line marks the year 1976.

4.2.2 Station OUT

In the OUT-15 core the ^{210}Pb/^{226}Ra equilibrium was reached in the 7-8 cm sample (Figure 4.3), substantially shallower than in the core from station IN. This lowest dated sample

(7.5cm) was dated to the year 1905 (112 (±10) years old). All core samples below 1905 are extrapolated and indicated with an asterisk (*). The ^{137}Cs record (Figure 4.4A) did not have a defined peak, but show a sharp increase to higher activity in the upper 5 cm, which indicate that these are post 1963 sediments. The ^{210}Pb dating places 1963 within the 4-5 cm sample, which is in good agreement with what the ^{137}Cs record suggests.

The unsupported ^{210}Pb record (Figure 4.4B) had a steep increase from core bottom up to 3.5 cm (1987) core depth, suggesting a slow but uniform sedimentation rate in this interval. Samples up to ~1987 had a mean sedimentation rate of 0.043±0.005 g/cm^2/year (Figure 4.5). In the upper 3 cm of the core (~1987 to 2015), the unsupported ^{210}Pb activity was virtually constant, indicating an increase in the sedimentation rate (Appleby and Piliposian, 2018, Appendix A). The increased sedimentation rate in the upper core centimetres had a mean value of 0.068 ±.,004 g/cm^2/y. When comparing the SAR to the dating of the core (Figure 4.5) it is evident that the sharp increase in SAR occurs around the same time at both stations (~1985-1990).

4.3 Particle size distribution

4.3.1 Station IN

There is a gradual fining-upward sequence in grain size from the bottom of the core towards surface sediments with some minor fluctuations (Figure 4.6A). The average sand content throughout the core was 33.3 %. Highest sand content (38.8%) was measured in the bottom core sample, and the lowest sand content (24.6 %) was measured in the surface sample (Figure 4.6A). The clay content remained relatively constant at 3-4 % throughout the core whereas the silt content increased up core, in response to the declining sand content. From the bottom core sample and up to 3cm (~2005) the sediment samples show similar grain size distribution (Figure 4.7), with the peak clearly centred around 80 µm particle size. In the upper 3cm of the core, marked with yellow in Figure 4.7, there was a transition to finer grain distribution, where the peak of the curve flattened out between 15 to 61 µm mean particle size.

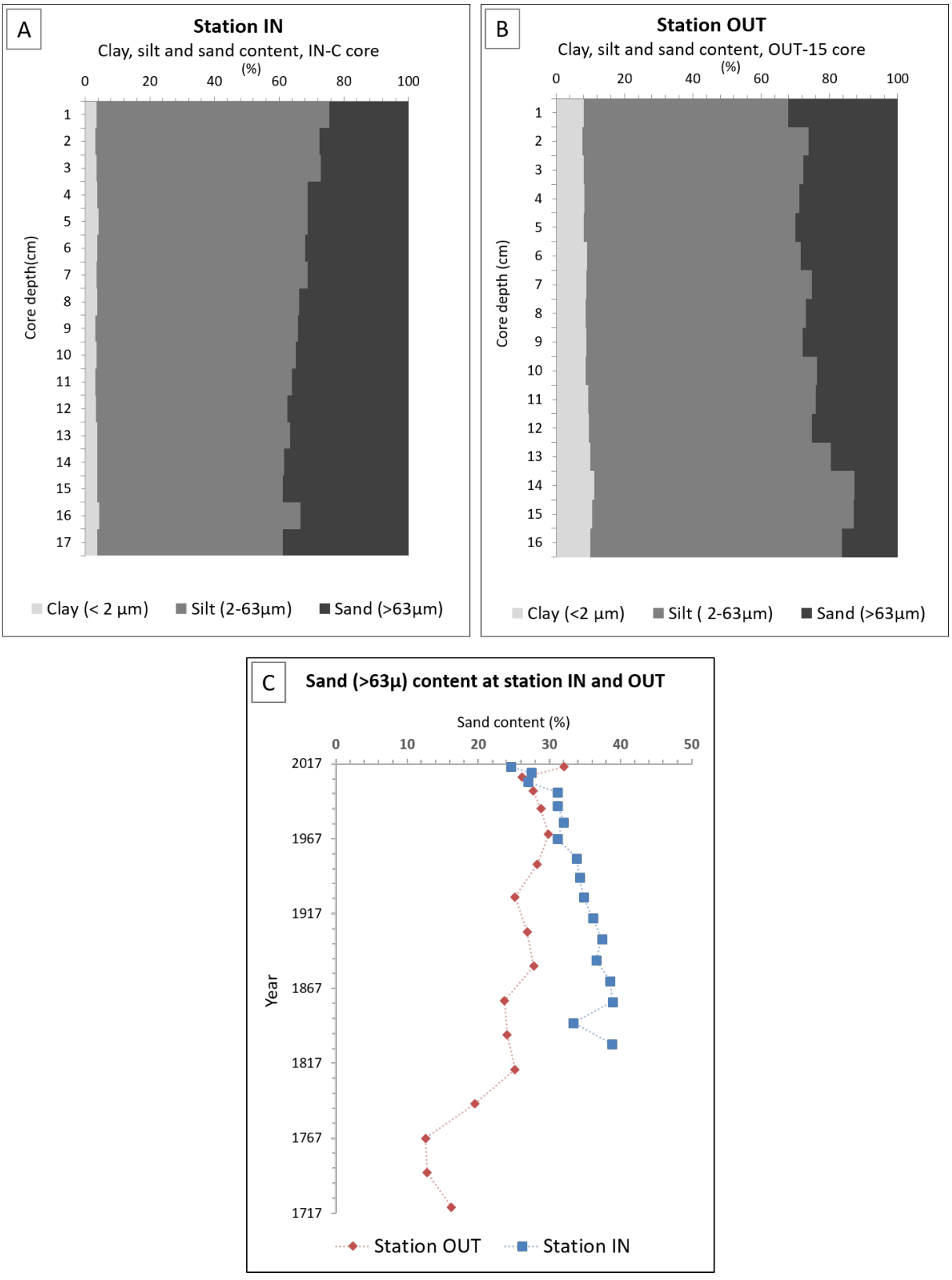

Figure 4.6: Percentage of particles within fraction of clay, silt and sand. **A:** Results from station IN. % of particles within clay (light grey), silt (grey) or sand (dark grey) vs. core depth (cm) **B:** Results from station OUT. % of particles of clay, silt and sand vs. core depth (cm). **C:** % of sand fraction from both cores vs. dated year of the core samples.

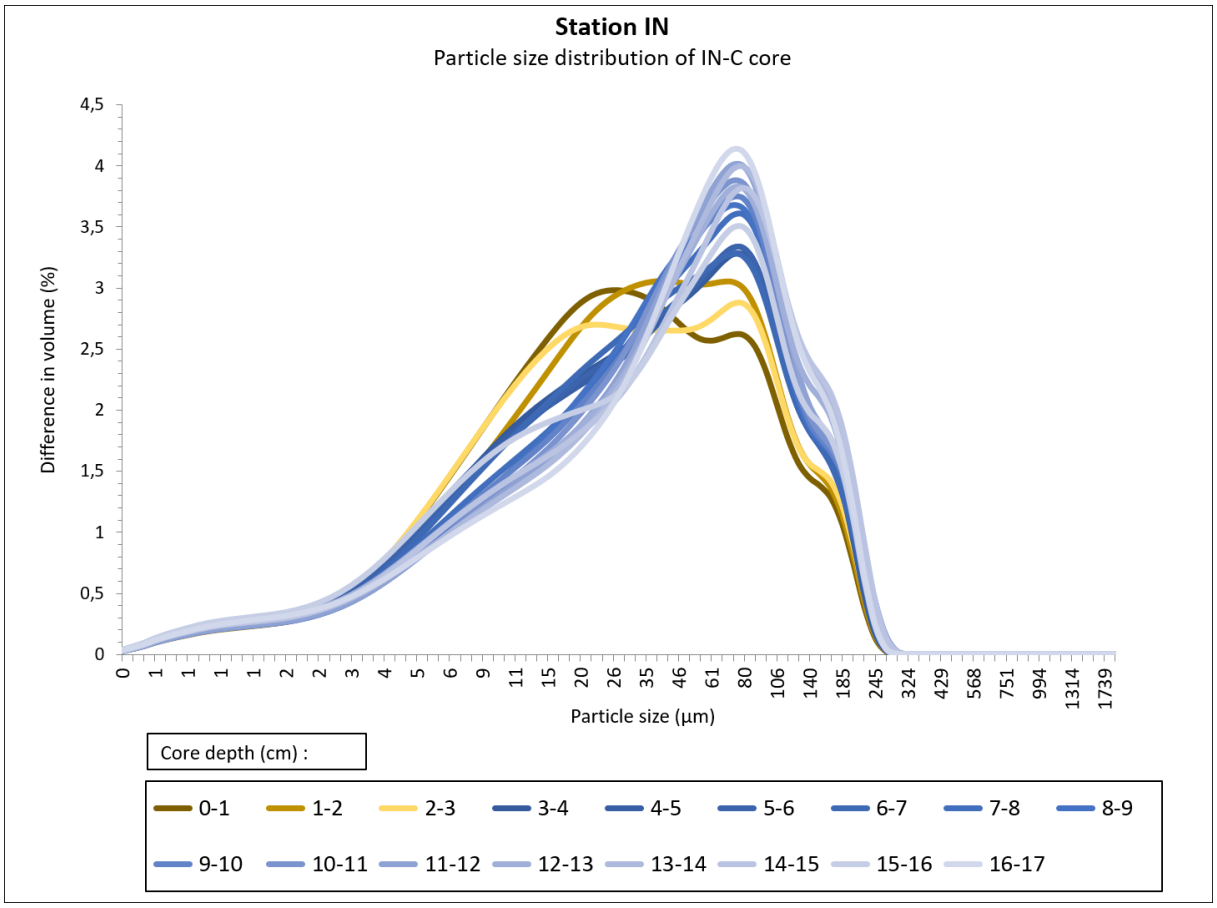

Figure 4.7: Differential volume of the complete grain size range of core IN-C from station IN.

4.3.2 Station OUT

From the grain size distribution diagram (Figure 4.8) a shift towards coarser mean particle size was observed at 12 cm core depth. The transition from smaller mean particle size (peak at 18 µm) in the bottom core to larger particle sizes (peak at 90 µm) is illustrated with the change in colour from purple to green (Figure 4.8). The average sand content below 12 cm core depth was 15% and above 12 cm the sand content gradually increased, averaging at 27% (Figure 4.6B). Little change in the clay content was observed. From the bottom of the core to 12 cm the mean clay content was about 10.5%. Above 12 cm the clay content was reduced to an average 8.5% (Figure 4.6B).

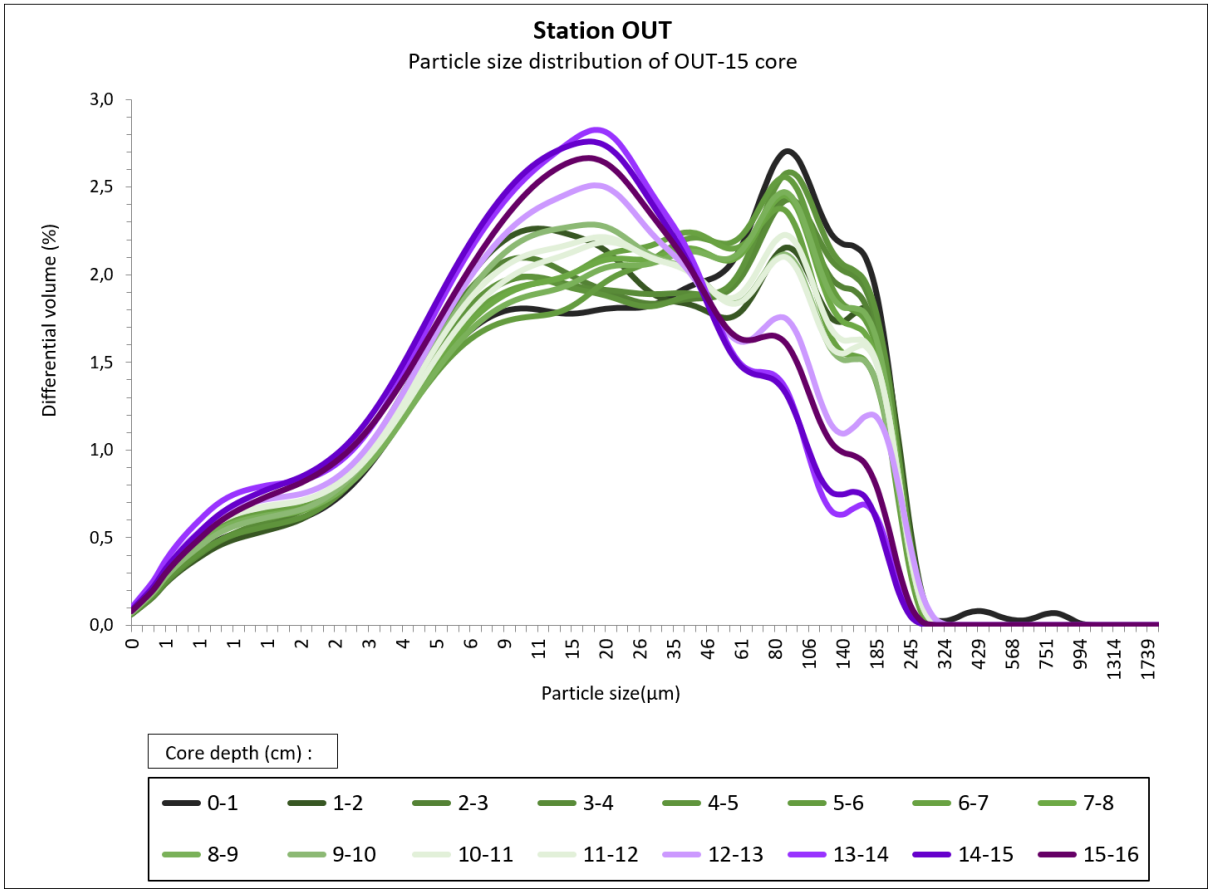

Figure 4.8: Differential volume of the complete grain size range of core OUT-15 from station OUT.

4.4 Total organic carbon (TOC) and nitrogen (TN) content

4.4.1 Station IN

There is a good correlation between the TOC and TN concentrations and accumulation rates up core (Figure 4.9). All TOC values presented are normalized and corrected to the sand fraction. The deviation between the two replicate analyses is marked with error bars in Figure 4.9A and are mostly low. Overall there is a general increasing trend in TOC and TN concentration throughout the whole core, but a more rapid and stable increase is observed in sediments above 6.5 cm (1967). The highest TOC concentration is measured in the 1-2cm (2011) sample with 3.85% TOC content. In the surface sample (2015) the concentration is slightly reduced to 3.82% TOC content. The TN concentration show the same trend and decreases from 0.36% TN in 2001 to 0.35% TN in 2015.

Between the lowest core depth and the 1900 dated sample (11-12 cm core depth) the average TOC accumulation rate was 13.3 g C/m^2/year (Figure 4.9B). From 1900 to 1967 the accumulation rate had some fluctuations with two peaks at 9.5 cm (1926) and 7.5 cm (1954) core depth. The TOC accumulation rate between 1900 to 1967 was on average a little higher at 15.0 g C/m^2/year. From 1967 (6.5 cm) and towards the top of the core (2015) the TOC accumulation rate increases much more rapidly. The TOC accumulation rate progressively increased from 17.0 to 32.5 g C/m^2/year from 1967 to 2015. The average rate in this period was 25.6 g C/m^2/year.

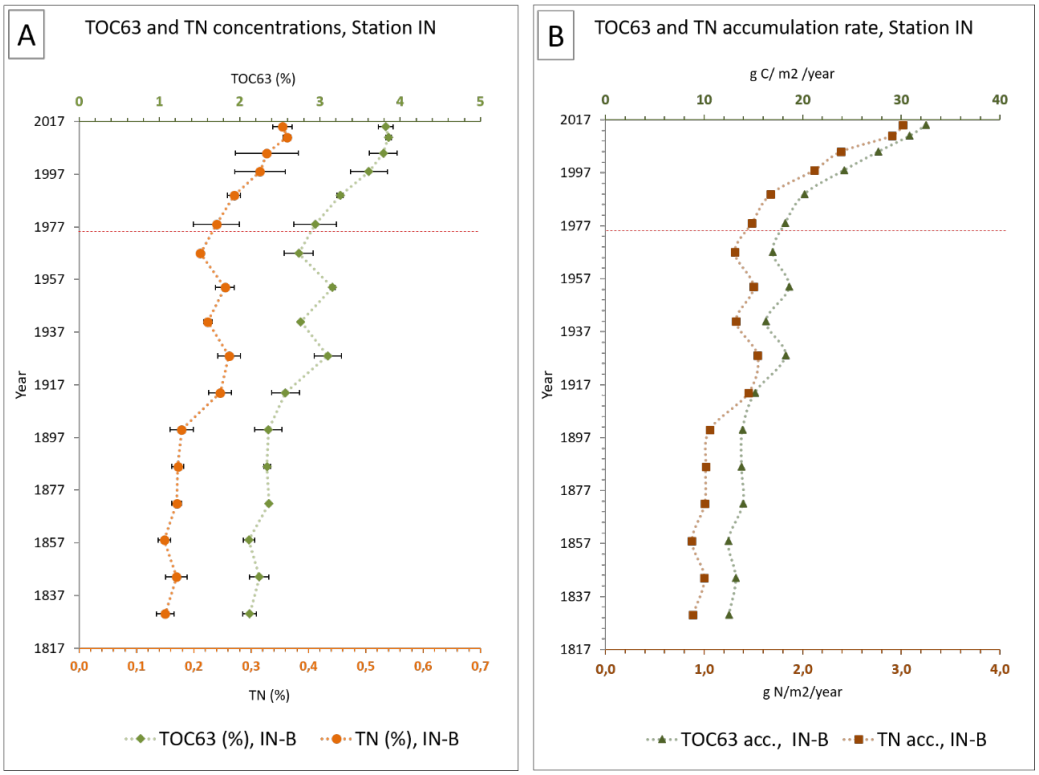

Figure 4.9: A: The IN-B-core measured TOC_{63} and TN concentrations in percent (%). Deviation between the two sets of measurements is indicated with error bars. **B**: The IN-B-core calculated TOC_{63} and TN accumulation rate in g/m^2/year. The red stippled line marks the year 1976.

4.4.2 Station OUT

The concentration and accumulation rate of TOC and TN in the graphs in Figure 4.10 illustrate the close correlation between the up-core trend between the TOC and TN analysis. The three bottom core samples (from 1721* to 1767*) have a stable TOC and TN content (Figure 4.10A). In this period the TOC concentration is 0.8% and TN concentration is 0.08%. From 1767* (13.5 cm core depth) and up through the whole core both TOC and TN concentration increases but with a much sharper increase in the samples above 5.5 cm (post-

1950 samples). The 1-2 cm core sample (2008) had the highest TOC concentration with 3.85% TOC. The highest TN concentration was measured in the surface sample with 0.41% TN content.

The TOC accumulation rate has a slow and steady increase in the pre-1950 samples (Figure 4.10B). TOC accumulation rate is stable at 3.6 g C/m^2/year in the three bottom-core samples, and the rate steadily increases towards 10.9 g C/m^2/year calculated in the 1950 sample. Average TOC accumulation rate for pre-1900 sediments is 5.6 g C/m^2/year, and average TOC accumulation rate between 1900 and 1950 is 9.7 g C/m^2/year. From 1950 to 1970 there is observed a sharp increase in accumulation rate. The deviation in the concentration between the two separate analyses illustrated in figure 4.10A indicate that there are some uncertainties whether this shift happened quick or more gradual. However, results from post-1970 samples have much lower deviation between the two analyses, and all together the TOC accumulation rate increased from 10.9 – 29.6 g C/m^2/year between 1950 and 2015. Average post-1950 TOC accumulation rate is 18.9 g C/m2/year, and therefore the accumulation rate has more than tripled since pre-1950 samples.

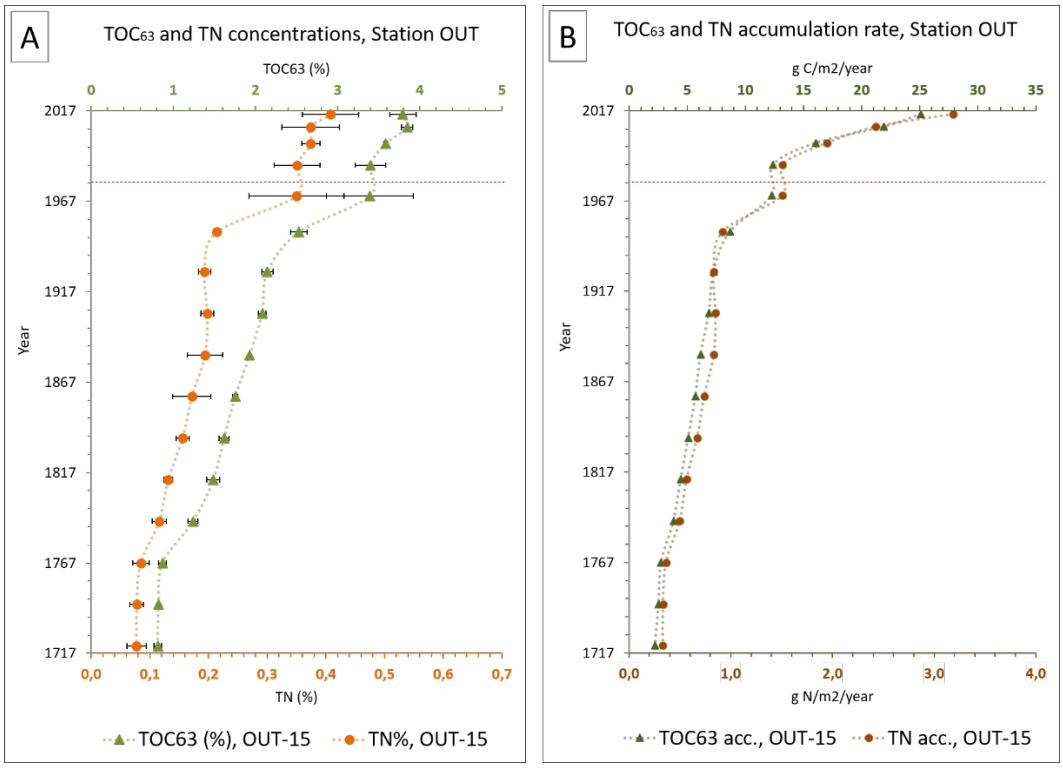

Figure 4.10: **A:** OUT-15-core TOC_{63} and TN concentration in percent (%). Deviation between the two sets of measurements is indicated with error bars. **B:** The OUT-15-core calculated TOC_{63} and TN accumulation rate in g/m^2/year.

4.5 C/N ratio

The TN and TOC concentrations show very high correlation both at station IN and OUT and therefore not a lot of variation in the up-core C/N ratio occurs (Figure 4.11). The up-core C/N ratio is stable at both stations with an average ratio of 9.6 at station IN and a little lower ratio at station OUT which averages of 8.0. The error margins between the two sets of analyses for each core can explain the quick reduction in the C/N ratio observed in the 1900-sample at station IN.

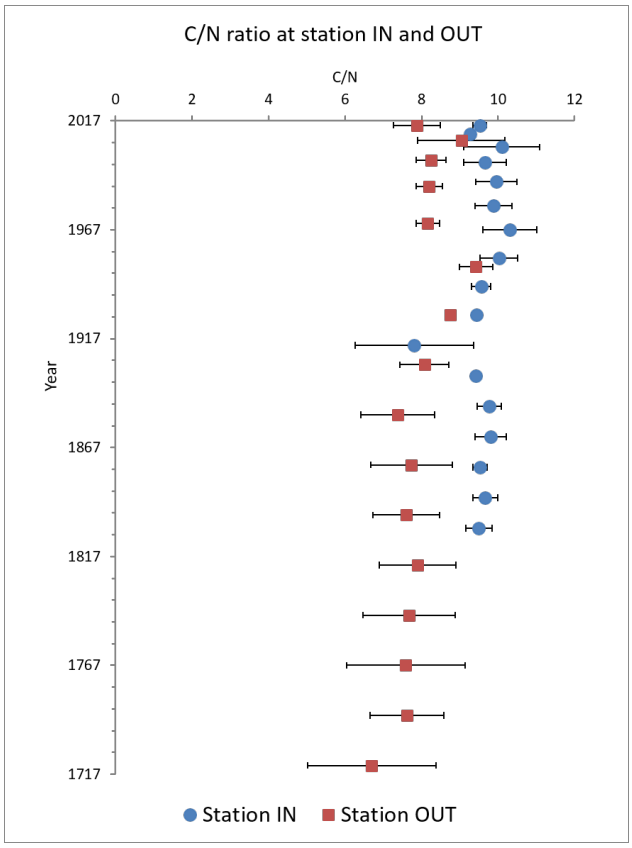

Figure 4.11: The C/N ratio at Station IN (blue) and Station OUT (red). The deviation between the two sets of analysis is illustrated with error bars.

4.6 Heavy metal concentrations

4.6.1 Station IN

As shown in Figure 4.12 the concentrations for all analysed heavy metals were well within 'good' or 'high' EcoQs. There is little change in concentration levels up-core. The concentration of Cu and Zn have a minor increase between 6.5 and 3.5 cm core depth where

the concentrations of these metal cross the limit between ‘high’ and ‘good’ EcoQs. From 3.5 cm to the surface sediments, the concentrations of Cu and Zn declines. Cr, Pb and Cd show very little variation in concentrations up-core. The exact quantities of Hg could not be measured with the ICP-MS and the results are therefore semi-quantitative measurements. However, the trendline of the Hg concentration indicates that there has been an increase in the concentration above 12 cm (~1900). Because the concentration of all heavy metals was far from the ‘moderate’ EcoQs classification, the accumulation rates were not calculated.

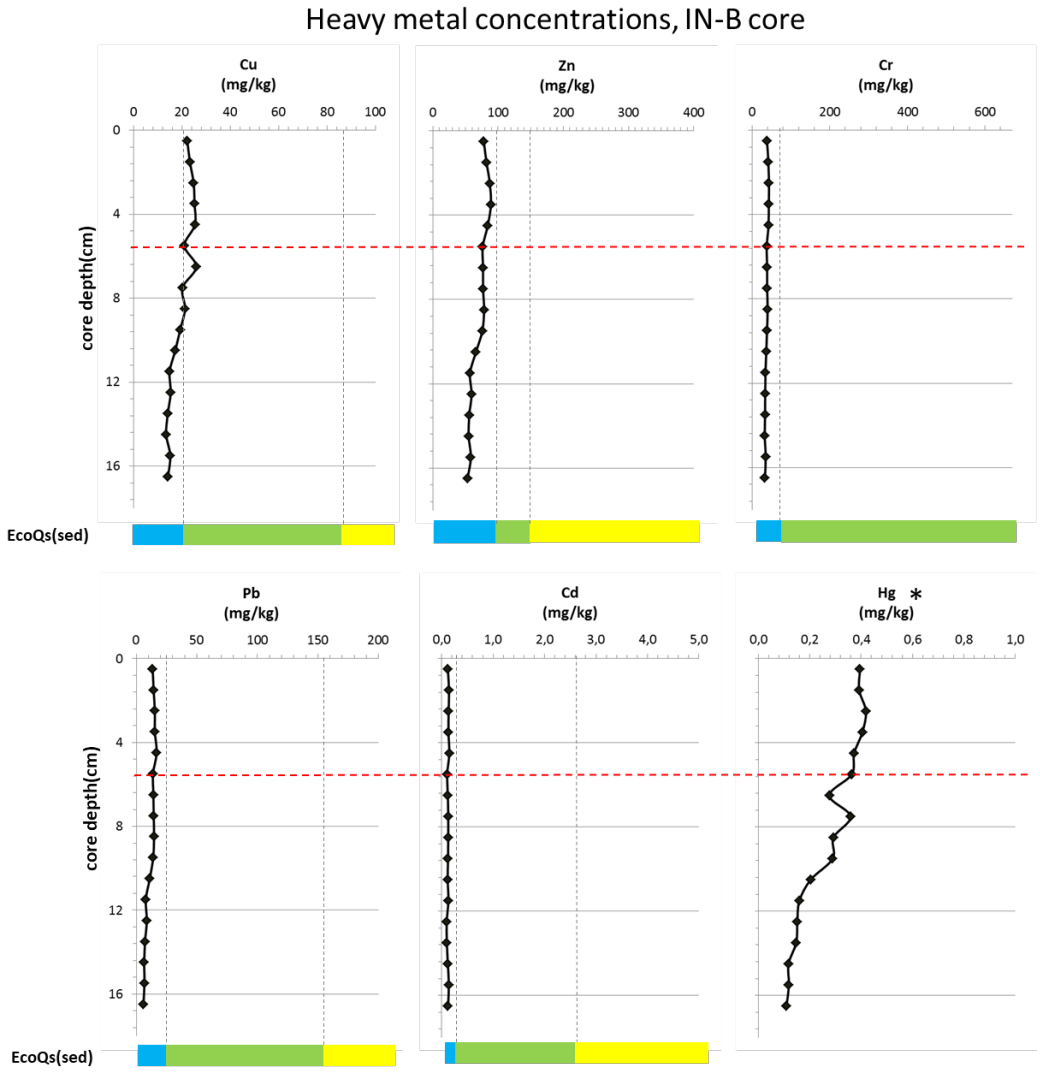

Figure 4.12: Down core concentrations of heavy metals from IN-B-core with corresponding environmental classification, EcoQs, as defined by Veileder M-608:2016 are indicated by corresponding colours. Semi-quantitative measurements for Hg* do not necessarily give the correct concentration, and the EcoQs can therefore not be used. The red dashed line marks the core depth dated to 1976.

4.6.2 Station OUT

All heavy metal concentrations fall within “high” or “good” EcoQs (Figure 4.13). The concentration for Cu, Zn and Cr all show a decreasing trend up core and have concentrations within “good” EcoQs in the lower core, and gradually increase and are within “high” EcoQs in the upper part of the core. Pb concentration has a very minor increase between 6 and 8cm but all concentrations are well within “high” EcoQs. There is virtually no up-core change in Cd concentrations. The semi-quantitative Hg concentrations show an increasing trend in from 8 cm (~1900) towards 4cm (~1976) where above this the concentrations fluctuates towards surface sediments.

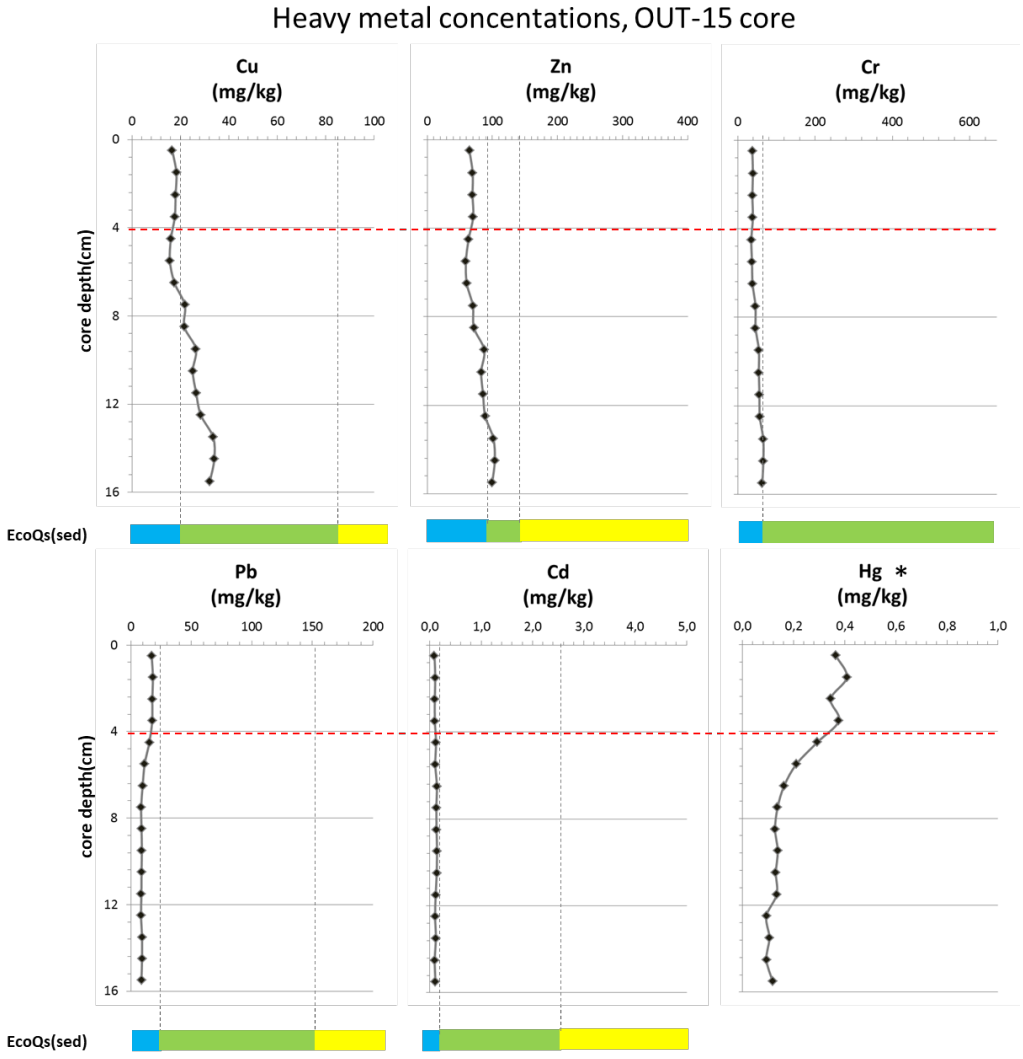

Figure 4.13: Down core concentrations of heavy metals from OUT-15-core with corresponding environmental classification, EcoQs (sed), as defined by Veileder M-608:2016. The red dashed line mark the core dating of 1976. Hg* measurements are semi-quantitative and therefore no EcoQs is given.

4.7 $CaCO_3$ content

Microscope inspection of the 63-500µm sand fraction for foraminifera indicated that the sediments at station IN were rich in foraminifera. The sediment was also abundant in mica and quarts fragments as well as some fine-grained aggregates and fecal pellets (Figure 4.14A).

Inspection of the 63-500µm fraction from station OUT indicated that almost the entire sample consisted of foraminifera (Figure 4.14B). The high abundance of foraminifera was mixed with quartz grains and thin mica flakes. There was not a lot of aggregates or fecal pellets observed at station OUT. The pictures in Figure 4.14 illustrate the typical 63-500µm sediment composition observed at each station and attempts to illustrate the higher abundance of foraminifera tests in the station OUT.

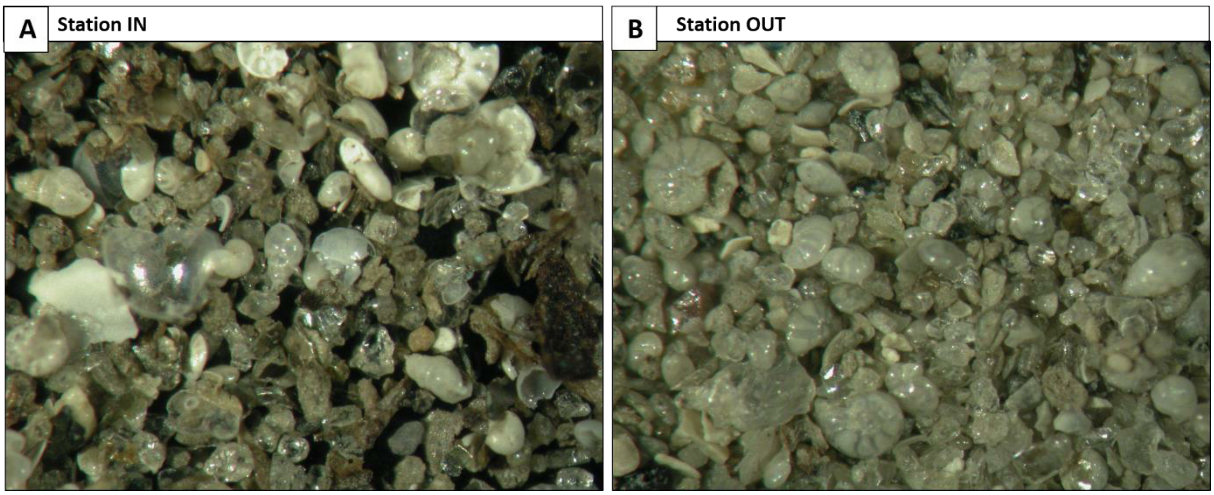

Figure 4.14: Pictures of the typical sediment composition of the 63-500µm sample fraction from each station. **A:** Picture of a small fraction of the 6-7cm sample from station IN (IN-B core). **B:** Picture of the 4-5cm sample from station OUT (OUT-15 core). Both picture show a 2.5 mm*2 mm section of the samples.

The weight (%) $CaCO_3$ content of the 63-500µm grain fraction showed a clear difference between the two stations (Figure 4.15). At station IN the average carbonate content was 17% and at station OUT the carbonate content was on average twice as high at 40%. The up-core carbonate content was relatively stable at both stations.

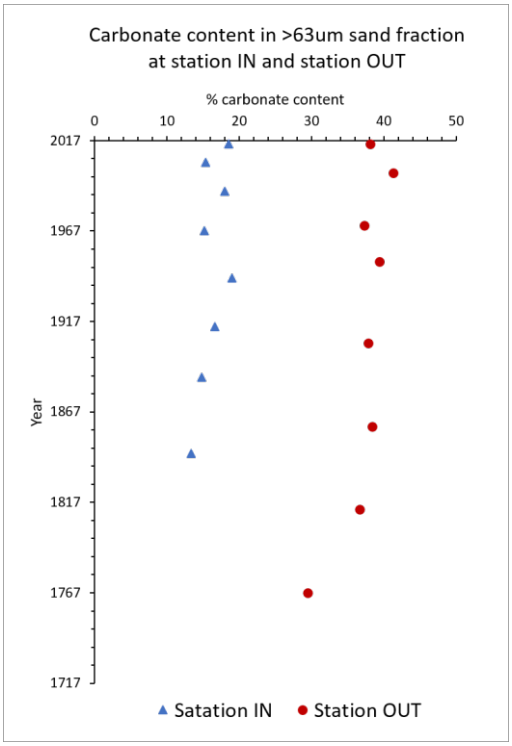

Figure 4.15. % weight (g) of the 63-500µm fraction of sediment that consisted of $CaCO_3$. Results from station IN are marked with blue triangular markers, and station OUT is marked with red circled markers.

4.8 Foraminifera

4.8.1 Station IN

From the lowest picked sample (15-16cm) and up to the 3-4 cm sample the foraminifera concentration was relatively stable with an average of 6700 ind/g. In the 1-2 cm sample the concentration peaked with 10000 ind/g before it declined again in the surface sediment, with the lowest concentration of 4685 ind/g. Even though the SAR increases in the upper 6 cm of the core (Figure 4.5), the concentration (ind/g) and benthic foraminiferal accumulation rate BFAR (ind/cm^2/year) curves follow each other very closely (Figure 4.16A). Apart from the peak observed in 1-2 cm sample (~2011), the BFAR was relatively stable in all analysed core sections and averaged at 408 ind/cm^2/year (466 ind/cm^2/year when 2011 sample is included).

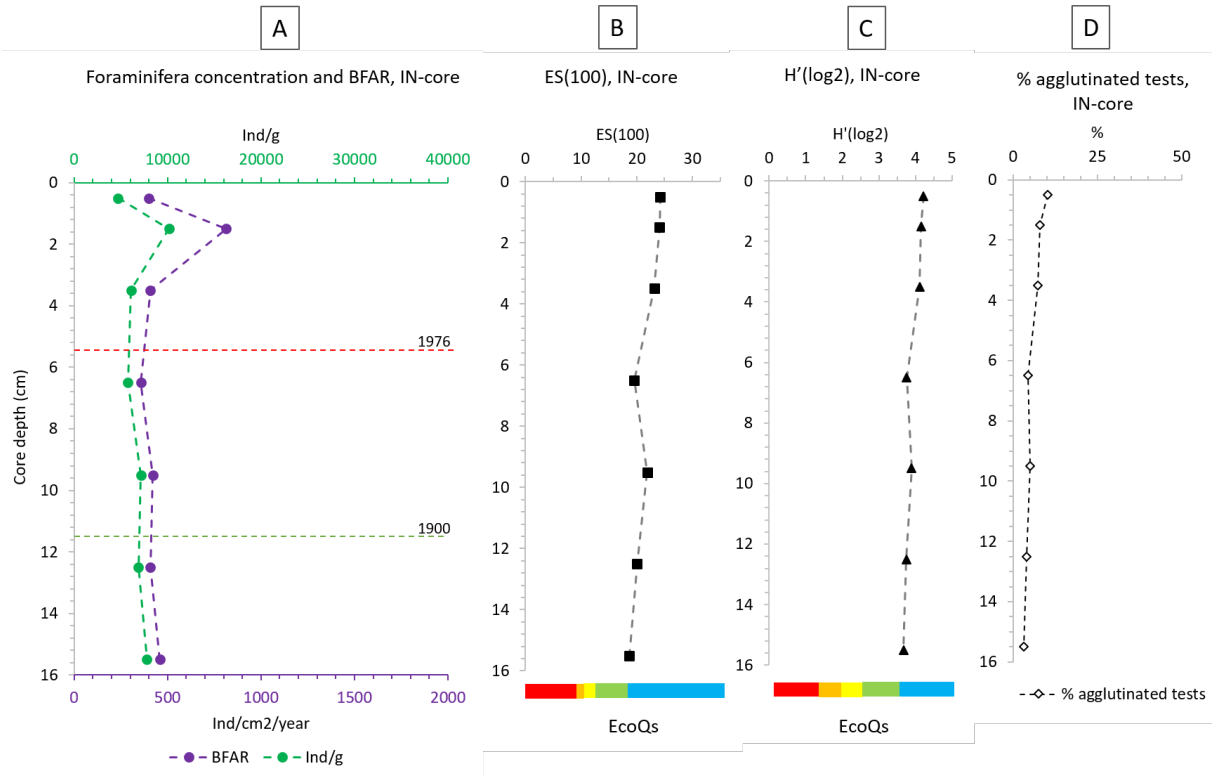

Figure 4.16: Results from foraminiferal analysis at station IN. The stippled line drawn between the markers is an assumption since not all samples were analysed. **A:** Foraminiferal concentration and BFAR at station IN, IN-C core. **B:** Diversity index ES(100) of IN-C core. **C:** Diversity index H'$_{(log2)}$ of IN-C core. **D:** % agglutinated species in IN-C core.

The diversity indices H'$_{(log2)}$ and ES(100) in all analysed samples were all within "high" EcoQs (Figure 4.16B and C). There was no significant temporal (up-core) change in either of the diversity indices. The average value for ES(100) was 21.6 and for H'$_{(log2)}$ it was 3.9 (Table 4-1).

Calcareous foraminifera dominate the assemblage and an average of 6% of agglutinated species were identified in the studied samples (Figure 4.8D). Agglutinated species had a slight increase in frequency in the surface samples.

In the 7 samples studied, a total of 53 benthic foraminiferal species were identified (Appendix C). The 6 most dominating species, with their following average abundance (%) were *Cassidulina reniforme* (19%) (Figure 4.17K), *Bulimina marginata* (14%) (Figure 4.17E), *Elphidium excavatum* (10%), *Stanforthia fusiformis* (9%) (Figure 4.17A), *Hyalinea balthica* (8%) (Figure 4.17C) and *Pullenia osloensis* (6%) (Figure 4.17O). Other common species present in all analysed samples, but with lower relative abundances, were *Buccella frigida* (5%), *Nonionella labradorica* (4%), Cassidulina laevigata (4%) (Figure 4.17M) and

Epistominella vitrea (2.5%) (Figure 4.17I). Of the agglutinated species *Cribrostomoides cf. kosterensis* and *Sprioplectammina biformis* were the most common and had an average abundance of about 1.5% each.

The average *Cassidulina reniforme* abundance was 22% in pre-1967 and decreased to 17% in post-1967 samples (Figure 4.17K). Although it decreased in the upper samples, *Cassidulina reniforme* had the highest relative abundance in all analysed samples. The other common species *Buliminia marginata* (Figure 4.17E), *Elphidium excavatum*, *Hyalina balthica* (Figure 4.17C), *Buccella frigida* and *Nonionella labradorica* showed no clear trend in relative abundance throughout the core, and was present around their average relative abundance in all analysed samples.

Stainforthia fusiformis (Figure 4.17A), *Pullina osloensis* (Figure 4.17O) and *Epistominella vitrea* (Figure 4.17I) showed the same trend with increasing relative abundance up-core, especially in the upper 3 core samples (1998-2015). *S.fusiformis* increased from an average relative abundance of 6% in pre-1998 samples to 13.5% in post-1998 samples, with the highest relative abundance in the surface sample (15%). *E. vitrea* increased from average 1% relative abundance in pre-1998 samples to 4% in the post 1998 samples. The increase in *P.osloensis* was less obvious and but on average increased from 4% to 7% in pre- to post-1998 samples.

The samples from station IN had a similarity of 73% (Figure 4.18). Above 73% similarity the pre-1998 and post-1998 assemblages show again higher similarities with each other. In the three post-1998 samples, the two upper samples (2011 and 2015) again show higher similarities (Figure 4.18). No samples show higher than ~83% similarity with each other. This difference in similarity is reflected in the MDS analysis (results from station IN in Figure 4.17) where no clear clustering occurs in any of the samples.

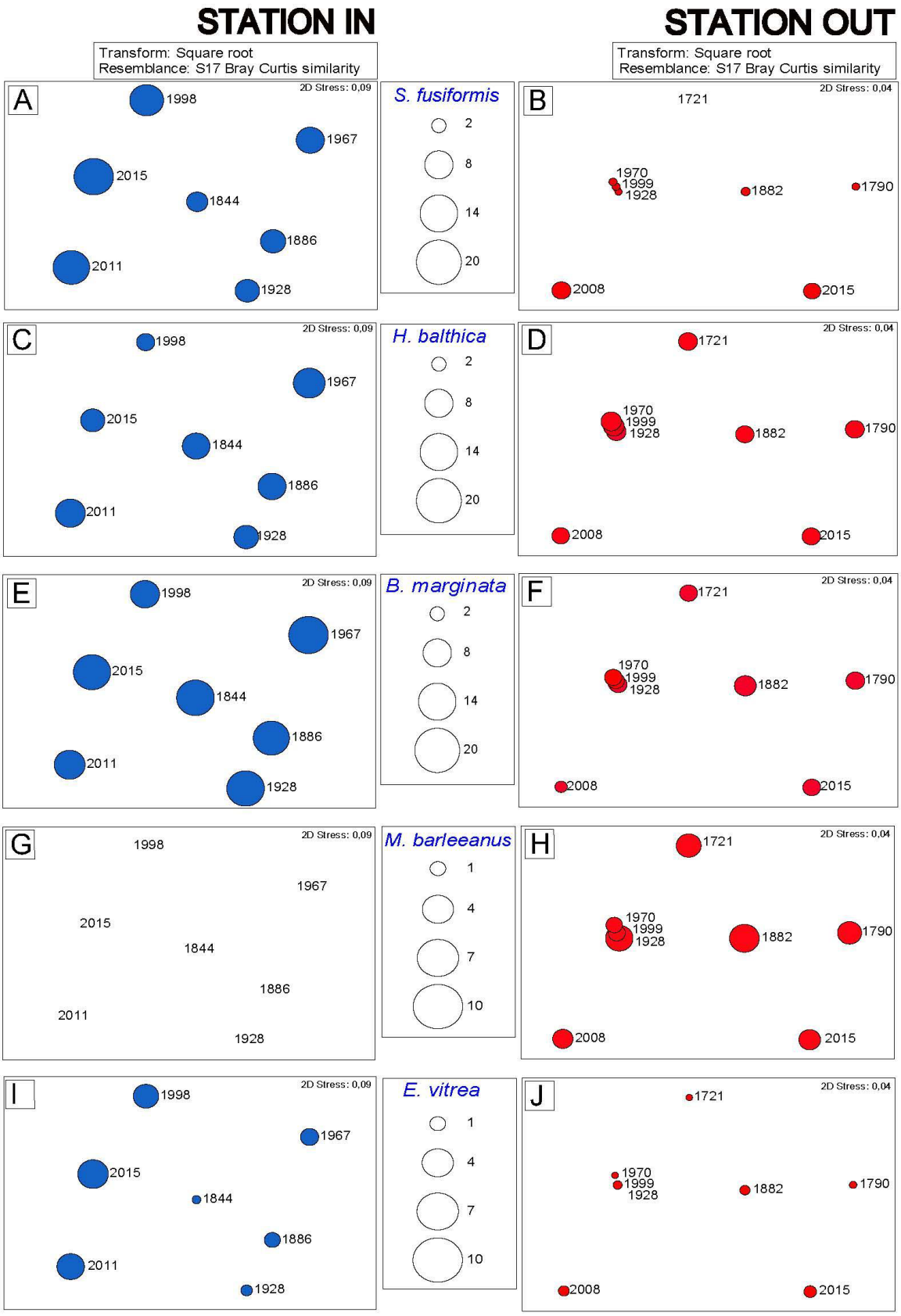
STATION IN
STATION OUT
Transform: Square root
Resemblance: S17 Bray Curtis similarity
Transform: Square root
Resemblance: S17 Bray Curtis similarity
A
2D Stress: 0,09
1998
1967
2015
1844
1886
2011
1928
S. fusiformis
2
8
14
20
B
2D Stress: 0,04
1721
1970
1999
1928
1882
1790
2008
2015
C
2D Stress: 0,09
1998
1967
2015
1844
1886
2011
1928
H. balthica
2
8
14
20
D
2D Stress: 0,04
1721
1970
1999
1928
1882
1790
2008
2015
E
2D Stress: 0,09
1998
1967
2015
1844
1886
2011
1928
B. marginata
2
8
14
20
F
2D Stress: 0,04
1721
1970
1999
1928
1882
1790
2008
2015
G
2D Stress: 0,09
1998
1967
2015
1844
1886
2011
1928
M. barleeanus
1
4
7
10
H
2D Stress: 0,04
1721
1970
1999
1928
1882
1790
2008
2015
I
2D Stress: 0,09
1998
1967
2015
1844
1886
2011
1928
E. vitrea
1
4
7
10
J
2D Stress: 0,04
1721
1970
1999
1928
1882
1790
2008
2015

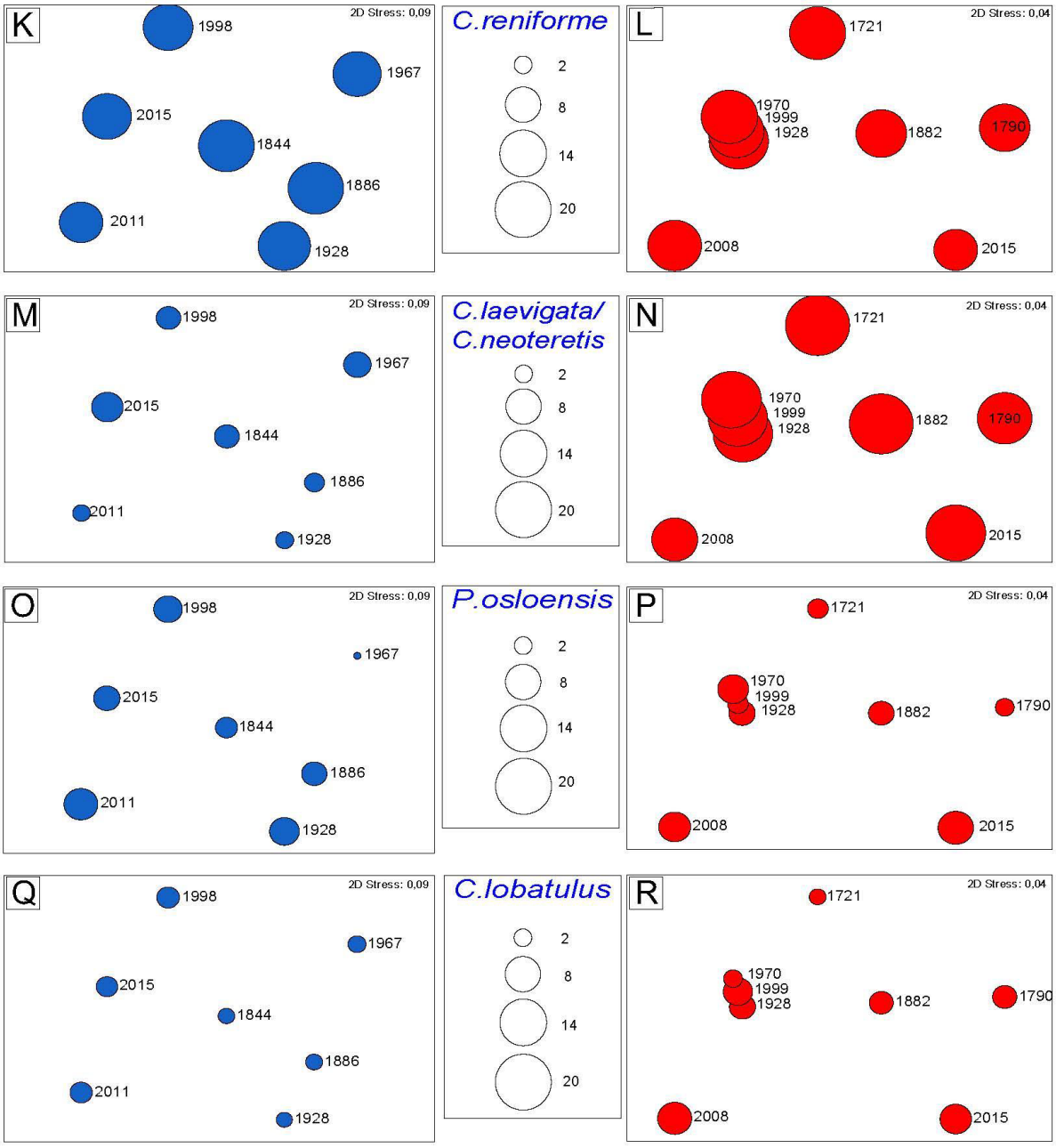

Figure 4. 17: Two-dimensional MDS-plots showing the relative occurrence of selected species analysed in the samples from station IN (diagrams to the left and marked with blue spheres) and station OUT (diagrams to the right and marked with red spheres). Bray-Curtis similarity analysis is used on all data which have been square root transformed. **A+B**: *S. fusiformis*, **C+D**: *H. balthica*, **E+F:** *B. marginata*, **G+H:** *M. barleeanus*, **I+J:** *E.vitrea*, **K+L:** *C. renifrome*, **M+N:** *C. laevigata / C. neoteretis* **O+P**: *P. osloensis*, **Q+R:** *C. lobatulus*. OBS. Notice that the scalebar for *M. barleeanus* and *E .vitrea* is from 1-10% relative abundance unlike 2-20% abundance like the rest of the plots.

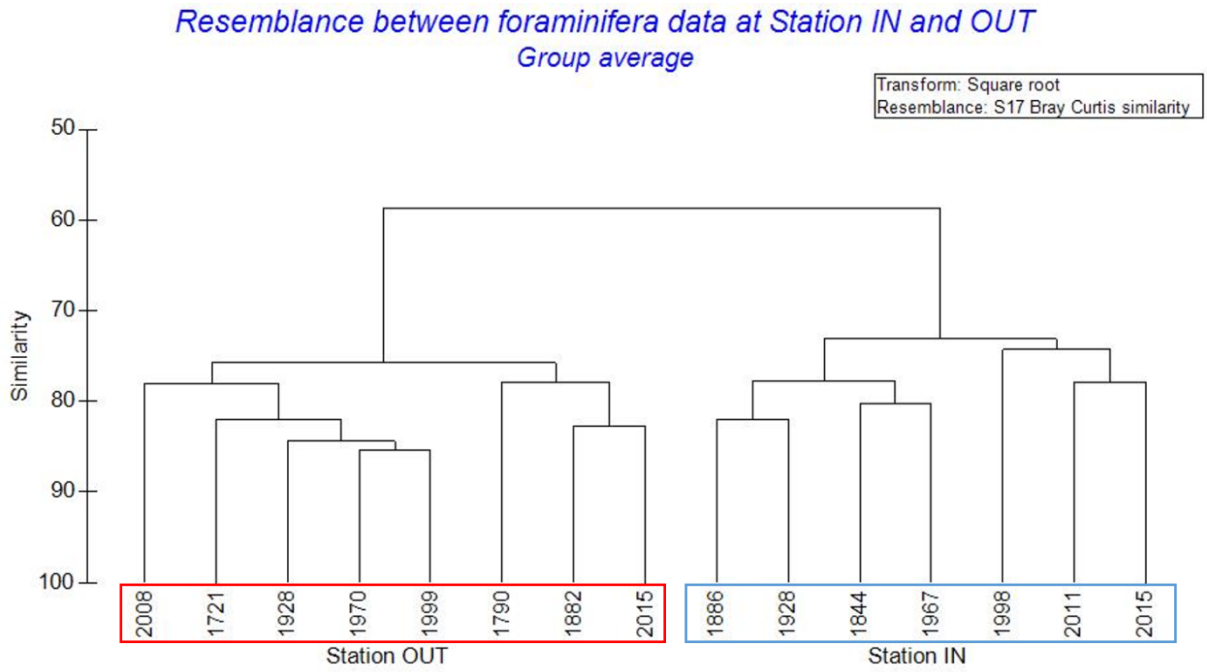

Figure 4.18: Dendrogram showing the similarities between all samples analysed. The diagram is a based on cluster analysis in PRIMER, which use Bray-Curtis similarity on the data which are √-transformed. Left: Samples from station OUT. Right: Samples from station IN.

4.8.2 Station OUT

The concentration of benthic foraminifera was very high throughout the core with an average of 18300 ind/g (Figure 4.19). Following the same trend as the foraminiferal concentration the BFAR was lowest in the samples from the bottom of the core (pre-1800* samples) with an average 306 ind/cm^2/year. The post-1800* samples had a much higher BFAR averaging at 1171 ind/cm^2/year. The diversity indices reveal that all samples were within "high" EcoQs (Average diversity indices: ES(100)= 21.5; $H'_{(log2)}$ = 4.0). There was little variation in the diversity indices.

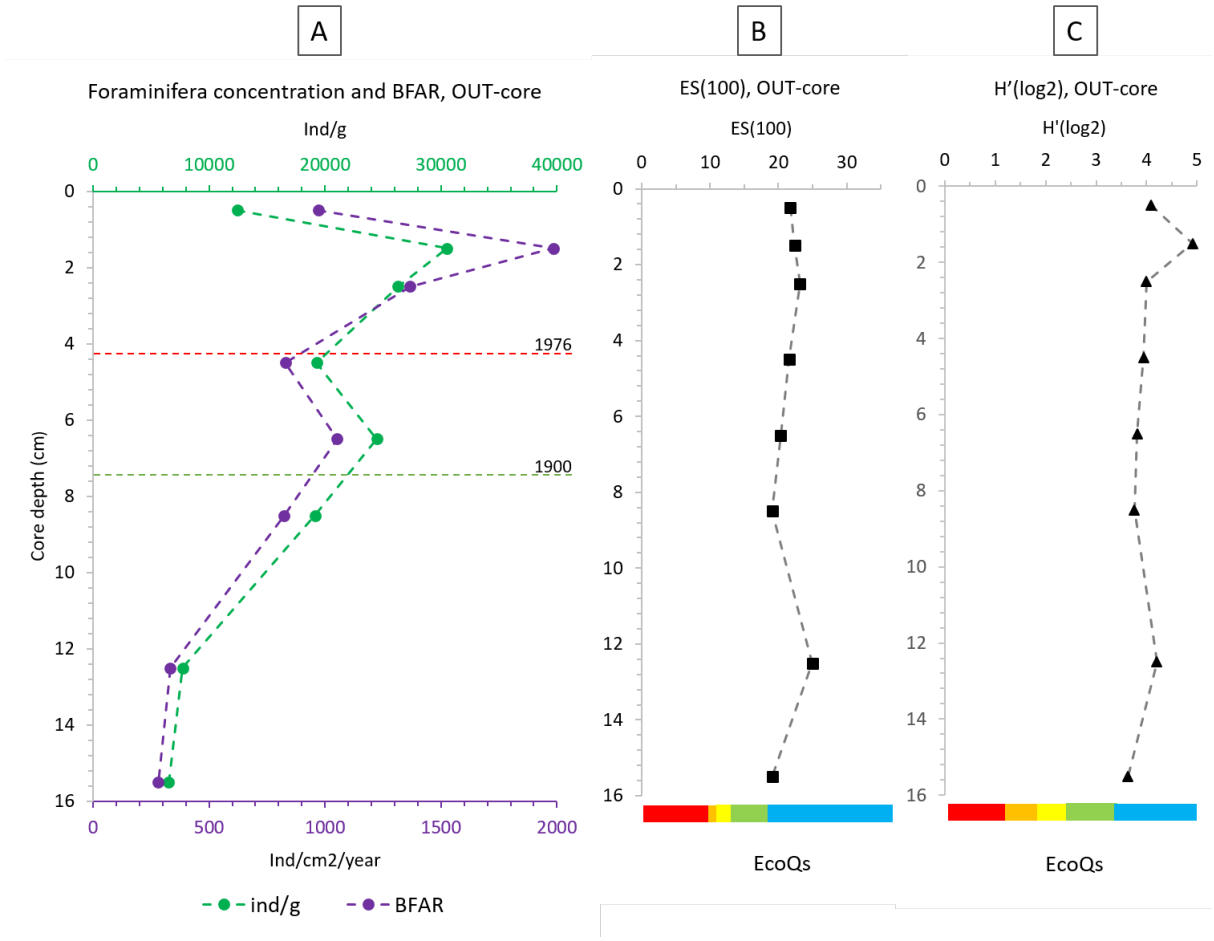

Figure 4.19: Results from foraminiferal analysis at station OUT. The stippled line drawn between the markers is an assumption since not all samples were analysed. **A:** Foraminiferal concentration and BFAR at station OUT, OUT-15 core. **B:** Diversity index ES(100) of OUT-15 core. **C:** Diversity index $H'_{(log2)}$ of OUT core.

In total, 54 benthic foraminiferal species were identified. Calcareous foraminifera dominated with 100% abundance, except for the 2-3 cm core sample where 3 agglutinated individuals were found.

Cassidulina reniforme was the clearly dominating species in all analysed samples with average relative abundance of 22% (Figure 4.17L). There was no typical trend in its up-core abundance and the analysed samples had an abundance close to its average %, apart from the surface sample. In the surface sample (0-1cm) *C. reniforme* had a relative abundance of 15%. Two other abundant species with are *Cassidulina neoteretis* (9%) and *Cassidulina laevigata* (10%). Because these two species look very similar they have been combined in Figure 4.17N. This is to prevent possible mistakes done in the sorting of the two species and to illustrate the difference in this species abundance between the two stations. Other common species are; *Pullenia osloensis* (6%) (Figure 4.17P), *Cibicides lobatulus* (6%) (Figure 4.17Q),

Elphidium excavatum (5%), *Cibicidoides mundulus* (5%), *Hyalinea balthica* (4%) (Figure 4.17D), *Discorbinella bertheloti* (4%), *Nonionella iridea* (3%) *Nonionella labradorica (3%), Trifarina angulosa* (3%), *Bulimina marginata* (3%) (Figure 4.17F) and *Melonis barleeanus (3%) (Figure 17H).*

Of the mentioned species only *C. lobatulus* and *P. osloensis* showed a clear changing trend in relative abundance up-core. *C. lobatulus* increased from an average abundance of 4% in pre-1999 samples to 8% abundance in the three upper core samples (post-1999) (Figure 4.17Q). *P. osloensis* increased from average 5% in the pre-1970 samples to 8% in the post-1970 samples. Another species that had an overall low relative abundance but increased in the upper two core samples was *S. fusiformis*. In samples deposited before 2008 *S. fusiformis* had an average abundance of 0.4% and increased to 3.2% in the upper two core samples (post-2008) (Figure 4.17B).

All analysed samples from station OUT showed a ~76% resemblance with each other (Figure 4.18). Three samples that showed a high similarity (~85%) with each other are the 1928, 1970 and 1999 samples. This resemblance is also illustrated in the MDS-plots in Figure 4.17, where these samples are highly clustered together. Apart from these samples, the similarity between other samples do not follow a typical trend with the age of the sample. For example, the 1889* and 2015 sample show a high similarity with each other.

5 Discussion

5.1 Sediment chronology

The dating horizon, i.e the level at which the unsupported Pb-activity reaches equilibrium with the supported activity, is dated to early 1900 at both stations, but happen at different core depths. The Pb dating for the two cores give reliable results based on relatively good correlation between ^{210}Pb and the corresponding ^{137}Cs used to validate the suggested post-1963 core depths. This holds especially for station IN where only a small correction was done to the post-1963 dates (Appleby and Piliposian, 2018). At station OUT the ^{137}Cs record did not show a clearly defined peak, but increased ^{137}Cs activity observed in the upper 5 cm correlates well with ^{210}Pb calculations (Figure 3.4A). Mixing of the surficial sediments from, for example bioturbation or slump failures, could cause errors in core dating, and thus core dating should generally be treated with caution unless supported by other evidence (Appleby, 2001; Appleby and Piliposian, 2018). Disturbance of the sediment sequence from such events will often be visible as perturbation in the up-core water content and particle size distribution.

The water content had smooth curves in cores from both stations (Figure 4.1). The gradual increase in water content towards core surfaces is due to less compaction of the sediments in the upper core. At station IN the particle size distribution was approximately uniform from core bottom up to the 1998-dated sample (17cm - 3cm core depth) (Figure 4.7). The upper 3 core samples (2005-2015) from station IN show a shift towards finer mean particle size, breaking the uniform distribution observed below. There is a close correlation between TOC and the <63µm particle fraction (Abballe and Chivas, 2017; Aure et al., 2002). The high TOC content (>3.7%) in these upper samples at station IN could therefore explain the increase in finer sediment particles (Figure 4.9A). The particle size distribution at station OUT show a similar distribution for samples above 12 cm core depth (Figure 4.8). Below 12 cm core depth the sediment had a higher content of fine grained particles. The transition to coarser particles at around 12 cm core depth in OUT-15 occurs gradually and therefore do not indicate that there have been any sudden shifts caused by for example slump failures.

What could be traces of bioturbation was only visually observed at station OUT. Appleby (2001) states that when using the CRS model, mixing caused by bioturbation will give a maximum error of less than 2 years in a sequence spanning over 10 years. Bioturbation has

presumably caused some mixing of the sediments at station OUT, and even though no traces were visible possibly also at station IN. However, an error within such a small time-scale is considered negligible in the bigger picture.

Considering the mentioned factors, there is no telling evidence of any sudden disruptions in the sediment sequence of the cores. The extrapolation of the lower core dates is therefore done on a presumably consistent depositional environment, and can contribute to narrow the possible errors of the extrapolated calculations. The general environmental conditions interpreted from sediments deposited before 1900 is the "reference" natural conditions of Kaldfjorden which has been used in this thesis. Extrapolations of the samples below 1900 (dating horizon) were calculated mainly to be able to plot the two stations against one another in the graphs, and will in further discussion be referred to pre-1900 sediments

5.2 Depositional environment

5.2.1 Sediment characteristics and accumulation rate

The sediment cores from the two stations had a clear visual difference. The patchy transition from light grey sediment to brown sediment observed at station OUT (pictures in Figure 4.2) was not present at station IN. The presence and source of this sediment characteristic is unknown and further research on the sedimentology would be interesting.

The results from core dating revealed that the two stations had a similar up-core trends in sediment accumulation rates, but different SAR. The trend seen at both stations is relatively stable accumulation rates from 1900 and towards ~1985, followed by sharp increases that continue towards the surface sediments (2015) (Figure 4.5). Between 1900-1985, SAR was on average 0,016 g/cm^2/year (37%) higher at station IN compared to station OUT. The intensification of SAR from pre- to post-1985 sediments was highest at station OUT, hence the difference in SAR between the two stations decrease towards 2015.

The total average SAR from 1900 to the present at station IN is 0.07 g/cm^2/year, and 0.05 g/cm^2/year at station OUT. Sediment cores collected in Onarheimsfjorden, Lysefjord, and Høgsfjord, all located in south-western Norway, have used the same methods as the present study to calculate the average up-core SAR from ~1900 to the present. In Onarheimsfjorden, a shallow basin (~ 127 m) on the western rim of Hardangerfjorden, two cores were collected.

One core was collected right next to a fish farm that has been active since early 1990's. The average SAR of this core was 0.18 g/cm^2/year. The other core from Onarheimsfjorden was located 500 m away from the fish farm (control core), and had an average SAR of 0.10 g/cm^2/year (Sjetne, 2017). In Lysefjord only one of three cores were dated back to around 1920 (situated in the mid fjord), and the average SAR at this station was 0.11 g/cm^2/year (C. J. Duffield et al., 2017). In Høgsfjord, located further seaward than Lysefjord, the average SAR from ~1900 to the present was 0.10 g/cm^2/year (C. J. Duffield et al., 2017). SAR in these fjords are on average two to three times higher than the SAR in Kaldfjorden

There are no available high-resolution SAR calculated from cores in close vicinity of Kaldfjorden. However, by use of sediment traps Wassmann et al., (1996) have reported the annual sedimentation of total particulate matter (TPM) from the inner to outer Malangen fjord. Malangen is located around 20 km south of Kaldfjorden, and its location is showed in Figure 2.4. Malangen is longer and wider than Kaldfjorden. Both fjords are on the other hand located close the coastal shelf and have deep sills, indicating that alike Kaldfjorden, waters masses of Malangen are well connected with the outer shelf water masses (Wassmann et al., 1996). The inner part of Malangen receives high fluvial input from Måselva river, located at the fjord head. The SAR around the fjord head of Malangen is therefore high (0.37 g/cm^2/year). The sediment supply by the river is relatively limited to the innermost part of the fjord (Wassmann et al., 1996), hence data from the sediment traps located further out are more representable to compare with Kaldfjorden. In the middle and outer part of Malangen the TPM supply in bottom-water sediment traps was reduced to between 0.18 g/cm^2/year (mid fjord) and 0.27 g/cm^2/year (outer fjord) (Wassmann et al., 1996). The SARs in Kaldfjorden, during the same time as the sediment traps were out in Malangen (1996), was three to four times lower (Figure 4.5). This means that Kaldfjorden does not only have a low SARs when compared to fjords in southern Norway, but also when compared to another fjord in northern Norway. The fact that SAR is so low in Kaldfjorden also addresses the question to whether the difference in SAR between station IN and OUT (0.016 g/cm^2/year) really is substantial in the grand scheme of things? For example, the two stations in Onarheimsfjorden, although only 500 m apart, had an average different SAR of 0.08 g/cm^2/year (Sjetne, 2017).

As mentioned in the introduction, the SAR in Norwegian fjords usually varies between 1-7 mm/year (Syvitski et al., 1987). In sediments younger than 1985 the SAR in Kaldfjorden was

lower than 1 mm/year. This might indicate that Kaldfjorden has an especially low SAR compared to other Norwegian fjords.

5.2.2 Temporal TOC accumulation rates

Pre-1900 sediments

In sediment accumulated before 1900 there was a substantial difference in TOC accumulation rate between station IN and OUT (Figure 5.1). The average TOC accumulation rate was 13.3 g C/m^2/year at station IN, and 5.6 g C/m^2/year at station OUT, in the pre-1900 sediments. Hence station IN naturally received over twice as high organic matter supply compared to station OUT.

Terrestrial organic material usually has a lower nitrogen content compared to marine organic material. Marine derived organic matter, for example from phytoplankton, is rich in nitrogen compounds and thus has a lower C/N ratio compared to terrestrial based organic matter (Meyers, 1994). The C/N ratio can therefore be used as an indicator to quantify in which degree the organic material in marine sediments is terrestrial-based or marine-based (Meyers, 1994). Terrestrial-based organic material usually has C/N ratio >10, and C/N ratio of marine-based organic material typically range between 4 -10 (Lamb et al., 2006; Meyers, 1994). The C/N ratio is on average higher by 1.6 at station IN (Figure 4.11), which indicates that there is a higher input of terrestrial material at this station. Inner Kaldfjorden is in a larger degree surrounded by vegetated land, whereas the steep, rocky hillsides surrounding the mid and outer fjord only are covered by a thin layer of sediment, with less vegetation (NGU, 2018). The fact that both stations have C/N ratios below 10 (average 9.6 at station IN and 8.0 at station OUT) suggest that organic material to the sediments is dominated by marine derived organic material (e.g. biogenic input from algal blooms) (Lamb et al., 2006; Meyers, 1994).

Since station IN receives a higher input of terrestrial organic matter it is likely that the transport of this material to the inner fjord also include input of siliciclastic material, which is a contributor to the higher SAR at station IN. The higher content of siliciclastic material at station IN was also visible during microscope inspection (picture in Figure 4.14A). It is worth mentioning the different hinterland geology surrounding the inner and outer fjord (Figure 2.3). Because the surrounding area of inner Kaldfjorden is much more flat and vegetated than

the mid and outer fjord there is a possibility that the different bedrock in this area is less resistant to weathering. Investigations of the mineralogy of the bottom sediments is needed to further discuss this hypothesis.

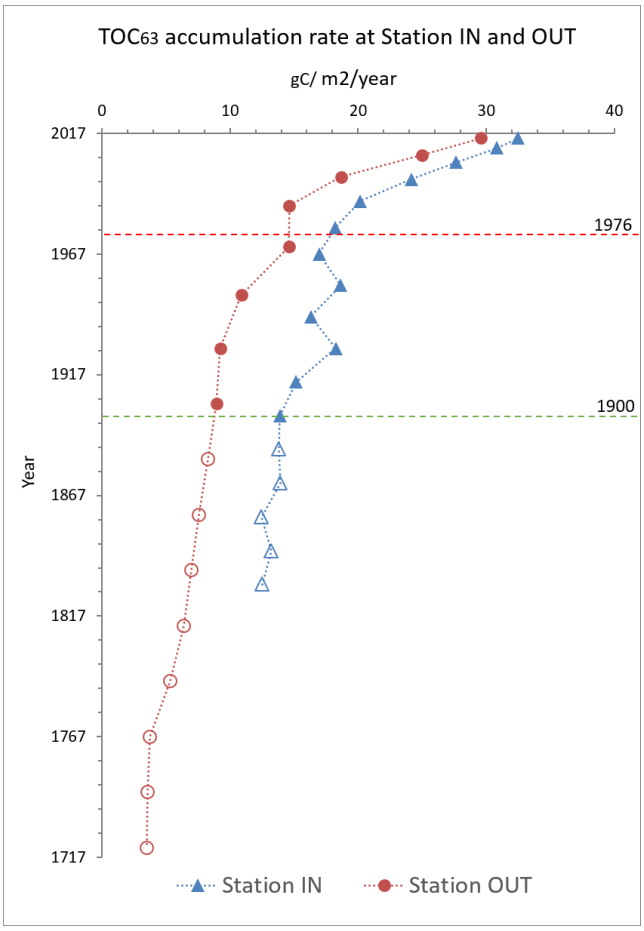

Figure 5.1: Combined results of TOC accumulation rate at station IN (blue) and station OUT (red). Green dotted line marks the transition between pre- and post- 1900 and the red dotted line mark 1976, the start of aquaculture in Kaldfjorden. Unfilled markers indicate that the age of the sample is extrapolated.

There is a very gradual increase in the TOC content from the bottom of the core and throughout the pre-1900 sediments (Figure 5.1). The pre-1900 period is believed to be before significant anthropogenic organic input to Kaldfjorden, and the reason why there is a small but steady increase observed in these sediments was interesting. This trend was for example not seen in pre-1900 sediments in Høgsfjord, where TOC accumulation rate was stable around 13 g C/m^2/year (C. J. Duffield et al., 2017). This rate is similar to the average pre-1900 TOC accumulation rate at station IN. TOC content analysed on a 400cm long sediment core collected in Ullsfjord, a fjord located further inland in Troms, reveal a similar pattern as observed in Kaldfjorden; a gradual increase in TOC content in pre-1900 sediments (Sauer et

al., 2016). Because there is limited high resolution TOC measurements from short cores in northern Norway, the upper core Ullsfjord is used to compare with Kaldfjorden. In the top 25 cm of the Ullsfjord core, the TOC content increases from ca. 2.4% at 25 cm to 2.6% at 10 cm in the core (Sauer et al., 2016). The average TOC accumulation rate in Ullsfjord from year 875 to present was 6.21 g C/m^2/year (Sauer et al., 2016), which is similar to the rate at station OUT. Syvitski et al., (1987) mention that with aging, buried organic matter may undergo bacterial degradation or, through low temperature diagenesis, the organic material can change to gas. The very gradual TOC increase in pre-1900 sediments in Kaldfjorden could possibly be due to this. The different TOC accumulation rate in pre-1900 sediments at the two stations is however more difficult to explain. It is partly explained by the natural factors causing the higher SAR at station IN, as discussed in the previous section.

Post -1900 sediments

From 1900 up to around 1960, the increasing trend in TOC accumulation rate continued but with a steeper slope at station OUT, and with some fluctuations at station IN (Figure 5.1). From around 1900 to ~1960 was also the period where there were some fluctuations observed in the otherwise stable C/N ratios (Figure 4.11). Available precipitation data only reach back to 1960 (Figure 2.5). There is also limited information of human activities that occurred around the village of Kaldfjord, and within the fjord, in this period. It is therefore difficult to draw a line to any sources to the slight increases. We know that the mechanical wastewater treatment plant was built in 1984 (Berg et al., 2009). It is likely that before this was built, wastewater from households in Kaldfjord was directly discharged to the fjord. This would have increased the nutrient input to the fjord, that could have supported larger plankton blooms than previously. However, it is clear from the TOC accumulation rates that the increase between 1900 and 1960 was much smaller than the post-1960 increase (Figure 5.1).

The TOC concentration in marine sediments are used as a supplementary parameter to regulate the degree of organic loading. The boundary between “good” and “moderate” classification of TOC content is 27 mg/g (2.7%) (Table 5-1). According to this classification TOC concentrations in pre-1950 sediments are within “high” and “good” status, and post-1950 sediments are within “moderate” and “poor” status at both stations (Figure 4.9A and Figure 4.10A).

Table 5-1: Classification of TOC_{63} content in marine sediments that are can be used as a supplementary parameter in classifying the EcoQs (retrieved from Veileder 02:2013).

Classification for TOC content in marine sediment according to STF Veileder 97:03					
	1	2	3	4	5
	High	Good	Moderate	Poor	Very poor
TOC content (mg/g):	0 - 20	20 - 27	27 - 34	34 - 41	41 - 200
TOC content (%):	0 - 2.0	2.0 - 2.7	2.7 - 3.4	3.4 - 4.1	4.1 - 20.0

TOC concentration of all post-1970 sediments at station OUT are higher than 3.4%, and therefore fall within "poor" conditions (Table 5-1). At station IN, TOC concentrations reach 3.4% in post-1990 sediments. The peak TOC concentration at the two station occurs between 2008-2011 with 3.9% at station IN and 3.8% at station OUT. The highest content at station IN (3.9%) are the same as found in an environmental survey conducted very close to this station in 2000 (Velvin et al., 2008). At the same station, repeated analysis in 2008 revealed that the TOC was reduced to 2.7% (Velvin et al., 2008). Such low TOC concentrations have not been found in any post-1990 samples in the present study.

In 2004 the TOC concentrations were analysed on 13 surface samples collected along Malangen fjord (Figure 5.2 A). The TOC concentrations from this study varies between 1-2% (Husum and Hald, 2004). In Ullsfjord the highest TOC content was measured to be 2.9% at 5 cm core depth (Sauer et al., 2016). There are no measurements of the surface sample in Ullsfjord. TOC content of these two fjords, also located in Troms county, are both lower than in Kaldfjorden. In a core collected right by the active fish farm in Onarheimsfjorden the TOC content in the surface sample was 3.4% (Sjetne, 2017). The control core, located 500 m away from the fish farm, had TOC content of 2.8% in the surface sample (Sjetne, 2017). Although stations in Kaldfjorden are situated more than 500 m away from any fish farms, they both have higher TOC content than from the core collected right by the fish farm in Onarheimsfjorden.

Accumulation rates were not measured in the 2004 study of TOC content in Malangen. By using Wassmann et al., (1996) measured TPM rates, the TOC accumulation rate in Malangen can be calculated to be between 18 - 36 g C /m^2/year. TOC accumulation rates from ~2000 to the present are 24 - 32 g C/m^2/year are at station IN and 19 - 30 g C/m^2/year at station OUT (Figure 5.1). This reveal that the accumulation rate between Kaldfjorden and Malangen are much more comparable than the TOC content. The consequence of the abnormally low SAR in Kaldfjorden is that burial of organic material will be much slower than in other fjords. It

might contribute to the high TOC content in the upper core samples. The stations in Onarheimsfjorden have, unlike Kaldfjorden, very different TOC accumulation rates in the upper core sample. TOC accumulation rate in the surface sample from the fish farm core was 42 g C/m^2/year. The other control core had 12 g C/m^2/year (Sjetne, 2017).

The fact that station OUT received a high increase in TOC accumulation around the same time as station IN is particularly interesting. All the potential sources for increased TOC accumulation were concentrated around the inner fjord area from around 1970. It was not before 1999 that aquaculture started in the outer fjord. The south to northern direction of the surface current in Kaldfjorden (Eriksen, 2016b) could possibly transport POM from the inner to outer fjord area. Another possibility for the simultaneous post-1967 increase at the two stations is that the change in nutrient supply could have led to larger and wider phytoplankton blooms in the fjord. The C/N values are constant and lower than 10 in the post-1976 sediments which indicate that the increased organic matter to the sediments is mainly from marine sources.

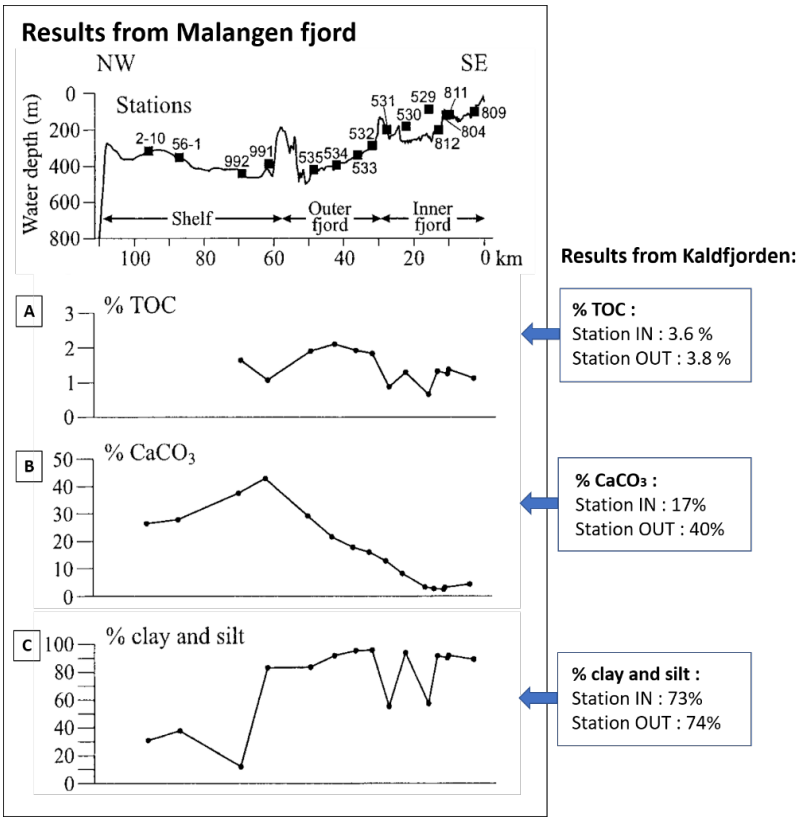

Figure 5.2: Results from analysis of 13 surface samples located from the inner fjord (SE) to the outer shelf (NW) in Malangen. **A:** TOC content (%) **B:** $CaCO_3$ content (%) **C:** Clay + silt content (%) (Illustration from Husum and Hald, 2004). Text boxes include results from Kaldfjorden; TOC and < 63 µm content is from the 2005-dated sample from station IN, and from the 2008-dated sample from station OUT.

5.2.3 Calcium Carbonate ($CaCO_3$) content

There is twice as high carbonate content in sediments at station OUT (~40%) compared to station IN (~17%) (Figure 4.15). The higher carbonate content at station OUT was also visible during microscope inspection (picture in Figure 4.14B), and in the post-1900 samples foraminifera concentration was over twice as high compared to station IN (Figure 4.16 A and Figure 4.19 A). The lower SAR in outer Kaldfjorden explains some of the higher concentration, since the sediment in this area is less diluted by siliciclastic material. Although SAR is lower at station OUT, the BFAR had an average rate of 1171 ind/cm^2/year in post-1800* dated samples, compared to the relatively stable BFAR of 408 ind/cm^2/year throughout the core from station IN. This tells us that the production rate of foraminifera shells, and likely also other calcium carbonate secreting organisms, is a lot higher in the outer fjord. Increased carbonate content in sediments from the inner to outer fjord is also seen in Malangen (Figure 5.2 B). There is however a slightly lower carbonate content in the outer Malangen fjord (~30%) (Husum and Hald, 2004), which is likely due to the higher SAR in this fjord. The carbonate content in Kaldfjorden is the same as measured in Malangsdjupet (st.991 and st. 992 in Figure 5.2 B). Location of Malangsdjupet is shown in Figure 2.4.

There is a considerable production of carbonate on the coastal platform and troughs outside Troms (Freiwald, 1998; Husum and Hald, 2004). A study of the sediments on the shallow coastal bank area north of Malangsdjupet reveal that the sediments in this region can have >90% carbonate content (Freiwald, 1998). Without going into details about the species level, Freiwald (1998) mentions that foraminifera, together with lots of other carbonate secreting organisms, are abundant in these carbonate-rich sands.

There is a high hydrodynamic energy at the shallow platform area, and transport and deposition of suspended carbonate particles from the platforms into outer fjord troughs can happen (Freiwald, 1998). It is therefore possible that the some of the foraminifera observed at station OUT, and perhaps even at station IN, are transported from this high productive environment outside Kaldfjorden. The higher BFAR at station OUT is likely a combination of higher production and transport of foraminiferal shells. It is impossible to know which species that could potentially have been transported to the stations. To be able to discuss and interpret the assemblages at the two stations it is therefore assumed that most species found in the sediments samples lived in the sediments analysed.

5.2.4 Sediment dispersal and bottom currents

Grain size distribution of the bottom sediment is generally a good indicator for the sediment transport and deposition controlled by the hydrodynamic energy (Boggs, 2014; Howe et al., 2000). In fjords with fluvial input it is often observed that the SAR and size of sediment particles decrease exponentially from the fjord head towards the fjord mouth (Syvitski et al., 1987). However, there is no river discharge to the inner Kaldfjorden, and the catchment area surrounding the inner fjord is not larger than the outer fjord (NVE, 2018).

The present study shows a transition from generally coarser sediments (with clay content of ~4%) and at station IN to higher content of finer particles (with clay content of ~8%) at the outer station. This relationship is in accordance with the general assumption that the deeper fjord area (station OUT is 28m deeper than station IN) are generally the areas with lowest current energy (Boggs, 2014; Syvitski et al., 1987). The up-core sand fraction (>63µm) at station IN and OUT have a reversed trend (decrease at station IN, and increase at station OUT) (Figure 4.6 C), and therefore the difference in sand content between the two stations is much smaller in the upper core.

A study of grain size distribution of 41 surface samples along the inner to outer fjord axis has been conducted on three neighbouring fjords in northern Norway; Vestfjord, Ofotfjord and Tysfjord (Faust, et al 2017). The study reveals that there is no spatial pattern in grain size distribution (except for the clay content which increases with water depth) between the inner and outer fjord area. A higher percent of the coarser fraction (>63µm) is observed in the inner fjord area of Tysfjord. Vestfjord and Ofotfjord, on the other hand, show little difference between the inner and outer fjord; both fjords are dominated by the <63µm fraction, with spatial occurrences of coarser samples. In Malangen, there is not either observed any trend in the % faction of clay and silt between the inner to outer fjord (Figure 5.2C) (Husum and Hald, 2004) . These findings indicate that a typical inner to outer fjord trend in particle sizes is not always the case. This is because the distribution and accumulation of particles in the fjords mentioned, as well as Kaldfjorden, is likely dependent on a more complex combination of factors such as the seafloor topography, basin geometry and annual and seasonal changes in the hydrodynamic regime within the fjords.

A reason to question the link between grain size distribution and the hydrodynamic regime in Kaldfjorden is the higher relative abundance of *Cibicides lobatulus* found at station OUT (Figure 4.17 R). *Cibicides lobatulus* is an epibenthic species (i.e. it lives on the sediment

surface), can occur over a wide range of organic flux rates and its presence appears to be closely linked to more powerful bottom currents (Altenbach et al., 1999). At station OUT the abundance of *Cibicides lobatulus* increase up-core with an average abundance of 8% in the upper 3 core centimetres. In addition, *Trifarina angulosa* has a much higher abundance (~3%) at station OUT. At station IN this species is only present a few samples with <1% relative abundance. *Trifarina angulosa* is commonly found in coarse sands that are affected by currents (Murray, 2001; Duffield et al., 2017 and references therein). *Cibicides lobatulus* and *Trifarina angulosa* are found to dominate the assemblage in the high energy and coarse grained environment on the coastal shelf area further south in Norway (63ºN) (Kristensen et al., 2002). High abundances of these two species are also found in the coarse grained sample on the shelf area outside Malangen fjord (st. 992 in Figure 5.2) (Husum and Hald, 2004). These two species do not dominate the assemblage at station OUT. However, their higher abundance is evidence that although finer particle sizes, there might still be higher energy in the bottom currents at station OUT. The fact that the percent (%) >63µm grain fraction and the abundance of *C. lobatulus* increase in the upper core centimetres at station OUT could be an indication that there has recently been a change to a higher energy environment at this station. As mentioned, there is a possibility that *C. lobatulus* has been transported from the high energy and high productive area outside Kaldfjorden. However, the increase in *C. lobatulus* in the upper core samples at station OUT would still mean that there has been a change in the currents that caused the increased transport of this species.

There is very limited data on the current regime in Kaldfjorden. Only one report, conducted next to the fish farm Rogndalen, was found (Eriksen, 2016b). There are therefore many uncertainties to how particles are dispersed in the fjord. If there are sufficient bottom current velocities, which can change over time, as interpreted from the station OUT core, there could be winnowing of the sediments in some areas. This could also be a potential explanation for the unusual sediment characteristics visually observed at station OUT (pictures in Figure 4.2). Winnowing of the sediments can cause an uneven distribution of grain size particles. The exact placement of a coring location can possibly have a significant impact on the grain size distribution.

5.3 Heavy metal concentrations

The results from the heavy metal analyses at station IN and OUT show generally low concentrations, and all values are classified within the “high” or “good” ecological status (Figure 4.12 and 4.13). Previous environmental surveys conducted on surface sediment samples in the inner Kaldfjorden, also show low concentrations of heavy metals (Velvin et al. 2008). In previous surveys all metals analysed were within the “high” status except mercury (Hg), which was within the “good” status (Velvin et al., 2008). Therefore post-1900 increase in the semi-quantitative measurements of Hg, occurring both at station IN and OUT, indicate that there has been a very small increase of this heavy metal in the fjord. Mercury is easily mobilized, deposited and re-mobilized in the environment (Goodsite et al., 2005). Because of its volatile nature, its source does not necessarily have to be located close to Kaldfjorden.

Copper (Cu) is a heavy metal that is usually associated with aquaculture operations. This heavy metal is often used as an anti-fouling impregnation on the net pen constructions (Skarbøvik et al., 2015). High levels of Cu are not observed in Kaldfjorden, and if the fish farm is using this as impregnation on the cages, it is not accumulating in the sediments.

The overall trend of heavy metal concentration differs between the two stations. From the lower to upper core samples, heavy metal concentrations show a gradual increase at station IN, and a decrease at station OUT. If all the heavy metal concentrations observed are Kaldfjorden’s natural background levels, there could be a correlation between heavy metals and the finer particles. Heavy metals have been found to be in close association with fine (< 7.8 µm) particles (Zonta et al., 1994). There is a gradual up-core increase in the percent of < 7.8 µm fraction at station IN (from 14% to 17%), whereas at station OUT the fraction decreases up-core (from 34% to 27%).

5.4 Foraminifera assemblages

5.4.1 Validation of foraminifera concentration and BFAR

The sediments at station IN and OUT both have a very high abundance of foraminifera. The average foraminifera concentration was 6930 ind/g at station IN and 18300 ind/g at station OUT. Therefore, a very small fraction of sediment (between 0,004-0,01g) was needed to pick >300 individuals. When working with such small weights, a minor error in weighing can lead

to large changes in the calculated concentrations (ind/g), which again is reflected in the BFAR. Therefore, the concentration and BFAR for both stations should be treated with caution.

Calcareous foraminifera dominate at both stations with the average 100% at station OUT and 94% at station IN. The calcareous shells were well preserved in all samples investigated. The abundance of agglutinated species increases from 3% in the lowest sample, to 10% in the surface sample at station IN. Agglutinated shells are more fragile than those of calcareous shells. Several agglutinated fragments, which could not be identified to species level, were found in lower core samples at station IN. The lower agglutinated abundance in the down-core samples at station IN could therefore likely due to some disintegration (Figure 4.16 D).

Because of the low SAR, and high BFAR in Kaldfjorden, the foraminifera concentration in the sediments at the two stations is anomalously high. In Onarheimsfjorden, Sjetne (2017) found what he describes an anomalously high concentration in the surface sample in the control core (500 m away from a fish farm) with 2120 ind/g. The BFAR of the same sample was 250 ind/cm^2/year (half the BFAR at station IN). Other studies from south-western Norway also show that foraminifera concentrations and BFAR are much lower than in Kaldfjorden (C. J. Duffield et al., 2017; Torper, 2017).

An extensive investigation of the foraminiferal assemblage along Malangen's inner fjord to outer shelf transect (NW-SE) was conducted in 2004 by Husum and Hald. The transect show, alike Kaldfjorden, that foraminifera concentration increase towards the coastal shelf area (Malangsdjupet) (Figure 5.3 A). The concentrations within Malangen fjord are lower than in Kaldfjorden (< 3000 ind/g, Figure 5.3A), which is partly explained by the higher SAR in this fjord. The concentration in Malangddjupet is 10000 ind/g and thus is comparable to concentrations in Kaldfjorden. Husum and Hald (2004) conclude that there is a very high abundance of well-preserved foraminifera in Malangen, which clearly is also is the case for Kaldfjorden. The factors that make up the favourable growth and living conditions for foraminifera species in Kaldfjorden and Malangen are not necessarily the case for other high-latitude, subarctic fjords. An investigation of the foraminifera assemblages in several fjords located around Svalbard reveal that concentrations in this region are much lower, usually varying around 100 ind/g (Hald and Korsun, 1997).

The % agglutinated species in inner Malangen was much higher than in Kaldfjorden (Figure 5.3 B). In one sample from inner Malangen fjord, the agglutinated assemblage actually dominated with only 44% calcareous species (Husum and Hald, 2004). However, the Malangen transect showed that % calcareous foraminifera increased towards the outer fjord (80-100%). Although agglutinated species were present with lower abundance at station IN, the two fjords show a similar trend, with clear dominance of calcareous species in the outer fjord.

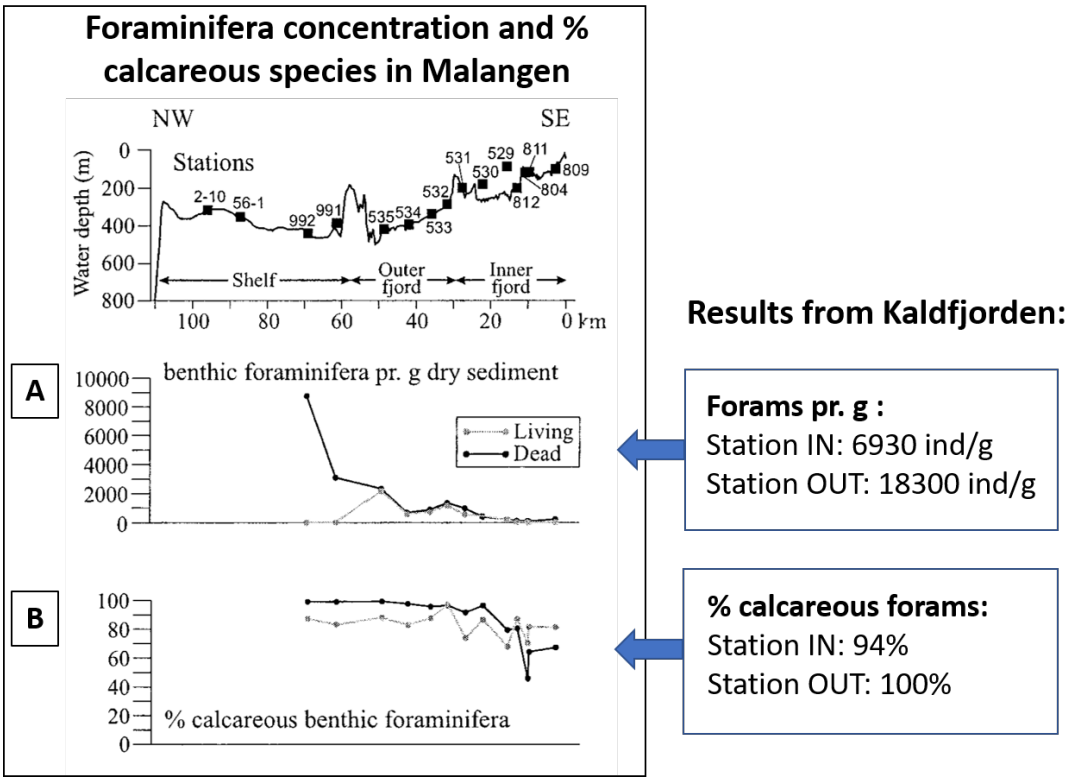

Figure 5.3: Results from foraminiferal analysis along the transect of Malangen. **A:** Benthic foraminifera pr. g dry sediment (ind/g) **B:** % calcareous benthic foraminifera along the fjord transect. Illustration of results is retrieved from Husum and Hald, 2004. Text boxes include average results from Kaldfjorden.

5.4.2 Difference in species assemblage

The foraminifera assemblage composition in the two cores shared common characteristics, both in terms of diversity ("high" EcoQs at both stations) and relative abundance of several different species. *Cassidulina reniforme* is one of these species, and is the dominating species at both stations (Table 5-2). *C. reniforme* is commonly restricted to high latitude regions (Murray, 2001), and is considered to be an arctic species by Sejrup and Guilbault (1980). A more recent review article by Murray and Alve (2016) shows that *C. reniforme* can occur at

lower latitudes, but only with minor abundances. At higher latitudes, *C. reniforme* can often be a dominating species (Husum and Hald, 2004; Murray and Alve, 2016). *C. reniforme* is classified as a Group I "Sensitive species" species by the Foram-AMBI sensitivity index (Alve et al., 2016). Group I species are classified as sensitive to organic matter enrichment. The small reduction of *C. reniforme* in the surface samples at both stations (Figure 4.17K and L) could therefore be because of the increased TOC content. Other common species that occurred at both stations with a relative abundance > 4% were *C. laevigata, E. excavatum, H. balthica,* and *P. osloensis* (Table 5-2).

Table 5-2: Table show the 9 most abundant species in each core from Kaldfjorden. The most abundant species is given in **bold** letters, and their relative abundance are indicated. Some species are within the top 9 most abundant species in both cores. "X" indicate that the species is not present in any samples at the station.

Station IN	Station OUT
***Bulimina marginata* (14%)**	*Bulimina marginata* (3%)
***Buccella frigida* (5%)**	*Buccella frigida* (*<0.2 %*)
***Cassidulina reniforme* (19%)**	***Cassidulina reniforme* (22%)**
X	***Cassidulina neoteretis* (9%)**
Cassidulina laevigata (4%)	***Cassidulina laevigata* (10%)**
Cibicides lobatulus (3%)	***Cibicides lobatulus* (6%)**
X	***Cibicidoides mundulus* (5%)**
Discorbinella bertheloti (1%)	***Discorbinella bertheloti* (4%)**
***Elphidium excavatum* (10%)**	***Elphidium excavatum* (5%)**
***Hyalinea balthica* (8%)**	***Hyalinea balthica* (4%)**
***Nonionella labradorica* (4%)**	*Nonionella labradorica (3%)*
***Pullenia osloensis* (6%)**	***Pullenia osloensis* (6%)**
***Stanforthia fusiformis* (9%)**	*Stanforthia fusiformis (1%)*

Although there are some similarities in the foraminiferal assemblages, the two stations also show distinct differences in assemblage compositions (Figure 4.18, Table 5-2). Since there is a clear difference in the assemblages at the two stations, they could not be presented in the same MDS-plots. Each station was therefore given individual MDS-plots in Figure 4.17.

After *C. reniforme,* the next most abundant species differs at the two stations. At station OUT *Cassidulina laevigata* and *Cassidulina neoteretis* make up a clear second and third most abundant species (Figure 4.17 N, Table 5-2). *C. neoteretis* does not occur at all at station IN, and the abundance observed in Figure 4.17 M is only the relative abundance of *C. laevigata* (4%). *C. laevigata* have previously been described to thrive in well-oxygenated water, and generally declining under low-oxygen conditions (Gustafsson and Nordberg, 2000 and references therein). The oxygen data is limited for the outer Kaldfjorden, but the data available indicate a slightly higher oxygen concentration in the outer fjord (Table 2-1, Figure 2.6). Previously, a seasonal drop in % O_2 saturation in bottom waters of inner Kaldfjorden (Velvin et al., 2008) has been observed. This indicates that there are seasonal variations in the oxygen concentrations in the inner fjord, opposed to possibly a more stable and a little higher saturation in the outer fjord.

M. barleeanus does not occur at all at station IN, whereas it is present around its relative abundance (3%) in all samples at station OUT (Figure 4.17G and H). In Malangen and Lysefjord *M. barleeanus* does not occur either in the inner fjord stations, but is abundant in outer fjord samples (Duffield et al., 2017; Husum and Hald, 2004). Malangen and Lysefjord both have fluvial input at the fjord heads, and the inner fjord are the most terrestrial influenced sites. *M. barleeanus* likely favours areas with low terrestrial input.

Stations located in mid and outer Malangen (st.531-st.535 in Figure 5.3) are dominated by *Brizalina skagerrakesnisis* and other mentioned abundant species are *C. neoteretis, C. lobatulus, Globobulimina turgida, P. osloensis, Astrononion gallowayi* and *H. balthica* (Husum and Hald, 2004). *B. skagerrakensis* and *G. turgida* are not found in any samples investigated in Kaldfjorden. The other mentioned common species in outer Malangen are also common at station OUT (Table 5-2). This is with exception of *A. gallowayi* which has a low relative abundance of 1% at station OUT. The results from outer Malangen indicate that although there are similarities between the outer fjord areas in the two neighbouring fjords, there are also clear differences in the species assemblages.

In average of all samples investigated at station IN, *B. marginata* is the second most dominating species at station IN. In the three upper-core (1998-2015) samples at station IN, *Stainforthia fusiformis* show slightly higher abundances compared to *B. marginata*. In the surface samples investigated in the inner Malangen fjord, both the dead and living foraminifera assemblage investigated are dominated by *C. reniforme* and *B. marginata*

(Husum and Hald, 2004). In Malangen the dead assemblage is dominated by *B. marginata* (relative abundance of 24%) followed by *C. reniforme*. The living assemblage is dominated by *C. reniforme* (Husum and Hald, 2004). Other common species in the inner Malangen are *N. labradorica, E. excavatum,* and *H. balthica* (Husum and Hald, 2004). The inner Malangen assemblage are similar to the results from station IN in Kaldfjorden (Table 5-2). This is apart from *S. fusiformis*, which is not mentioned in the study of Malangen. *B. marginata* are classified as a Group III "Tolerant species" by the Foram-AMBI index, and the species can thrive over a wide range of TOC concentrations (Alve et al., 2016). Inner Malangen fjord have lower TOC contents of ~1.2% (Figure 5.2 A) compared to the inner Kaldfjorden (~3.8 in 2005 sample). It could seem that the high abundance of *B. marginata* in the inner fjord areas of Kaldfjorden and Malangen are more related to other environmental characteristics than the naturally higher TOC content at station IN.

At station IN the foraminiferal species composition of the three upper-core samples (1998 - 2015) differs slightly compared to the pre-1998 investigated samples (Figure 4.18). This up-core change in assemblage composition is not as clearly identified at station OUT. At station IN abundance of *Stainforthia fusiformis* increases from average 6% to 13% in pre- to post-1998 samples (Figure 4.17A). *S. fusiformis* is therefore one of the species contributing to the higher similarity of the post-1998 samples at station IN. Although with a much lower relative abundance, *S. fusiformis* also increases in the two upper core samples at station OUT (Figure 4.17 B). The observation of increased *S. fusiformis* abundances in upper core samples are confirmed by living (rose Bengal stained) benthic foraminifera analysis of surface samples in Kaldfjorden (Klootwijk, 2018, unpublished data). Klootwijk's (2018) data shows that in the living assemblage, *S. fusiformis* has a relative abundance of 10% and 14% in two surface samples from the inner Kaldfjorden, and 11% and 24% in two surface samples from the mid/outer Kaldfjorden. *S. fusiformis* is well documented as an opportunistic species, and is commonly associated with dominating in organic rich and oxygen-depleted sediments (Alve and Murray, 1997; Duffield et al., 2015 and references therin). *S. fusiformis* is one of only two species that have been classified within Group V "1st order opportunistic species" by the Foram ABMI index (Alve et al., 2016). As the proportion of *S. fusiformis* increases in the upper core samples. *S. fusiformis* could be an important indicator that the foraminiferal assemblage in Kaldfjorden is showing some stress related to the post-1967 increased organic supply to the sediments. In the study of Malangen, occurrence of *S. fusiformis* is not

mentioned at all, which indicate that this species is not present with high abundances in this fjord.

5.5 The impact of anthropogenic organic carbon discharges in Kaldfjorden

The natural "reference" conditions between the IN- and OUT-core show clear differences in several geochemical parameters analysed. There was observed a naturally higher SAR, TOC content, TOC accumulation rate and sand content in the pre-1900 sediments at station IN compared to station OUT (Table 5-3). During the period from 1900 to ~1960 there are some fluctuations in the TOC accumulation rate at station IN, opposed to a more slow and gradual increase at station OUT (Figure 5.1). The two periods of fluctuations in TOC accumulation rate at station IN, with peaks at around ~1926 and ~1954, implies that small increases in pre-aquaculture sediments in Kaldfjorden do occur. However, the increased TOC accumulation rates in these periods were brief, and decreased again after short time. Between 1900-1976 the differences of the mentioned parameters slightly decrease between the two stations (Table 5-3). In post-1976 the largest intensifications of SAR, TOC content, TOC accumulation rate occurs at both stations. Station OUT receives the biggest change compared to its reference conditions, which results in that the recent (post-1976) sediment show more similarities between the two stations.

Table 5-3: Average results of analysed parameters of sediments accumulated before 1900, between 1900 and 1976 and in sediments younger than 1976 (post-aquaculture) at station IN and station OUT.

	Station IN			Station OUT		
	pre-1900	1900-1976	post -1976	pre-1900	1900-1976	post -1976
SAR (g/cm2/year)	0.059*	0.059	0.071	0.043*	0.043	0.06
TOC content (%)	2.2	2.8	3.5	1.3	2.5	3.7
TOC acc. rate (g C/m2/year)	13.2	16.5	25.6	5.7	10.9	22.0
Sand content (>63 µm) (%)	37	34	29	20	27	29
OM source	Dominantly marine with some terrestrial			Domminantly marine		
BFAR (ind/cm2/year)	433	389	540	479	938	1440
Diversity indices: ES(100)	19.4	20.7	23.8	21.0	21.0	22.4
Diversity indices: H'(log2)	3.7	3.8	4.2	3.9	3.9	4.3

The timing of increased SARs and TOC accumulation rates at the two stations, correlate well with the onset of the two major sources of organic carbon discharges to Kaldfjorden; the shrimp factory (1970) and the fish farms (~1976). Because the rapid increase of TOC accumulation rate occurs around the start of these known sources the results could be viewed as chronostratigraphic evidence that further validate the age model of the two cores. In 2009 the fish farm company in Kaldfjorden received a second MAB-licence, and the fish farm production was doubled (see section 2.5 for further information). The increase in production can explain the observed continuous high increase in organic matter to the sediments towards present time. The absolute highest TOC accumulation rate occurs in the surface sediments with 32.5 g C/m^2/year at station IN and 29.7 g C/m^2/year at station OUT. Precipitation data reach back to 1960, and do not indicate that there have been any substantial changes in precipitation over the last ~60 years (Figure 2.5). The possible explanation that a recent increase of OM to the sediments can be caused by natural climate variations is therefore minimized.

Analysed parameters in the present study has been compared to Malangen. According the Directorate of Fisheries map-tool, Malangen has two fish farms located in the outer fjord, and several fish farms located within Malangens many fjord-arms (Directortate of Fisheries, 2018c). In fact, the entire outer coastal area of Troms county is perforated with aquaculture localities according to this map. The present study has therefore not been able to compare recent surface TOC accumulation rates or content values with a pristine fjord in the Troms region. This highlights the importance of this study, where we have been able to compare the TOC accumulation rate with Kaldfjordens own “pristine” conditions. The results from Kaldfjorden point in the direction that the most recent TOC accumulation rate (~2015) at station IN is over twice, and station OUT more than four times as high as observed in pre-1900 sediments. Although high compared to is reference conditions, post-1976 TOC accumulation rates in Kaldfjorden are not particularly higher than other fjords with aquaculture activity (e.g 42 g C/ m^2/year in Onarheimsfjorden and 18-36 g C/m^2/year in Malangen).

The natural differences in the depositional environment in the outer and inner fjord are factors contributing to the difference in the foraminiferal concentration (ind/g), assemblage and the BFAR observed at the two stations. Recent hydrographic parameters retrieved from Kaldfjorden reveal that there is a slight difference between the two stations (slightly higher

bottom water temperatures, salinities and oxygen saturation in the outer fjord) (Table 2-1, Figure 2.6). Although the difference in hydrographic parameters is small, these hydrographic parameters are likely also contributing to the differences in species assemblage.

The BFAR at station IN is relatively stable with exception of the increase observed in the ~2011 sample (1-2 cm core depth) (Figure 4.16A), whereas the BFAR show much more variations up-core at station OUT. At station OUT, BFAR peaks in the ~2008 sample (1-2 cm core depth) (Figure 4.19A). Keeping in mind the mentioned possible errors of the BFAR, there is a similar trend at the two stations with peak BFARs in this period (2008-2011) at the two stations (Table 5-2). These dated samples also had the highest TOC content measured in Kaldfjorden (3.8 - 3.9%) (TOC_{63}% in Figure 4.9A and Figure 4.10A). The BFAR will typically increase with increasing organic flux, but only to the extent where the oxygen concentrations still are stable and high (Duffield et al., 2015). Oxygen measurements in Kaldfjorden reveal that there are high concentrations in the bottom waters. This is with exception for the summer months where there was observed O_2 consumption in bottom waters in the inner Kaldfjorden. Kaldfjorden is assumedly well flushed with annual deep-water renewals (see chapter 2.3 for more information). Although some limitations in CTD data, the increased organic matter accumulated in the sediments do not seem to affect the bottom water oxygen concentrations, and could explain the recent increased benthic foraminifera production.

Although TOC accumulation rate has highly increased there has not been observed major changes in the diversity of the foraminiferal assemblages in the upper core samples. Diversity of the foraminiferal assemblages is stable within “high” EcoQs throughout the cores at both stations (Table 5-2). We don’t know how concentrated the fish farm production in the inner Kaldfjorden has been since 2000, but because of the opening of the larger cage at Rogndalen in 1999, it can be assumed that production in the inner fjord has somewhat decreased since early 2000s. However, the TOC accumulation rate at station IN has still increased from 24.2 to 32.5 g/m^2/year between 1998 and 2015. At station IN the upper core also show a higher content of finer (<63µm) particles, which could be a sign that the bottom sediments are change towards having a more sludge consistence. The *S. fusiformis* thrive in organic rich and muddy sediments (Murray, 2001), and its increase in both the living and dead assemblage is a clear indication that the assemblage composition is experiencing some stress related to the organic matter increase. The increasing presence of *S. fusiformis* in the upper core samples at

both station could be viewed at an early warning sign. It is important to keep in mind that both stations are with distance from the fish farms. The benthic ecology of foraminifera at stations in direct vicinity of the fish farms is unknown.

Although several km apart, the two stations experienced an increase in SAR and TOC accumulation rate around the same time. This indicate that the discharge of organic matter to Kaldfjorden influences areas with distances (>500m) from the potential sources. Since only two cores are analysed in Kaldfjorden, there is insufficient data to conclude with high certainty that POM is dispersed over the larger fjord area. A similar study as Husum and Hald (2014) conducted in Malangen, with continuous sampling from the inner to outer fjord, would give a much better overview of how organic matter is dispersed in the fjord. The limited knowledge on the current regime both in upper water layers and bottom water is a cause for high uncertainties to how the organic matter is dispersed in the fjord.

6 Conclusions

- The sediment core from inner (station IN) and outer Kaldfjorden (station OUT) were successfully dated back to ~1900. The two analysed sediment cores have been collected in a likely undisturbed area.

- The sediment accumulation rate (SAR), which was on the average 0.07 g/cm^2/year at station IN and 0.05 g/cm^2/year at station OUT from 1900 to the present, are a lot lower compared to other southern Norwegian fjords, and to a neighbouring fjord in Troms county.

- The SAR and TOC accumulation rate at the two stations show different rates but a similar and clear temporal trend. Station IN has naturally higher rates compared to station OUT. The trend seen at both stations show a slow linear increase up to ~1976. From ~1976 both stations experienced an increasing exponential trend towards the present. The average TOC accumulation rate from pre- to post-1976 sediments increased from 15 to 26 g C/m^2/year at station IN, and from 7 to 22 g C/m^2/year at station OUT.

- The beginning of increased TOC accumulation rates correlates well with the beginning of aquaculture activity (~1976) and other potential anthropogenic organic carbon sources (~1970) located in Kaldfjorden. The increased TOC accumulation rate to the sediment is likely due to a combination of these sources.

- The highest TOC content and accumulation rates were measured in the upper core samples at both stations. Although post-1976 values are a lot higher than the reference condition at each station, recent values are not higher compared to other fjords with aquaculture. Station OUT receives the largest increase compared to it reference conditions, and thus TOC content and accumulation rate in the upper core cm at the two stations are much more similar than before 1976. The results from TOC accumulations rates in Kaldfjorden do not show any sign of decreased trend in recent times.

- The C/N ratio of sediments in Kaldfjorden indicates that organic matter in sediments at both stations are predominantly marine based. There is a slightly higher C/N ratio at station IN (9.6) compared to OUT (8.0), which indicate that the inner fjord receives slightly more input of terrestrial organic matter. The C/N ratio values in Kaldfjorden is relatively stable through time.

- There is no evidence of increased heavy metal concentrations in Kaldfjorden.

- Although SAR is low in Kaldfjorden, the BFAR is high compared to other available fjord data used in the present study. On the coastal shelf area outside Kaldfjorden there has previously been documented high concentration of foraminifera. The outer coastal area of Troms which Kaldfjorden is a part of, seem to favour a general high production of calcium carbonate secreting organisms like foraminifera.

- The natural differences in the depositional environment and small differences in hydrographic parameters between the outer and inner fjord are factors contributing to the natural higher BFAR observed in the outer Kaldfjorden. It may also explain the clear differences in foraminiferal assemblage observed at the two stations.

- The increased TOC accumulation rates do not seem to have a highly affect the diversity of the foraminiferal assemblages. Diversity of the foraminiferal assemblages is stable within “high” EcoQs throughout all samples investigated. However, the three upper core samples from station IN show a clear change in assemblage composition opposed to lower core samples.

- Increased relative abundance of the opportunistic species *S. fusiformis* occurs in upper core samples at both stations. Increasing relative abundance of *S. fusiformis* can be viewed as an early warning sign that the assemblages are showing some degree of stress related to the increased organic matter supplied to the sediments.

References

Abballe, P. A., & Chivas, A. R. (2017). Organic matter sources, transport, degradation and preservation on a narrow rifted continental margin: Shoalhaven, southeast Australia. *Organic Geochemistry*, *112*, 75–92. https://doi.org/10.1016/J.ORGGEOCHEM.2017.07.001

Ackerfors, H., & Enell, M. (1994). The release of nutrients and organic matter from aquaculture systems in Nordic countries. *Journal of Applied Ichtyology*, *10*(4), 225–241. https://doi.org//10.1111/j.1439-0426.1994.tb00163.x

Altenbach, A. V., Pflaumann, U., Schiebel, R., Thies, A., Timm, S., & Trauth, M. (1999). Scaling precentages and distributional patterns of benthic forminifera with flux rates of organic carbon. *Journal of Foraminiferal Research*, *29*, 173–185.

Alve, E. (1995). Benthic foraminiferal responses to estuarine pollution: a review. *Journal of Foraminiferal Research*, *25*(3), 190-203.

Alve, E. (1991). Foraminifera, climatic change, and pollution: a study of late Holocene sediments in Drammensfiord, southeast Norway. *The Holocene*, *1*(3), 243–261. https://doi.org/https://doi.org/10.1177/095968369100100306

Alve, E., Korsun, S., Schönfeld, J., Dijkstra, N., Golikova, E., Hess, S., … Panieri, G. (2016). Foram-AMBI: A sensitivity index based on benthic foraminiferal faunas from North-East Atlantic and Arctic fjords, continental shelves and slopes. *Marine Micropaleontology*, *122*, 1–12. https://doi.org/10.1016/j.marmicro.2015.11.001

Alve, E., & Murray, J. W. (1997). High benthic fertility and taphonomy of foraminifera: a case study of the Skagerrak, North Sea. *Marine Micropaleontology*, *31*(3–4), 157–175. https://doi.org/10.1016/S0377-8398(97)00005-4

Alve, E., Lepland, A., Magnusson, J., & Backer-Owe, K. (2009). Monitoring strategies for re-establishment of ecological reference conditions: possibilities and limitations. *Marine Pollution Bulletin*, *59*(8-12), 297-310.

Appleby, P. G. (2001). Chronostratigraphic techniques in recent sediments. In Springer (Ed.), *Tracking environmental change using lake sediments* (1st ed., pp. 171–203). Dordrecht.

Appleby, P. G., Nolan, P. J., Gifford, D. W., Godfrey, M. J., Oldfield, F., Anderson, N. J., & Battarbee, R. W. (1986). 210Pb dating by low background gamma counting. *Hydrobiologia*, 143 (1): 21-27.

Appleby, P. G., & Piliposian, G. . (2018). *Radiometric Dating of two marine sedimentcores from Kaldfjorden, northern Norway*.

Aure, J., Dahl, E., Green, N., Johnsen, T., Lømsland, E., Magnusson, J., … Walday, M. (2002). Langtidsovervåking av miljøkvaliteten i kystområdene av Norge. 10-års rapport, 1990-1999. Statlig program for forurensningsovervåking Kystovervåkingsprogrammet., 131.

Aure, J., & Østensen, Ø. (1993). Hydrografiske normaler og langtidsvariasjoner i norske kystfarvann. *Hydrografiske Normaler Og Langtidsvariasjoner i Norske Kystfarvann*, (6), 67.

Beckman Coulter LS 320 Laser Diffraction Particle Size Analyser, User Manual, *Beckman Coulter, Inc.* Brea, CA, 2011

Berg, I., Johansen, F. M., Johnsen, T. A., Kjelstrup, S., Lejon, R., Matheussen, G., & Tjeldflåt, A. (2009). *Vann og avløp Tromsø kommune - Hovedplan avløp og vannmiljø 2009-2018*. Tromsø. Retrieved from

https://www.tromso.kommune.no/getfile.php/1813311.1308.yqsvardxuv/Hovedplan_avlop_og_vannmiljo_v2.pdf

Bergh, S. G., Kullerud, K., Armitage, P. E. B., Zwaan, K. B., Corfu, F., Ravna, E. J. K., & Myhre, P. I. (2010). Neoarchaean to svecofennian tectono-magmatic evolution of the West Troms Basement complex, North Norway. *Norsk Geologisk Tidsskrift*, *90*(1–2), 21–48.

Boggs, S. (2014). Transport and Deposition of Siliciclastic Sediment. In *Sedimentology and Stratigraphy* (5th ed., pp. 19–43). Pearson.

Bouchet, V. M. P., Alve, E., Rygg, B., & Telford, R. J. (2012). Benthic foraminifera provide a promising tool for ecological quality assessment of marine waters. *Ecological Indicators*, *23*, 66–75. https://doi.org/10.1016/J.ECOLIND.2012.03.011

Brooks, K. M., & Mahnken, C. V. . (2003). Interactions of Atlantic salmon in the Pacific northwest environment: II. Organic wastes. *Fisheries Research*, *62*(3), 255–293. https://doi.org/https://doi.org/10.1016/S0165-7836(03)00064-X

Brown, J. R., Gowen, R. J., & McLusky, D. S. (1987). The effect of salmon farming on the benthos of a Scottish sea loch. *Journal of Experimental Marine Biology and Ecology*, *109*(1), 39–51. https://doi.org/10.1016/0022-0981(87)90184-5

Carroll, M. L., Cochrane, S., Fieler, R., Velvin, R., & White, P. (2003). Organic enrichment of sediments from salmon farming in Norway: Environmental factors, management practices, and monitoring techniques. *Aquaculture*, *226*(1–4), 165–180. https://doi.org/10.1016/S0044-8486(03)00475-7

Curtin, R., & Prellezo, R. (2010). Understanding marine ecosystem based management: A literature review. *Marine Policy*, *34*(5), 821–830. https://doi.org/10.1016/J.MARPOL.2010.01.003

Directorate of Fisheries. (2018a). Akvakultur/Akvakulturstatistikk/Totalt, hele næringen. Retrieved March 1, 2018, from https://www.fiskeridir.no/Akvakultur/Statistikk-akvakultur/Akvakulturstatistikk-tidsserier/Totalt-hele-naeringen

Directorate of Fisheries. (2018b). Fiskeridirektoratet/Akvakultur/Registre og skjema/ Akvakulturregisteret. Retrieved April 29, 2018, from https://www.fiskeridir.no/Akvakultur/Registre-og-skjema/Akvakulturregisteret

Directorate of Fisheries. (2018c). Map-tool. Retrieved May 20, 2018, from https://kart.fiskeridir.no/akva

Dolven, J. K., Alve, E., Rygg, B., & Magnusson, J. (2013). Defining past ecological status and in situ reference conditions using benthic foraminifera: A case study from the Oslofjord, Norway. *Ecological Indicators*, *29*, 219–233. https://doi.org/10.1016/J.ECOLIND.2012.12.031

Duffield, C. J., Alve, E., Andersen, N., Andersen, T. J., Hess, S., & Strohmeier, T. (2017). Spatial and temporal organic carbon burial along a fjord to coast transect: A case study from Western Norway. *Holocene*, *27*(9), 1325–1339. https://doi.org/10.1177/0959683617690588

Duffield, C. J., Hess, S., Norling, K., & Alve, E. (2015). The response of Nonionella iridea and other benthic foraminifera to “fresh” organic matter enrichment and physical disturbance. *Marine Micropaleontology*, *120*, 20–30. https://doi.org/10.1016/J.MARMICRO.2015.08.002

Eklima.no. (2018). Climate database of the Norwegian Meterological Institute. Retrieved April 4, 2018, from eklima.no

Eriksen, S. D. (2016a). *B-undersøkelse på oppdrettslokalitet Rogndalen*. Tromsø.

Eriksen, S. D. (2016b). *Sjurelv Fiskeoppdrett AS, Strømmåling Rogndalen; 5m, 15m, spredning- og brunnstrøm*. Tromsø.

FAO. (2016). *The State of World Fisheries and Aquaculture: Contributing to food security and nutrition for all*. Rome. https://doi.org/10.5860/CHOICE.50-5350

Faust, J. C., Scheiber, T., Fabian, K., Vogt, C., & Knies, J. (2017). Geochemical characterisation of northern Norwegian fjord surface sediments: A baseline for further paleo-environmental investigations. *Continental Shelf Research*, *148*(August), 104–115. https://doi.org/10.1016/j.csr.2017.08.015

Freiwald, A. (1998). Modern nearshore Cold-Temperate Calcareous Sediments in the Troms Distric, Northern Norway. *Journal of Sedimentray Research*, *68*(5), 763–776. https://doi.org/10.1306/D426886F-2B26-11D7-8648000102C1865D

Goodsite, M., Cole, A., Dastoor, A., Douglas, T., Durnford, D., Goodsite, M., … Christensen, J. (2005). Where Does Mercury in the Arctic Environment Come From , and How Does it Get There ? In *AMAP Assessment 2011:Mercury in the Arctic* (pp. 9–193).

Gustafsson, M., & Nordberg, K. (2000). Living (Stained) benthic Foraminifera and their response to the seasonal hydrographic cycle, periodic hypoxia and to primary production in Havstens Fjord on the Swedish west coast. *Estuarine, Coastal and Shelf Science*, *51*(6), 743–761. https://doi.org/10.1006/ecss.2000.0695

Hald, M., & Korsun, S. (1997). Distribution of modern benthic foraminifera from fjords of Svalbard, European Arctic. *Journal of Foraminiferal Research*, *27*(2), 101–122. https://doi.org/https://doi.org/10.2113/gsjfr.27.2.101

Herguera, J. (1992). Deep-sea benthic foraminifera and biogenic opal: Glacial to postglacial productivity changes in the western equatorial Pacific. *Marine Micropaleontology*, *19*(1–2), 79–98. https://doi.org/10.1016/0377-8398(92)90022-C

Hermansen, H. O. (2015). *Sedimentære avsetningsmiljøer og deglasiasjonshistorie i Kaldfjorden , Kvaløya , Troms Fylke*.

Howe, J. A., Austin, W. E. N., Forswick, M., & Paetzel, M. (2000). *Fjord Systems and Archives*. London: The Geological Scociety.

Hulbert, S. H. (1971). The Nonconcept of Species Diversity: A Critique and Alternative Parameters. *Ecology*, *52*(4), 577–586. https://doi.org/https://doi.org/10.2307/1934145

Husum, K., & Hald, M. (2004). Modern Foraminiferal Distribution in the Subarctic Malangen Fjord and Adjoining Shelf, Northern Norway. *The Journal of Foraminiferal Research*, *34*(1), 34–48. https://doi.org/10.2113/0340034

Jørgensen, B. B., & Richardson, K. (1996). *Coastal and Eustarine Studies - Eutrophication in Coastal Marine Ecosystems*. Washington DC: American Geophysical Union.

Keeley, N. B., Forrest, B. M., & Macleod, C. K. (2015). Benthic recovery and re-impact responses from salmon farm enrichment: Implications for farm management. *Aquaculture*, *435*, 412–423. https://doi.org/10.1016/J.AQUACULTURE.2014.10.007

Klitgaard-Kristensen, D., Sejrup, H. F., & Haflidason, H. (2002). Distribution of recent calcareous benthic foraminifera in the northern North Sea and relation to the environment. *Polar Research*, *21*(2), 275–282. https://doi.org/10.1111/j.1751-8369.2002.tb00081.x

Klootwijk, T. A.(2018) Retrieved data from work in progress (unpublished data)

Kutti, T., Ervik, A., & Hansen, P. K. (2007a). Effects of organic effluents from a salmon farm on a fjord system. I. Vertical export and dispersal processes. *Aquaculture*, *262*(2–4), 367–381. https://doi.org/10.1016/J.AQUACULTURE.2006.10.010

Kutti, T., Ervik, A., & Høisæter, T. (2008). Effects of organic effluents from a salmon farm on a fjord system. III. Linking deposition rates of organic matter and benthic productivity. *Aquaculture*, *282*(1–4), 47–53. https://doi.org/10.1016/J.AQUACULTURE.2008.06.032

Kutti, T., Hansen, P. K., Ervik, A., Høisæter, T., & Johannessen, P. (2007b). Effects of organic effluents from a salmon farm on a fjord system. II. Temporal and spatial patterns in infauna community composition. *Aquaculture*, *262*(2–4), 355–366. https://doi.org/10.1016/J.AQUACULTURE.2006.10.008

Lamb, A. L., Wilson, G. P., & Leng, M. J. (2006). A review of coastal palaeoclimate and relative sea-level reconstructions using δ13C and C/N ratios in organic material. *Earth-Science Reviews*, *75*(1–4), 29–57. https://doi.org/10.1016/J.EARSCIREV.2005.10.003

Lyons, B. P., Thain, J. E., Stentiford, G. D., Hylland, K., Davies, I. M., & Vethaak, A. D. (2010). Using biological effects tools to define Good Environmental Status under the European Union Marine Strategy Framework Directive. *Marine Pollution Bulletin*, *60*(10), 1647–1651. https://doi.org/10.1016/J.MARPOLBUL.2010.06.005

MAREANO. (2018) Retrieved May 20, 2018, from http://mareano.no/kart/mareano.html

Mankettikkara, R. (University of T. (2013). Hydrophysical characteristics of the northern Norwegian coast and fjords. *Dissertation for the Degree of Philosophiae Doctor*, (August).

Meyers, P. A. (1994). Preservation of elemental and isotopic source identification of sedimentary organic matter. *Chemical Geology*, *114*(3–4), 289–302. https://doi.org/10.1016/0009-2541(94)90059-0

Mikkola, F., Pedersen, G., Velvin, R., & Carroll, M. (2000). *Resipientundersøkelse i kaldfjorden for Tromsø Reker AS, 200*. Tromsø.

Ministry of Fisheries. (2016). Biomasse. Retrieved April 11, 2018, from https://www.fiskeridir.no/Akvakultur/Drift-og-tilsyn/Biomasse

Murray, J. W. (2001). *Ecology and Applications of Benthic Foraminifera*.

Murray, J. W., & Alve, E. (2016). Benthic foraminiferal biogeography in NW European fjords: A baseline for assessing future change. *Estuarine, Coastal and Shelf Science*, *181*, 218–230. https://doi.org/10.1016/J.ECSS.2016.08.014

NGU-Norges Geologiske Undersøkelser. (2018). Nasjonal løsmassedatabase. Retrieved May 1, 2018, from http://geo.ngu.no/kart/losmasse/

NVE- Norges vassdrags- og energidirektorat (2018). Nedbørsfelt REGINE. Retrieved May 5, 2018, from https://temakart.nve.no/link/?link=nedborfelt

Østrem, A. K. (2018). *Personal communication, recieved CTD data collected by Havforskningsinstituttet (Unpublished data)*. Bergen.

Pedersen, T., & Mikkola, F. (2001). *Oppfølgende undersøkelse av vannkvalitet i Kaldfjord - Tromsø Reker AS*. Tromsø.

Pinet, P. R. (2013). The Human Presence in the Ocean. In *Invitation to Oceanography* (6th ed., pp. 492–526). New York: Jones and Bartlett Learning.

Roger Bray, J., & Curtis, J. T. (1957). An Ordination of the Upland Forest Communities of Southern Wisconsin. *Ecological Monographs*, *27*(4), 326–349. https://doi.org/https://doi.org/10.2307/1942268

Sætre, R. (2007). *The Norwegian Coastal Current - Oceanography and Climate*. Tapir Academic Press. Trondheim.

Sauer, S., Hong, W.-L., Knies, J., Lepland, A., Forwick, M., Klung, M., … Schubert, C. J. (2016). Sources and turnover of organic carbon and methane in fjord and shelf sediments off northern Norway. *Geochemistry, Geophysics, Geosystems*, *17*(10), 4011–4031. https://doi.org/https://doi.org/10.1002/2016GC006296

Sejrup, H. P., & Guilbault, J. P. (1980). Cassidulina reniforme and C. obtusa (Foraminifera), taxonomy, distribution, and ecology. *Sarsia*, *65*(2), 79–85. https://doi.org/https://doi.org/10.1080/00364827.1980.10431476

Shannon, C. E., & Weaver, W. (1964). *The Mathimatical Theory of Communication*. Urbana: University of Illinois.

Sigvaldsen, L., & Lindkjenn, K. T. (1992). *Rensing av Avløpsvann*. Retrieved from https://www.nb.no/items/URN:NBN:no-nb_digibok_2007100100052

Sjetne, L. B. (2017). *Organic carbon accumulation in Hardangerfjorden - A micropaleontological and geochemical study of benthic environmental impact from fish farming*. (Master thesis) University of Oslo. Retrieved from https://www.duo.uio.no/

Skarbøvik, E., Allan, I., Stålnacke, P., Hagen, A. G., Greipsland, I., Høgåsen, T., … Beldring, S. (2015). *Riverine inputs and direct discharges to Norwegian coastal waters -2014*. NIVA. Retrieved from http://miljodirektoratet.no/Documents/publikasjoner/M439/M439.pdf

Smith, R. W., Bianchi, T. S., Allison, M., Savage, C., & Galy, V. (2015). High rates of organic carbon burial in fjord sediments globally. *Nature Geoscience*, (8.6), 450–453.

Statistisk Sentralbyrå (SSB). (2018). Tabell: 04317:Folkemengde, etter grunnkrets (G) 199-2018. Retrieved April 11, 2018, from https://www.ssb.no/statbank/table/04317/?rxid=2e974a58-a715-4e2f-a376-32175b15f469

Sundby, S. (1984). Influence of bottom topography on the circulation at the continentat shelf of northern Norway. *Fiskeridirektoratets Skrifter, Serie Havundersøkelser*, *17*, 501–519. https://doi.org//10.1016/0924-7963(95)00037-2

Svåsand, T., Grefsrud, E. S., Karlsen, Ø., Kvamme, B. O., Glover, K., Husa, V., & Kristiansen, T. S. (2017). Risikorapport norsk fiskeoppdrett 2017. *Fisken Og Havet*, *2*, 179.

Svåsand, T., Karlsen, Ø., Kvamme, B. O., Stien, L. H., Taranger, G. L., & Boxaspen, K. K. (2016). Risikovurdering av norsk fiskeoppdrett 2016. *Fisken Og Havet*, *2*, 192.

Sweetman, A. K., Norling, K., Gunderstad, C., Haugland, B. T., & Dale, T. (2014). Benthic ecosystem functioning beneath fish farms in different hydrodynamic environments. *Limnology and Oceanography*, *59*(4), 1139–1151. https://doi.org/10.4319/lo.2014.59.4.1139

Syvitski, J. P. M., Burrell, D. C., & Skei, J. M. (1987). *Fjords: Processes and Products*. New York: Springer-Verlag New York Inc. https://doi.org/10.1007/978-1-4632-9

Tårnesvik, G. (2012, December 21). 250 000 laks kvalt i merdene. *Nordlys*. Retrieved from https://www.nordlys.no/naring/250-000-laks-kvalt-i-merdene/s/1-79-6407025

Torper, M. (2017). *Den historiske utviklingen av organisk karbon og naturtilstanden i dypbassenget til*

Lurefjorden , Hordaland - En mikropaleontologisk og geokjemisk studie. (Master thesis) University of Oslo. Retrieved from https://www.duo.uio.no/

Valdemarsen, T., Hansen, P. K., Ervik, A., & Bannister, R. J. (2015). Impact of deep-water fish farms on benthic macrofauna communities under different hydrodynamic conditions. *Marine Pollution Bulletin*, *101*(2), 776–783. https://doi.org/10.1016/J.MARPOLBUL.2015.09.036

Velvin, R., Evenset, A., Forberg, K., & Vogele, B. (2008). *Resipientundersøkelser i Ramfjord , Kaldfjord og Ersfjord*. Tromsø.

Veileder 02:2013 – revidert 2015: Kalssifisering av miljøtilstand i vann – Økologisk og kjemisk klassifieringssystem for kystvann, grunnvann, innsjøer og elver.

Veileder M:633 (2016). Bløtbunnsfauna som indikator for miljøtilstand i kystvann.

Veileder M:608 (2016). Grenseverdier for klassifisering av vann, sediment og biota.

Velvin, R., & Worum, B. (2012). *Sjurelv Fiskeoppdrett: C undersøkelse Kræmarvika 2012*. Tromsø.

Walker, E. (2018). *Pelagic-Benthic Coupling in a Northern Norwegian Fjord Over Winter : Considering Seasonality in High-Latitude Aquaculture*. (Unpublished Master thesis) University of Akureyri.

Wassmann, P., Reigstad, M., Øygarden, S., & Rey, F. (2000). Seasonal variation in hydrography, nutrients, and suspended biomass in a subarctic fjord: Applying hydrographic features and biological markers to trace water masses and circulation significant for phytoplankton production. *Sarsia*, *85*(3), 237–249. https://doi.org/10.1080/00364827.2000.10414576

Wassmann, P., Svendsen, H., Keck, A., & Reigstad, M. (1996). Selected aspects of the physical oceanography and particle fluxes in fjords of northern Norway. *Journal of Marine Systems*, *8*(1–2), 53–71. https://doi.org/10.1016/0924-7963(95)00037-2

Zonta, R., Zaggia, L., & Argese, E. (1994). Heavy metal and grain-size distributions in estuarine shallow water sediments of the Cona Marsh (Venice Lagoon, Italy). *Science of the Total Environment, The*, *151*(1), 19–28. https://doi.org/10.1016/0048-9697(94)90482-0

Zwaan, K. B. (1995). Geology of the West Troms Basement Complex, northern Norway, with emphasis on the Senja Shear Belt: a prelimi- nary account. *Geological Survey of Norway Bulletin*, *427*, 33–36. Retrieved from http://www.ngu.no/filearchive/NGUPublikasjoner/Bulletin427_33-36.pdf

Appendices:

Appendix A: Lab report from sediment dating

Radiometric Dating of two marine sediment cores from Kaldfjorden, northern Norway

P.G.Appleby and G.T.Piliposian
Environmental Radioactivity Research Centre
University of Liverpool

Methods

Dating by ^{210}Pb and ^{137}Cs was carried out on marine sediment cores 46-C and D-15 collected from Kaldfjorden in northern Norway. Sub-samples from each core were analysed for ^{210}Pb, ^{226}Ra, and ^{137}Cs by direct gamma assay in the Liverpool University Environmental Radioactivity Laboratory, using Ortec HPGe GWL series well-type coaxial low background intrinsic germanium detectors (Appleby *et al*. 1986). ^{210}Pb was determined via its gamma emissions at 46.5 keV, and ^{226}Ra by the 295 keV and 352 keV γ-rays emitted by its daughter radionuclide ^{214}Pb following 3 weeks storage in sealed containers to allow radioactive equilibration. ^{137}Cs was measured by its emissions at 662 keV. The absolute efficiencies of the detectors were determined using calibrated sources and sediment samples of known activity. Corrections were made for the effect of self-absorption of low energy γ-rays within the sample (Appleby *et al.* 1992).

Results

The results of the radiometric analyses carried out on each core are given in Tables 1–2 and shown graphically in Figures 1.i–2.i. Supported ^{210}Pb activity was assumed to be equal to the measured ^{226}Ra activity, and unsupported ^{210}Pb activity calculated by subtracting supported ^{210}Pb from the measured total ^{210}Pb activity.

Kaldfjorden Core 46-C

Lead-210 Activity
Total ^{210}Pb activity (Figure 1.i(a)) reached equilibrium with the supporting ^{226}Ra at a depth of around 12 cm. Unsupported ^{210}Pb concentrations (Figure 1.i(b)) decline relatively uniformly with depth though with a reduced gradient in the upper sections of the core that may indicate a recent increase in the sedimentation rate.

Artificial Fallout Radionuclides
^{137}Cs concentrations have a relatively well-defined peak in the 6-7 cm sample (Figure 1.i(c)) that most probably records the peak levels of fallout in the 1960s from the atmospheric testing of nuclear weapons.

Core Chronology
^{210}Pb dates calculated using the CRS (Appleby and Oldfield 1978) place 1963 at a depth of around 7 cm, in relatively good agreement with the 1963 depth suggested by the ^{137}Cs record. A small correction has been made to the post-1963 dates using the ^{137}Cs date as a reference point (Appleby 2001). Pre-1963 dates have been calculated using the mean sedimentation rate of 0.059 ± 0.006 g cm^{-2} y^{-1} (0.08 cm y^{-1}) determined from the gradient of the ^{210}Pb record below 6.5 cm. The results, shown in Figure 1.ii and given in detail in Table 3, further suggest a significant increase in recent decades to a contemporary value of 0.077 g cm^{-2} y^{-1} (0.18 cm y^{-1})

Kaldfjorden Core D-15

Lead-210 Activity
^{210}Pb/^{226}Ra equilibrium in this core is reached at a depth of around 8 cm (Figure 2.i(a)), significantly shallower than in 46-C. The unsupported ^{210}Pb record (Figure 2.i(b)) has two distinct parts. A steep and more-or-less exponential decline in concentrations in the lower half (below 4 cm) suggests slow but uniform sedimentation in the earlier part of the record. In the upper part of the record, particularly

in sediments above 3 cm, concntrations are virtually constant. This could indicate either a recent increase in the sedimentation rate, or sediment mixing of the surficial sediments.

Artificial Fallout Radionuclides

Although the ^{137}Cs record in this core (Figure 2.i(c)) does not have a clearly defined peak, relatively high values in the uppermost 5 cm of the core may identify post-1963 sediments. The lack of a distinct record may simply be due to the poor retention of ^{137}Cs, presumably because of its greater mobility in sea water. In both cores concentrations are nearly two orders of magnitude lower than ^{210}Pb.

Core Chronology

^{210}Pb dates calculated using the CRS model place 1963 within the 4-5 cm sample, in relatively good agreement with the suggestion that sediments above 5 cm post-date the early 1960s weapons test fallout maximum. The ^{210}Pb calculations indicate a relatively uniform sediment rate through most of the 20th century with a mean value during that time of 0.043 ± 0.005 g cm^{-2} y^{-1} (0.05 cm y^{-1}). They further suggest that in recent years this may have increased significantly, to a contemporary value of around 0.068 g cm^{-2} y^{-1} (0.14 cm y^{-1}). The results are shown in Figure 2.ii and given in detail in Table 4. In view of the poor ^{137}Cs record and possibility that the ^{210}Pb record has been affected by mixing these results must however be treated with caution unless supported by other evidence.

References

Appleby PG, 2001. Chronostratigraphic techniques in recent sediments, in *Tracking Environmental Change Using Lake Sediments Volume 1: Basin Analysis, Coring, and Chronological Techniques*, (eds W M Last & J P Smol), Kluwer Academic, pp171-203.

Appleby PG, PJ Nolan, DW Gifford, MJ Godfrey, F Oldfield, NJ Anderson & RW Battarbee, 1986. ^{210}Pb dating by low background gamma counting. *Hydrobiologia*, **141**:21-27.

Appleby PG & F Oldfield, 1978. The calculation of ^{210}Pb dates assuming a constant rate of supply of unsupported ^{210}Pb to the sediment. *Catena*, **5**:1-8

Appleby PG, N Richardson, & PJ Nolan, 1992. Self-absorption corrections for well-type germaniun detectors. *Nucl. Inst.& Methods B*, **71**: 228-233.

Table 1. Fallout radionuclide concentrations in the Kaldfjorden sediment core 46-C

Depth		^{210}Pb						^{137}Cs	
		Total		Unsupported		Supported			
cm	g cm^{-2}	Bq kg^{-1}	±	Bq kg^{-1}	±	Bq kg^{-1}	±	Bq kg^{-1}	±
0.5	0.14	211.2	9.4	189.5	9.6	21.7	1.5	3.1	0.8
1.5	0.50	206.2	9.6	185.8	9.7	20.5	1.5	2.7	0.8
2.5	0.96	187.4	7.6	164.7	7.8	22.8	1.4	4.3	0.9
3.5	1.46	170.7	7.3	148.9	7.5	21.9	1.4	3.1	0.9
4.5	2.04	139.0	6.8	117.8	6.9	21.2	1.2	4.2	0.7
5.5	2.70	117.6	6.4	94.6	6.5	23.0	1.1	4.1	0.8
6.5	3.41	103.3	5.7	78.8	5.8	24.5	1.2	6.2	0.9
7.5	4.15	77.0	5.0	53.3	5.1	23.7	1.0	3.0	0.7
8.5	4.91	55.1	3.3	31.9	3.3	23.2	0.8	2.3	0.4
9.5	5.70	41.4	3.7	21.3	3.8	20.1	0.8	0.6	0.4
10.5	6.52	39.7	3.3	15.9	3.4	23.8	0.8	0.1	0.5
11.5	7.35	26.8	3.1	5.6	3.2	21.2	0.7	0.0	0.0
12.5	8.20	30.3	3.3	8.4	3.3	21.9	0.7	0.0	0.4
13.5	9.07	29.7	3.2	8.0	3.3	21.6	0.7	0.6	0.4
14.5	9.94	25.2	2.5	3.4	2.5	21.9	0.6	0.8	0.3
16.5	11.75	24.8	2.7	3.6	2.8	21.2	0.6	0.0	0.3

Table 2. Fallout radionuclide concentrations in the Kaldfjorden sediment core D-15

Depth		^{210}Pb						^{137}Cs	
		Total		Unsupported		Supported			
cm	g cm^{-2}	Bq kg^{-1}	±	Bq kg^{-1}	±	Bq kg^{-1}	±	Bq kg^{-1}	±
0.5	0.21	180.4	8.0	164.2	8.1	16.3	1.4	4.4	0.8
1.5	0.67	189.8	7.5	172.0	7.6	17.8	1.3	4.6	0.8
2.5	1.21	189.3	7.3	168.0	7.5	21.3	1.3	3.9	0.9
3.5	1.80	152.6	6.4	133.9	6.5	18.8	1.3	3.7	0.8
4.5	2.51	109.3	6.7	89.7	6.8	19.6	1.2	3.9	0.8
5.5	3.37	57.8	5.4	38.7	5.5	19.2	1.1	1.8	0.6
6.5	4.31	36.9	3.3	16.6	3.4	20.3	0.7	1.8	0.4
7.5	5.28	31.5	2.6	9.9	2.7	21.6	0.5	0.9	0.4
8.5	6.28	29.9	3.1	8.7	3.2	21.2	0.7	1.4	0.3
9.5	7.29	27.5	4.0	4.0	4.1	23.5	0.8	1.2	0.4
10.5	8.30	26.7	3.2	0.8	3.3	25.8	0.8	1.5	0.5
11.5	9.29	23.4	3.2	-2.5	3.3	25.9	0.8	0.9	0.4
12.5	10.32	28.6	3.2	5.0	3.3	23.6	0.7	0.6	0.3
14.5	12.39	18.5	3.3	-6.9	3.4	25.5	0.7	0.0	0.0

Table 3 ^{210}Pb chronology of the Kaldfjorden sediment core 46-C

Depth		Chronology			Sedimentation Rate		
		Date	Age				
cm	g cm^{-2}	AD	y	±	g cm^{-2} y^{-1}	cm y^{-1}	± (%)
0.0	0.00	2017	0	0			
0.5	0.14	2015	2	2	0.085	0.25	5.8
1.5	0.50	2011	6	2	0.080	0.20	6.0
2.5	0.96	2005	12	2	0.073	0.15	5.8
3.5	1.46	1998	19	2	0.067	0.12	6.3
4.5	2.04	1989	28	3	0.062	0.10	7.3
5.5	2.70	1978	39	5	0.062	0.09	8.6
6.5	3.41	1967	50	5	0.062	0.08	9.9
7.5	4.15	1954	63	6	0.059	0.08	10.0
8.5	4.91	1941	76	6	0.059	0.08	10.0
9.5	5.70	1928	89	7	0.059	0.07	10.0
10.5	6.52	1914	103	8	0.059	0.07	10.0
11.5	7.35	1900	117	9	0.059	0.07	10.0

Table 4. ^{210}Pb chronology of the Kaldfjorden sediment core D-15

Depth		Chronology			Sedimentation Rate		
		Date	Age				
cm	g cm^{-2}	AD	y	±	g cm^{-2} y^{-1}	cm y^{-1}	± (%)
0.0	0.00	2017	0	0			
0.5	0.21	2015	2	2	0.078	0.17	6.3
1.5	0.67	2008	9	2	0.065	0.13	6.3
2.5	1.21	1999	18	2	0.052	0.09	7.1
3.5	1.80	1987	30	2	0.043	0.07	9.0
4.5	2.51	1970	47	3	0.043	0.05	12.4
5.5	3.37	1950	67	5	0.043	0.05	12.4
6.5	4.31	1928	89	8	0.043	0.04	12.4
7.5	5.28	1905	112	10	0.043	0.04	12.4

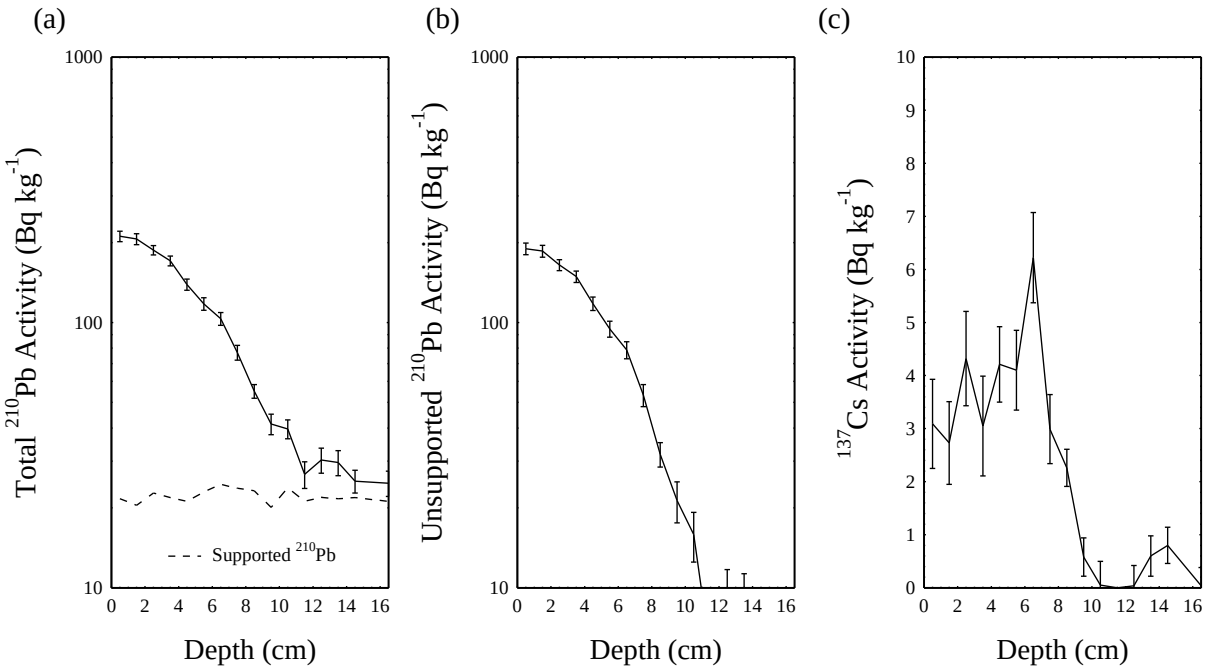

Figure 1.i. Fallout radionuclides in the Kaldfjorden sediment core 46-C showing (a) total and supported ^{210}Pb, (b) unsupported ^{210}Pb, (c) ^{137}Cs concentrations versus depth.

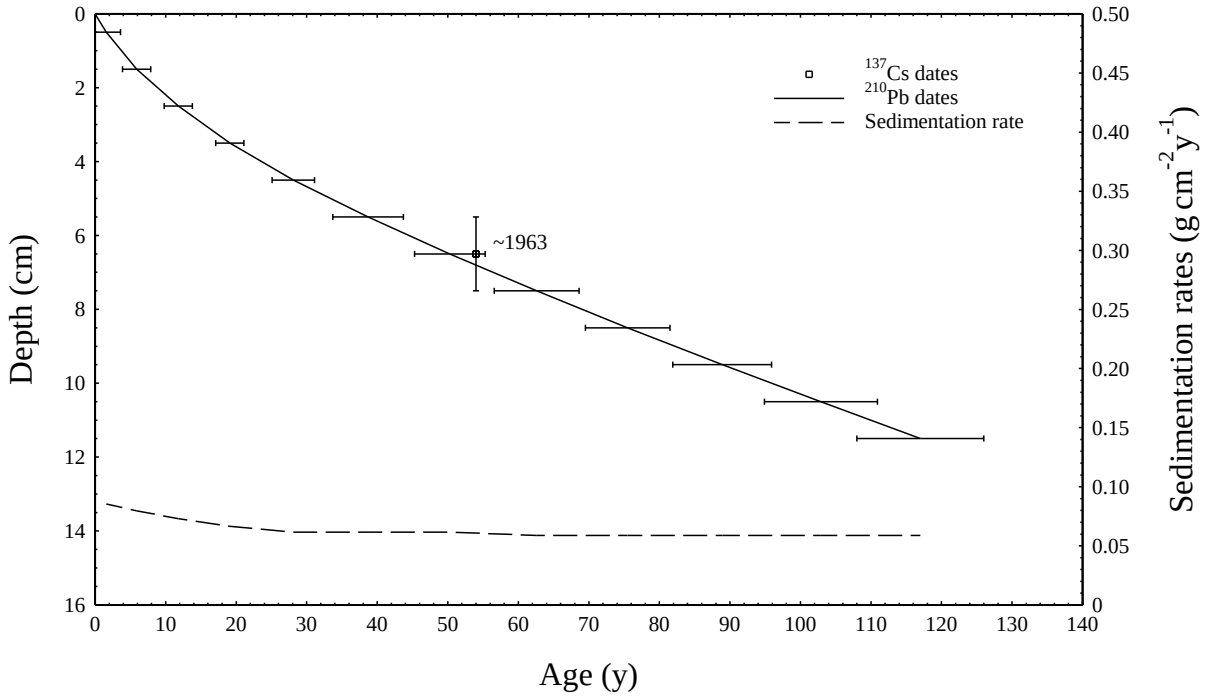

Figure 1.ii. Radiometric chronology of the Kaldfjorden sediment core 46-C showing the ^{210}Pb dates and sedimentation rates and possible 1963 depth suggested by the ^{137}Cs fallout record.

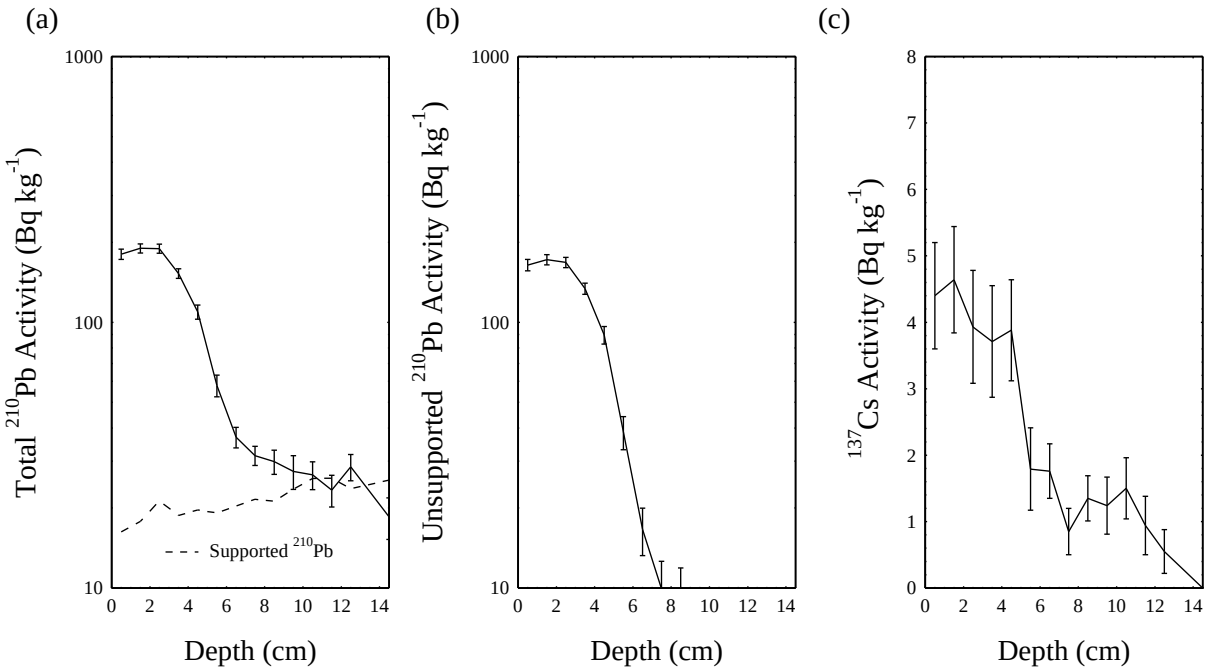

Figure 2.i. Fallout radionuclides in the Kaldfjorden sediment core D-15 showing (a) total and supported ^{210}Pb, (b) unsupported ^{210}Pb, (c) ^{137}Cs concentrations versus depth.

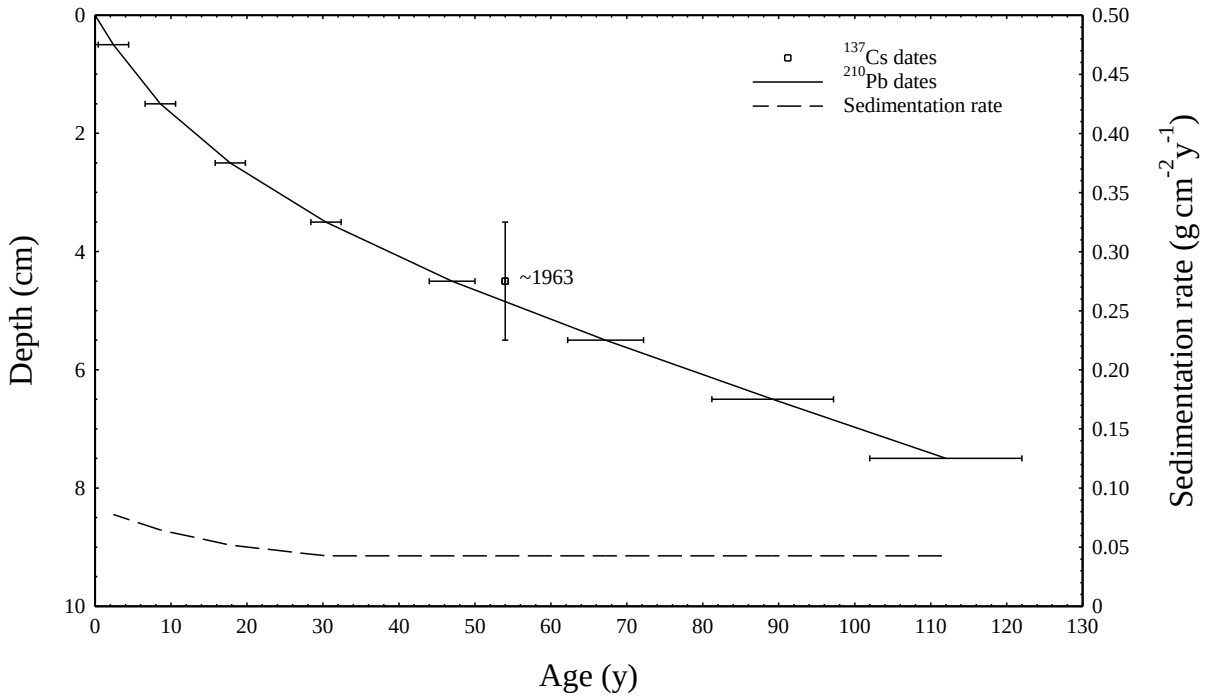

Figure 2.ii. Radiometric chronology of the Kaldfjorden sediment core D-15 showing the ^{210}Pb dates and sedimentation rates and the possible 1963 depth suggested by the ^{137}Cs fallout record.

Appendix B: Results from geochemical analysis

Station IN, IN-C and IN-B core									
Analysis preformed on:		IN-C	IN-C	IN-C	IN-B	IN-C	IN-C	IN-C	IN-C
Core interval (cm)	Core depth (cm)	Sediment age (years AD)	SAR (g/cm2/ year)	Water (%)	Water (%)	Clay (<2µm) (%)	Silt (2-63µm) (%)	Sand (>63µm) (%)	CaCO3 (%)
0-1	0,5	2015	0,085	73,5	67,8	3,5	71,9	24,6	18,5
1-2	1,5	2011	0,080	63,0	63,0	3,2	69,3	27,4	
2-3	2,5	2005	0,073	61,7	60,4	3,6	69,4	27,0	15,4
3-4	3,5	1998	0,067	57,0	59,5	3,8	65,0	31,2	
4-5	4,5	1989	0,062	53,7	56,3	4,2	64,6	31,2	18,0
5-6	5,5	1978	0,062	49,8	52,9	3,7	64,3	32,0	
6-7	6,5	1967	0,062	47,7	50,5	3,7	65,2	31,1	15,2
7-8	7,5	1954	0,059	47,0	48,5	3,7	62,4	33,9	
8-9	8,5	1941	0,059	46,3	48,9	3,3	62,5	34,3	19,0
9-10	9,5	1928	0,059	44,3	47,6	3,5	61,7	34,8	
10-11	10,5	1914	0,059	43,7	43,6	3,3	60,6	36,1	16,6
11-12	11,5	1900	0,059	43,5	41,7	3,3	59,3	37,4	
12-13	12,5	1886*		42,3	41,1	3,9	59,6	36,6	14,8
13-14	13,5	1872*		42,0	41,4	3,8	57,7	38,5	
14-15	14,5	1858*		41,4	40,5	3,7	57,4	38,9	
15-16	15,5	1844*		40,1	39,5	4,3	62,3	33,4	13,4
16-17	16,5	1830*		40,1	39,6	3,9	57,4	38,8	

Station IN, IN-C and IN-B core											
Analysis preformed on:		IN-B	IN-B	IN-B	IN-B	IN-B	IN-B	IN-B	IN-B	IN-B	IN-B
Core interval (cm)	Core depth (cm)	TN(%)	TOC(%)	TOC63 (%)	C/N	Cu (mg/kg)	Zn (mg/kg)	Cd (mg/kg)	Pb (mg/kg)	Cr (mg/kg)	Hg* (mg/kg)
0-1	0,5	0,35	3,38	3,82	9,5	22,2	78,0	0,1	13,5	38,4	0,4
1-2	1,5	0,36	3,36	3,86	9,3	23,3	82,2	0,1	14,3	41,9	0,4
2-3	2,5	0,33	3,30	3,79	10,1	24,8	87,3	0,1	15,3	43,6	0,4
3-4	3,5	0,32	3,05	3,61	9,7	25,2	88,9	0,1	15,4	43,0	0,4
4-5	4,5	0,27	2,69	3,25	10,0	25,4	84,1	0,1	16,8	42,4	0,4
5-6	5,5	0,24	2,36	2,94	9,9	21,1	76,4	0,1	13,8	37,8	0,4
6-7	6,5	0,21	2,18	2,74	10,3	25,9	77,0	0,1	14,1	38,8	0,3
7-8	7,5	0,25	2,55	3,16	10,0	20,3	76,9	0,1	14,4	38,8	0,4
8-9	8,5	0,22	2,15	2,76	9,6	21,3	78,5	0,1	14,7	40,1	0,3
9-10	9,5	0,26	2,47	3,10	9,4	19,3	75,8	0,1	13,9	38,6	0,3
10-11	10,5	0,25	1,92	2,57	7,8	17,3	66,0	0,1	11,1	36,5	0,2
11-12	11,5	0,18	1,68	2,36	9,4	14,9	57,0	0,1	7,9	34,5	0,2
12-13	12,5	0,17	1,68	2,34	9,8	15,4	59,4	0,1	8,7	33,7	0,2
13-14	13,5	0,17	1,67	2,36	9,8	14,2	55,7	0,1	7,2	33,5	0,1
14-15	14,5	0,15	1,42	2,12	9,5	13,5	54,9	0,1	6,5	32,6	0,1
15-16	15,5	0,17	1,64	2,24	9,7	15,2	58,2	0,1	6,7	35,0	0,1
16-17	16,5	0,15	1,43	2,12	9,5	14,3	53,1	0,1	5,9	33,3	0,1

Station OUT, OUT-15 core								
Core interval (cm)	Core depth (cm)	Sediment age (years AD)	SAR (g/cm2/year)	Water (%)	Clay (<2µm) (%)	Silt (2-63µm) (%)	Sand (>63µm) (%)	CaCO3 (%)
0-1	0,5	2015	0,08	65	8	60	32	38
1-2	1,5	2008	0,07	59	8	66	26	
2-3	2,5	1999	0,05	57	8	64	28	41
3-4	3,5	1987	0,04	53	8	63	29	
4-5	4,5	1970	0,04	45	8	62	30	37
5-6	5,5	1950	0,04	39	9	63	28	39
6-7	6,5	1928	0,04	39	9	66	25	
7-8	7,5	1905	0,04	37	9	65	27	38
8-9	8,5	1882*		36	9	63	28	
9-10	9,5	1859*		37	9	68	24	38
10-11	10,5	1836*		37	9	66	24	
11-12	11,5	1813*		37	10	65	25	37
12-13	12,5	1790*		35	10	70	20	
13 -14	13,5	1767*		35	11	76	13	29
14-15	14,5	1744*		36	11	77	13	
15-16	15,5	1721*		36	10	74	16	

Station OUT, OUT-15 core											
Core interval (cm)	Core depth (cm)	TN (%)	TOC (%)	TOC63 (%)	C/N	Cu (mg/kg)	Zn (mg/kg)	Cd (mg/kg)	Pb (mg/kg)	Cr (mg/kg)	Hg* (mg/kg)
0-1	0,5	0,4	3,2	3,8	7,9	16,7	64,6	0,1	17,3	37,5	0,4
1-2	1,5	0,4	3,4	3,8	9,0	18,4	69,7	0,1	18,2	39,0	0,4
2-3	2,5	0,4	3,1	3,6	8,3	18,0	69,5	0,1	17,8	37,6	0,3
3-4	3,5	0,4	2,9	3,4	8,2	17,7	70,4	0,1	17,7	38,9	0,4
4-5	4,5	0,3	2,9	3,4	8,2	16,1	63,4	0,1	15,3	34,9	0,3
5-6	5,5	0,2	2,0	2,5	9,4	15,7	59,3	0,1	11,5	36,6	0,2
6-7	6,5	0,2	1,7	2,1	8,8	17,6	60,6	0,1	9,8	38,2	0,2
7-8	7,5	0,2	1,6	2,1	8,1	21,8	69,9	0,1	8,5	45,8	0,1
8-9	8,5	0,2	1,4	1,9	7,4	21,7	71,7	0,1	8,8	46,2	0,1
9-10	9,5	0,2	1,3	1,8	7,7	26,4	87,4	0,1	9,1	54,5	0,1
10-11	10,5	0,2	1,2	1,6	7,6	25,1	82,8	0,1	8,9	54,5	0,1
11-12	11,5	0,1	1,0	1,5	7,9	26,5	85,6	0,1	8,8	55,9	0,1
12-13	12,5	0,1	0,9	1,2	7,7	28,5	89,0	0,1	8,4	56,9	0,1
13 -14	13,5	0,1	0,6	0,9	7,6	33,5	101,5	0,1	9,3	65,7	0,1
14-15	14,5	0,1	0,6	0,8	7,6	34,0	103,7	0,1	9,3	66,0	0,1
15-16	15,5	0,1	0,5	0,8	6,7	32,2	99,8	0,1	8,8	63,3	0,1

Appendix C: Foraminifera data, total counts and diversity indices

Foram counts (63-500µm)	Station IN (IN-C core)							Station OUT (OUT-15 core)							
Core depth (cm)	0,5	1,5	3,5	6,5	9,5	12,5	15,5	0,5	1,5	2,5	4,5	6,5	8,5	12,5	15,5
Sediment age (year)	2015	2011	1998	1967	1928	1886*	1844*	2015	2008	1999	1970	1928	1882*	1790*	1721*
Core interval (cm)	0-1	1-2	3-4	6-7	9-10	12-13	15-16	0-1	1-2	2-3	4-5	6-7	8-9	12-13	15-16
agglutinated															
Adercotryma glomerata/wrighti	8	8	1	2	1	4									
Ammoscalaria gullmarensis	3														
Cribrostomoides cf. kosterensis	1	6	9	5	5	5	6			2					
Cuneata arctica	5		1												
Eggerelloides medius	5	2	1				2								
Eggerelloides scaber	1														
Eggerella europea			1												
Recurvoides trochamminiformis	4	2			2										
Reophax dentaliniformis	3	1													
Reophax micaceus		1													
Spiroplectammina biformis	5	6	4	3	3	1	7								
Trochammina sp.			1		2	1				1					1
Textulaia sp.		6			1	1									
Textulaia earlandi		1													
Textularia kattegatensis	1														
Textularia cf. contorta			1												
calcareous															
Astrononion gallowayi	5	2		2	5	1	5	8		2	1	3	8	3	2
Bolivina sp.			1					1	1	1	1			1	2
Bolivina pseudopunctata	11	4	5	6	4	4	11		2	9	2	4	5	1	4
Buccella frigida	16	4	12	14	13	15	28			2	4		1		
Bulimina marginata	51	43	24	38	43	42	75	8	5	14	13	13	36	12	14
Bulimina sp								1							
Buliminella elegantissima		3					3								
Cassidulina obtusa				2				4	1				10	4	
Cassidulina laevigata	26	10	12	13	7	9	23	17	32	74	41	52		6	88
Cassidulina reniforme	61	59	48	39	58	68	113	35	70	108	100	107	142	63	102
Cassidulina neoteretis								29	4	12	38	24	158	46	6
Cassidulinoides brodyi										2	2				1
Cassidulinoids sp.														1	
Cibicides refulgens														1	
Cibicides lobatulus	13	17	11	6	6	7	11	20	31	33	12	23	35	16	10
Cibicidoides mundulus								11	22	23	14	18	45	20	20
Comuspira involvens															1
Discorbinella bertheloti	2	3	3	6	2		3	11	6	18	15	13	28	17	17
Elphidium albiumbilicatum	1	6	1	3		9	8	3	10	6	5	3	10	5	4
Elphidium excavatum	38	29	21	22	31	34	60	9	14	20	22	18	25	20	45
Elphidium cf. subarcticum	9	10	12	3		3	12		12	16	19	18		8	8
Elphidium sp.										2	2				
Epistominella vitrea	17	17	9	4	2	4	2	2	2	2	1		4	1	1
Fissurina lagenoides			1	1											
Fissurina marginata			1		4	2								6	
Fissurina orbignyana		1												1	
Fissurina sp.	4	7	1				2	3	3	3	1	1	3		2
Gavelinopsis praegeri	2			1	1			1	4	4	4	4	3		1
Globocassidulina subglobosa									1						
Guttulina communis			1												
Guttulina sp									1	1					
Hyalinea balthica	23	43	10	26	20	27	43	9	11	22	19	17	27	13	17
Islandiella islandica											4				
Islandiella norcrossi		1			4	3			6	5	8	3			
Islandiella sp.														1	
Lenthiculina sp		1						2		1			1	2	
Lagenamnia arenulata	1			1											
Lagena distoma				1		1									
Lagena sp.		1			1							1			
Melonis barleeanus								6	7	7	6	16	34	10	14
Miliolinella subrotunda													1		
Nodosaria sp.															1
Nonionella iridea	13	3	9		4		3	13	12	17	20	6	10	19	5
Nonionella frigida	1	3													
Nonionella turgida										3	2	1	3		
Nonionellina labradorica	11	13	6	9	12	13	22	5	10	17	5	12	39	10	23
Parafissurina sp.										1				1	
Parafissurina fusuliformis														2	
Patellina corrugata	2	1	3		2		2		2	1		2			
Pullenia osloensis	20	40	18	1	21	16	20	26	28	17	34	24	41	10	16
Pullenia bulloides								1						2	
Quinqueloculina stalkeri			1												
Quinqueloculina sp.		1				3							2		
Rosalina sp.														2	
Robertina arctica									1					2	
Stainforthia fusiformis	53	56	30	18	17	19	22	7	11	3		2	6	2	
Stainforthia concave	7	4	1		7	2	5	1		2	6	4	13	4	11,00
Stainforthia schreibersiana					5	2								3	
Trifarina angulosa	6	4				1	1	7	7	8	10	10	35	10	9,00
Triloculina tricarinata									2			1			
Uvigerina peregrina			2												
Sum counted tests	342	419	262	226	283	297	489	240	318	459	411	400	725	325	425
No tests/g dry sediment	4685	10163	6088	5766	7128	6899	7782	12443	30515	26293	19289	24474	19139	7736	6509
BFAR (ind/cm2/year)	398	813	408	358	421	407	459	971	1984	1367	829	1052	823	333	280
% agglutinated tests	10	8	7	4	5	4	3	0	0	0,7	0	0	0	0	0,2
% calcareous tests	90	92	93	96	95	96	97	100	100	99	100	100	100	100	100
nr. of species	29	37	33	24	28	27	25	26	29	35	29	27	27	35	27
ES100	24,2	24,1	23,2	19,5	21,9	20,0	18,7	21,7	22,4	23,1	21,6	20,3	19,1	24,9	19,1
H' (log2)	4,2	4,2	4,1	3,8	3,9	3,8	3,7	4,1	4,9	4,0	3,9	3,8	3,8	4,2	3,6

Appendix D: Foraminifera data, relative species abundance (%)

Relative abundance (%)	Station IN (IN-C core)							Station OUT (OUT-15 core)							
Core depth (cm)	0,5	1,5	3,5	6,5	9,5	12,5	15,5	0,5	1,5	2,5	4,5	6,5	8,5	12,5	15,5
Sediment age (year)	2015	2011	1998	1967	1928	1886*	1844*	2015	2008	1999	1970	1928	1882*	1790*	1721*
Core interval (cm)	0-1	1-2	3-4	6-7	9-10	12-13	15-16	0-1	1-2	2-3	4-5	6-7	8-9	12-13	15-16
Adercotryma glomerata/wrighti	2,3	1,9	0,4	0,9	0,4	1,3	0,0	0,0	0,0	0,0	0,0	0,0	0,0	0,0	0,0
Ammoscalaria gullmarensis	0,9	0,0	0,0	0,0	0,0	0,0	0,0	0,0	0,0	0,0	0,0	0,0	0,0	0,0	0,0
Ammoscalaria tenuimargo	0,0	0,0	0,0	0,0	0,0	0,0	0,0	0,0	0,0	0,0	0,0	0,0	0,0	0,0	0,0
Cribrostomoides crassimargo	0,0	0,0	0,0	0,0	0,0	0,0	0,0	0,0	0,0	0,0	0,0	0,0	0,0	0,0	0,0
Cribrostomoides jeffreysii	0,0	0,0	0,0	0,0	0,0	0,0	0,0	0,0	0,0	0,0	0,0	0,0	0,0	0,0	0,0
Cribrostomoides cf. kosterensis	0,3	1,4	3,4	2,2	1,8	1,7	1,2	0,0	0,0	0,4	0,0	0,0	0,0	0,0	0,0
Cuneata arctica	1,5	0,0	0,4	0,0	0,0	0,0	0,0	0,0	0,0	0,0	0,0	0,0	0,0	0,0	0,0
Eggerelloides medius	1,5	0,5	0,4	0,0	0,0	0,0	0,4	0,0	0,0	0,0	0,0	0,0	0,0	0,0	0,0
Eggerelloides scaber	0,3	0,0	0,0	0,0	0,0	0,0	0,0	0,0	0,0	0,0	0,0	0,0	0,0	0,0	0,0
Eggerella europea	0,0	0,0	0,4	0,0	0,0	0,0	0,0	0,0	0,0	0,0	0,0	0,0	0,0	0,0	0,0
Haplophragmoides bradyi	0,0	0,0	0,0	0,0	0,0	0,0	0,0	0,0	0,0	0,0	0,0	0,0	0,0	0,0	0,0
Leptohalysis scottii	0,0	0,0	0,0	0,0	0,0	0,0	0,0	0,0	0,0	0,0	0,0	0,0	0,0	0,0	0,0
Liebusella goësi	0,0	0,0	0,0	0,0	0,0	0,0	0,0	0,0	0,0	0,0	0,0	0,0	0,0	0,0	0,0
Recurvoides trochamminiformis	1,2	0,5	0,0	0,0	0,7	0,0	0,0	0,0	0,0	0,0	0,0	0,0	0,0	0,0	0,0
Reophax dentaliniformis	0,9	0,2	0,0	0,0	0,0	0,0	0,0	0,0	0,0	0,0	0,0	0,0	0,0	0,0	0,0
Reophax fusiformis	0,0	0,0	0,0	0,0	0,0	0,0	0,0	0,0	0,0	0,0	0,0	0,0	0,0	0,0	0,0
Reophax micaceus	0,0	0,2	0,0	0,0	0,0	0,0	0,0	0,0	0,0	0,0	0,0	0,0	0,0	0,0	0,0
Spiroplectammina biformis	1,5	1,4	1,5	1,3	1,1	0,3	1,4	0,0	0,0	0,0	0,0	0,0	0,0	0,0	0,0
Trochammina sp.	0,0	0,0	0,4	0,0	0,7	0,3	0,0	0,0	0,0	0,2	0,0	0,0	0,0	0,0	0,2
Textulaia sp.	0,0	1,4	0,0	0,0	0,4	0,3	0,0	0,0	0,0	0,0	0,0	0,0	0,0	0,0	0,0
Textulaia earlandi	0,0	0,2	0,0	0,0	0,0	0,0	0,0	0,0	0,0	0,0	0,0	0,0	0,0	0,0	0,0
Textularia kattegatensis	0,3	0,0	0,0	0,0	0,0	0,0	0,0	0,0	0,0	0,0	0,0	0,0	0,0	0,0	0,0
Textularia cf. contorta	0,0	0,0	0,4	0,0	0,0	0,0	0,0	0,0	0,0	0,0	0,0	0,0	0,0	0,0	0,0
Agglutinated fragments	0,0	0,0	0,0	0,0	0,0	0,0	0,0	0,0	0,0	0,0	0,0	0,0	0,0	0,0	0,0
Astrononion gallowayi	1,5	0,5	0,0	0,9	1,8	0,3	1,0	3,3	0,0	0,4	0,2	0,8	1,1	0,9	0,5
Bolivina sp.	0,0	0,0	0,4	0,0	0,0	0,0	0,0	0,4	0,3	0,2	0,2	0,0	0,0	0,3	0,5
Bolivina pseudopunctata	3,2	1,0	1,9	2,7	1,4	1,3	2,2	0,0	0,6	2,0	0,5	1,0	0,7	0,3	0,9
Buccella frigida	4,7	1,0	4,6	6,2	4,6	5,1	5,7	0,0	0,0	0,4	1,0	0,0	0,1	0,0	0,0
Bulimina marginata	14,9	10,3	9,2	16,8	15,2	14,1	15,3	3,3	1,6	3,1	3,2	3,3	5,0	3,7	3,3
Bulimina sp	0,0	0,0	0,0	0,0	0,0	0,0	0,0	0,4	0,0	0,0	0,0	0,0	0,0	0,0	0,0
Buliminella elegantissima	0,0	0,7	0,0	0,0	0,0	0,0	0,6	0,0	0,0	0,0	0,0	0,0	0,0	0,0	0,0
Cassidulina obtusa	0,0	0,0	0,0	0,9	0,0	0,0	0,0	1,7	0,3	0,0	0,0	0,0	1,4	1,2	0,0
Cassidulina laevigata	7,6	2,4	4,6	5,8	2,5	3,0	4,7	7,1	10,1	16,1	10,0	13,0	0,0	1,8	20,7
Cassidulina reniforme	17,8	14,1	18,3	17,3	20,5	22,9	23,1	14,6	22,0	23,5	24,3	26,8	19,6	19,4	24,0
Cassidulina neoteretis	0,0	0,0	0,0	0,0	0,0	0,0	0,0	12,1	1,3	2,6	9,2	6,0	21,8	14,2	1,4
Cassidulinoides brodyi	0,0	0,0	0,0	0,0	0,0	0,0	0,0	0,0	0,0	0,4	0,5	0,0	0,0	0,0	0,2
Cassidulinoids sp.	0,0	0,0	0,0	0,0	0,0	0,0	0,0	0,0	0,0	0,0	0,0	0,0	0,0	0,3	0,0
Cibicides refulgens	0,0	0,0	0,0	0,0	0,0	0,0	0,0	0,0	0,0	0,0	0,0	0,0	0,0	0,3	0,0
Cibicides lobatulus	3,8	4,1	4,2	2,7	2,1	2,4	2,2	8,3	9,7	7,2	2,9	5,8	4,8	4,9	2,4
Cibicidoides mundulus	0,0	0,0	0,0	0,0	0,0	0,0	0,0	4,6	6,9	5,0	3,4	4,5	6,2	6,2	4,7
Cornuspira involvens	0,0	0,0	0,0	0,0	0,0	0,0	0,0	0,0	0,0	0,0	0,0	0,0	0,0	0,0	0,2
Discorbinella bertheloti	0,6	0,7	1,1	2,7	0,7	0,0	0,6	4,6	1,9	3,9	3,6	3,3	3,9	5,2	4,0
Elphidium albiumbilicatum	0,3	1,4	0,4	1,3	0,0	3,0	1,6	1,3	3,1	1,3	1,2	0,8	1,4	1,5	0,9
Elphidium excavatum	11,1	6,9	8,0	9,7	11,0	11,4	12,3	3,8	4,4	4,4	5,4	4,5	3,4	6,2	10,6
Elphidium cf. subarcticum	2,6	2,4	4,6	1,3	0,0	1,0	2,5	0,0	3,8	3,5	4,6	4,5	0,0	2,5	1,9
Elphidium sp.	0,0	0,0	0,0	0,0	0,0	0,0	0,0	0,0	0,0	0,4	0,5	0,0	0,0	0,0	0,0
Epistominella vitrea	5,0	4,1	3,4	1,8	0,7	1,3	0,4	0,8	0,6	0,4	0,2	0,0	0,6	0,3	0,2
Fissurina lagernoides	0,0	0,0	0,4	0,4	0,0	0,0	0,0	1,3	0,0	0,0	0,2	0,0	0,4	0,0	0,0
Fissurina marginata	0,0	0,0	0,4	0,0	1,4	0,7	0,0	0,0	0,0	0,0	0,0	0,0	0,0	1,8	0,0
Fissurina orbignyana	0,0	0,2	0,0	0,0	0,0	0,0	0,0	0,0	0,0	0,0	0,0	0,0	0,0	0,3	0,0
Fissurina sp.	1,2	1,7	0,4	0,0	0,0	0,0	0,4	0,0	0,9	0,7	0,0	0,3	0,0	0,0	0,5
Gavelinopsis praegeri	0,6	0,0	0,0	0,4	0,4	0,0	0,0	0,4	1,3	0,9	1,0	1,0	0,4	0,0	0,2
Globobulimina turgida	0,0	0,0	0,0	0,0	0,0	0,0	0,0	0,0	0,0	0,0	0,0	0,0	0,0	0,0	0,0
Globocassidulina subglobosa	0,0	0,0	0,0	0,0	0,0	0,0	0,0	0,0	0,3	0,0	0,0	0,0	0,0	0,0	0,0
Guttulina communis	0,0	0,0	0,4	0,0	0,0	0,0	0,0	0,0	0,0	0,0	0,0	0,0	0,0	0,0	0,0
Guttulina sp	0,0	0,0	0,0	0,0	0,0	0,0	0,0	0,0	0,3	0,2	0,0	0,0	0,0	0,0	0,0
Hyalinea balthica	6,7	10,3	3,8	11,5	7,1	9,1	8,8	3,8	3,5	4,8	4,6	4,3	3,7	4,0	4,0
Islandiella islandica	0,0	0,0	0,0	0,0	0,0	0,0	0,0	0,0	0,0	0,0	1,0	0,0	0,0	0,0	0,0
Islandiella norcrossi	0,0	0,2	0,0	0,0	1,4	1,0	0,0	0,0	1,9	1,1	1,9	0,8	0,0	0,0	0,0
Islandiella sp.	0,0	0,0	0,0	0,0	0,0	0,0	0,0	0,0	0,0	0,0	0,0	0,0	0,0	0,3	0,0
Lenthiculina sp	0,0	0,2	0,0	0,0	0,0	0,0	0,0	0,8	0,0	0,2	0,0	0,0	0,1	0,6	0,0
Lagena mollis	0,0	0,0	0,0	0,0	0,0	0,0	0,0	0,0	0,0	0,0	0,0	0,0	0,0	0,0	0,0
Lagenamnia arenulata	0,3	0,0	0,0	0,4	0,0	0,0	0,0	0,0	0,0	0,0	0,0	0,0	0,0	0,0	0,0
Lagena distoma	0,0	0,0	0,0	0,4	0,0	0,3	0,0	0,0	0,0	0,0	0,0	0,0	0,0	0,0	0,0
Lagena sp.	0,0	0,2	0,0	0,0	0,4	0,0	0,0	0,0	0,0	0,0	0,0	0,3	0,0	0,0	0,0
Melonis barleeanus	0,0	0,0	0,0	0,0	0,0	0,0	0,0	2,5	2,2	1,5	1,5	4,0	4,7	3,1	3,3
Miliolinella subrotunda	0,0	0,0	0,0	0,0	0,0	0,0	0,0	0,0	0,0	0,0	0,0	0,0	0,1	0,0	0,0
Nodosaria sp.	0,0	0,0	0,0	0,0	0,0	0,0	0,0	0,0	0,0	0,0	0,0	0,0	0,0	0,0	0,2
Nonionella iridea	3,8	0,7	3,4	0,0	1,4	0,0	0,6	5,4	3,8	3,7	4,9	1,5	1,4	5,8	1,2
Nonionella frigida	0,3	0,7	0,0	0,0	0,0	0,0	0,0	0,0	0,0	0,0	0,0	0,0	0,0	0,0	0,0
Nonionella turgida	0,0	0,0	0,0	0,0	0,0	0,0	0,0	0,0	0,0	0,7	0,5	0,3	0,4	0,0	0,0
Nonionellina labradorica	3,2	3,1	2,3	4,0	4,2	4,4	4,5	2,1	3,1	3,7	1,2	3,0	5,4	3,1	5,4
Parafissurina sp.	0,0	0,0	0,0	0,0	0,0	0,0	0,0	0,0	0,0	0,2	0,0	0,0	0,0	0,3	0,0
Parafissurina fusuliformis	0,0	0,0	0,0	0,0	0,0	0,0	0,0	0,0	0,0	0,0	0,0	0,0	0,0	0,6	0,0
Patellina corrugata	0,6	0,2	1,1	0,0	0,7	0,0	0,4	0,0	0,6	0,2	0,0	0,5	0,0	0,0	0,0
Pullenia osloensis	5,8	9,5	6,9	0,4	7,4	5,4	4,1	10,8	8,8	3,7	8,3	6,0	5,7	3,1	3,8
Pullenia bulloides	0,0	0,0	0,0	0,0	0,0	0,0	0,0	0,4	0,0	0,0	0,0	0,0	0,0	0,6	0,0
Pyrgo williamsoni	0,0	0,0	0,0	0,0	0,0	0,0	0,0	0,0	0,0	0,0	0,0	0,0	0,0	0,0	0,0
Quinqueloculina seminula	0,0	0,0	0,0	0,0	0,0	0,0	0,0	0,0	0,0	0,0	0,0	0,0	0,0	0,0	0,0
Quinqueloculina stalkeri	0,0	0,0	0,4	0,0	0,0	0,0	0,0	0,0	0,0	0,0	0,0	0,0	0,0	0,0	0,0
Quinqueloculina sp.	0,0	0,2	0,0	0,0	0,0	1,0	0,0	0,0	0,0	0,0	0,0	0,0	0,0	0,3	0,0
Rosalina sp.	0,0	0,0	0,0	0,0	0,0	0,0	0,0	0,0	0,0	0,0	0,0	0,0	0,0	0,6	0,0
Robertina arctica	0,0	0,0	0,0	0,0	0,0	0,0	0,0	0,0	0,3	0,0	0,0	0,0	0,0	0,6	0,0
Stainforthia fusiformis	15,5	13,4	11,5	8,0	6,0	6,4	4,5	2,9	3,5	0,7	0,0	0,5	0,8	0,6	0,0
Stainforthia concave	2,0	1,0	0,4	0,0	2,5	0,7	1,0	0,4	0,0	0,4	1,5	1,0	1,8	1,2	2,6
Stainforthia schreibersiana	0,0	0,0	0,0	0,0	1,8	0,7	0,0	0,0	0,0	0,0	0,0	0,0	0,0	0,9	0,0
Trifarina angulosa	1,8	1,0	0,0	0,0	0,0	0,3	0,2	2,9	2,2	1,7	2,4	2,5	4,8	3,1	2,1
Triloculina tricarinata	0,0	0,0	0,0	0,0	0,0	0,0	0,0	0,0	0,6	0,0	0,0	0,3	0,0	0,0	0,0
Uvigerina peregrina	0,0	0,0	0,8	0,0	0,0	0,0	0,0	0,0	0,0	0,0	0,0	0,0	0,0	0,0	0,0

Appendix E: Taxonomic list of benthic foraminifera

Species are listed in alphabetical order. The list is based on the World Register of Marine Species (WoRMS, 2018).

Adercotryma glomerata (Brady) = *Lituola glomerata* Brady 1878.
Adercotryma wrighti Brönnimann & Whittaker 1987.
Ammodiscus gullmarensis Höglund 1948
Astrononion gallowayi Loeblich & Tappan 1953.
Bolivina pseudopunctata Höglund 1947.
Buccella frigida (Cushman) = *Pulvinulina frigida* Cushman 1922.
Bulimina marginata d'Orbigny 1826.
Buliminella elegantissima (d'Orbigny) = *Bulimina elegantissima* d'Orbigny 1839.
Cassidulina laevigata d'Orbigny 1826.
Cassidulina neoteretis Seidenkrantz 1995.
Cassidulina obtusa Williamson 1858.*Cassidulina reniforme* Nørvang 1945.
Cassidulinoides bradyi – Cassidulina bradyi Norman 1881.
Cibicides lobatulus (Walker & Jacob) = *Nautilus lobatulus* Walker & Jacob 1798.
Cibicides refulgens de Montfort 1808.
Cibicidoides mundulus (Brady, Parker & Jones) = *Truncatulina mundula* Brady, Parker & Jones 1888.
Cornuspira involvens (Reuss) = *Operculina involvens* Reuss 1850.
Cribrostomoides kosterensis (Höglund) = *Labrospira kosterensis* Höglund 1947.
Discorbinella bertheloti (d'Orbigny) = *Rosalina bertheloti* d'Orbigny 1839.
Eggerella europea (Christiansen) = *Verneuilina europeum* Christiansen 1958.*Eggerelloides medius* (Höglund) = *Verneuilina media* Höglund 1947.
Eggerelloides scaber (Williamson) = *Bulimina scabra* Williamson 1858.
Elphidium albiumbilicatum (Weiss) = *Nonion pauciloculum* (Cushman) subsp. *albiumbilicatum* Weiss 1954.
Elphidium excavatum (Terquem) = *Polystomella excavata* Terquem 1875
Elphidium subarcticum Cushman 1944.
Epistominella vitrea Parker 1953.
Fissurina marginata (Montagu) = *Vermiculum marginatum* Montagu 1803
Fissuringa orbignyana Seguenza 1862.

Gavelinopsis praegeri (Heron-Allen & Earland) = *Discorbina praegeri* Heron-Allen & Earland 1913.

Globocassidulina subglobosa (Brady) = *Cassidulina subglobosa* Brady 1881.

Guttulina communis (d'Orbigny) = *Polymorphia communis* d'Orbigny 1826.

Hyalinea balhica (Schröter) = *Nautilus balthicus* Schröter 1783.

Islandiella islandica Nørvang 1945.

Islandiella norcrossi (Cushman) = *Cassidulina norcrossi* Cushman 1933.

Lagenammina arenulata (Skinner) = Reophax difflugiformis subsp. *arenulata* Skinner 1961.

Lagena distoma Parker & Jones 1864.

Melonis barleeanus (Williamson) = *Nonionina barleeana* Williamson 1858.

Miliolinella subrotunda (Montagu) = *Vermiculum subrotundum* 1803.

Nonionella iridea Heron-Allen & Earland 1932.

Nonionella turgida (Williamson) = *Rotalina turgida* Williamson 1858

Nonionellina labradorica (Dawson) = *Nonionina scapha* var. *labradorica* Dawson 1860.

Parafissurina fusuliformis Loeblich & Tappan 1953.

Patellina corrugata Williamson 1858.

Pullenia bulloides (d'Orbigny) = *Nonionina bulloides* d'Orbigny 1846.*Pullenia osloensis* Feyling-Hanssen 1954.

Quinqueloculina stalkeri Loeblich & Tappan 1953.

Recurvoides trochamminiformis Höglund 1947.

Reophax dentaliniformis (Brady) = *Lituola (Reophax) dentaliniformis* Brady 1881.

Reophax micaceus Earland 1934.

Robertina arctica d'Orbigny 1846.

Spiroplectammina biformis (Parker & Jones) = *Textularia agglutinans* var. *biformis* Parker & Jones 1865.

Stainforthia fusiformis (Williamson) = *Bulimina pupoides* d'Orbigny var. *fusiformis* Williamson 1858.

Stainforthia concava (Höglund) = *Virgulina concava* Höglund 1947.

Stanforthia schreibersiana Czjzek = *Virgulina schreibersiana* Czjzek 1848

Textularia earlandi Parker 1952.

Textularia kattegatensis Höglund 1948.

Textularia contorta Höglund 1947.

Trifarina angulosa (Williamson) = *Uvigerina angulosa* Williamson 1858.

Triloculina tricarinata d'Orbigny 1826.

Uvigerina peregrina Cushman 1923.